VISUAL DETECTION OF CANCER BIOMARKERS WITH APTAMER FUNCTIONALIZED-GOLD NANOPARTICLES

A Dissertation
Submitted to the Graduate Faculty
of the
North Dakota State University
of Agriculture and Applied Science

By

Anant Singh Gurung

In Partial Fulfillment of the Requirements
for the Degree of
DOCTOR OF PHILOSOPHY

Major Department:
Chemistry and Biochemistry

May 2014

Fargo, North Dakota

North Dakota State University

Graduate School

Title

Visual Detection of Cancer Biomarkers with Aptamer-Functionalized Gold Nanoparticles

By

Anant Singh Gurung

The Supervisory Committee certifies that this ***disquisition*** complies with North Dakota State University's regulations and meets the accepted standards for the degree of

DOCTOR OF PHILOSOPHY

SUPERVISORY COMMITTEE:

Dr. Guodong Liu
Chair

Dr. D.K. Srivastava

Dr. Wenfang Sun

Dr. Eugene Berry

Approved:

November 19, 2015
Date

Dr. Gregory R. Cook
Department Chair

ABSTRACT

Cancer biomarkers may hold the key for the early detection of cancer, distinguishing between benign and malignant cells, and differentiating tumor types. The detection of cancer biomarkers can be used for cancer diagnosis, monitoring the response to therapy, and providing real-time prognostic information for cancer patients. Most of the traditional cancer biomarker detections are based on specific antibodies or expensive instrumentations/complex operations. In this dissertation, we have developed aptamer-based bioassays for visual detection of cancer protein biomarkers with low-cost and short assay time. Aptamers with specific sequences are immobilized on gold nanoparticle (AUNP) surface through self-assembling process. Combining the excellent molecular recognition properties of aptamers and the unique optical properties of AUNPs, colorimetric assay for carcinoembryonic antigen (CEA) and mucin 1 (MUC1) (breast cancer biomarkers) and lateral flow assay for platelet-derived growth factor (PDGF) and thrombin have been developed. The methods were applied to detect protein biomarkers in human plasma and blood successfully. The sensitivities of the assays were further improved by using enzyme-coated AUNP dual labels and designing the cross-flow test strips. The developed approaches have the potential to be extended for detecting other biomarkers, and show great promise for point-of-care or in-field detection.

ACKNOWLEDGMENTS

I would like to thank my advisor Dr. Guodong Liu for his support and guidance throughout graduate school. Dr. Liu has helped me with all my problems in the five years that we have known each other. I thank you Dr. Liu as your excellent knowledge and expertise has inspired me a lot. Working under your excellent guidance has taught me a lot about research. I have always looked up to you as my mentor and will always come to you for advice for any future endeavors.

I would also like to thank my committee members Dr. D.K. Srivastava, Dr. Wenfang Sun and Dr. Eugene Berry for their excellent guidance with my graduate studies and research. I thank all of you for your time and support.

I would like to thank Dr. Xun Mao for all the initial training on lateral flow biosensors when I first joined the lab in 2009. Thank you for your patience, support and all the training which helped me greatly with all my graduate research.

Importantly, I would like to acknowledge the financial support from NSF and NDEPSCoR, without which none of the research in this dissertation would have been possible.

I would also like to thank my colleagues Meenu Baloda and Hui Xu for making graduate school a fun experience. Thank you guys for making the lab a fun place to work.

Finally, I would like to thank my parents Dr. Anup Singh Gurung and Anika Gurung for their love, support and encouragement.

DEDICATION

This dissertation is dedicated to my parents **Dr. Anup Singh Gurung** and **Anika Gurung**, and also to my brother **Arjun Singh Gurung**. Thank you for all your unconditional love and support.

"The most important thing in this world is to learn to give out love, and let it come in."

~Morrie Schwartz

TABLE OF CONTENTS

LIST OF FIGURES

CHAPTER 1. INTRODUCTION

The motivation behind the research described in this dissertation is the development of ultrasensitive assays for the detection of cancer biomarkers. Biomarkers are measurable characteristics which indicate the presence, severity and prognosis of a disease. There are several types of biomarkers, but the discovery of protein biomarkers and their accurate correlation with the progression of several diseases have made them increasingly important. Once validated, cancer biomarkers can be used for cancer diagnosis, monitoring the response to therapy, and providing real-time prognostic information for cancer patients. Cancer is one of the leading causes of deaths in the United States with 1,660,290 expected new cases in 2013. Early detection and diagnosis of cancer greatly improves the odds of successful treatment and survival. Several clinical studies have shown that protein biomarkers have been successful in detecting and monitoring the progression of cancer. Some common protein detection techniques are enzyme-linked immunosorbent assay, fluorescence, radioimmunoassay and surface enhanced Raman spectroscopy. Although these techniques are sensitive and selective for protein detection, they suffer from drawbacks like time consuming sample purification, sample pre-treatment, incubation, washing steps, costly instrumentation, need of specialized equipment and experienced personals. Liu et al. recently developed gold nanoparticle-aptamer based lateral flow strips for the detection of proteins. These lateral flow strips incorporated the use of aptamers instead of the traditional antibodies used for protein detection. Aptamers, which are single stranded oligonucleotides (DNA or RNA) exhibited exceptional binding affinity and selectivity for their protein target as compared to the antibody. Advantages like low-cost manufacturing, longer shelf-life, and ease of modification with no cross reactivity clearly proved that the aptamer based lateral flow strips were far more promising than the antibody based strips. Offering a wide range of advantages over antibodies, at all stages of

development, production, and commercial application; antibodies are slowly being replaced by aptamers for conventional detection and diagnosis.

In this dissertation, we studied the development of lateral flow biosensors incorporating aptamers and AUNPs for the multiple detection of protein targets (PDGF-BB and Thrombin) and whole cells (MCF-7 breast cancer cells). Amplification techniques using enzyme-coated AUNP dual labels and the cross-flow test strips were also developed to increase the sensitivity of the lateral flow strips. The detection principal was also used to develop a colorimetric system based on magnetic beads, aptamers and horseradish peroxidase for the detection of breast cancer biomarkers (CEA and MUC1).

1.1. Nanoparticles

Particles or dispersions in the nanometer (nm) size range are called Nanoparticles (NPs). NPs are divided into groups based on their sizes and shapes. Two broad groups of NPs are fine NPs which range from 100 nm to 2500 nm and ultrafine NPs which range from 1 nm to 100 nm.[1] Several studies have been conducted to test the structures NPs form when they are combined together. One such popular structure are the "nanoclusters" which have at least one dimension ranging from 1 nm to 10 nm.[2] NPs have a wide range of applications depending on whether it is a suspension (solid in liquids), aerosol (solid or liquid in air) or emulsion (two liquid phases).[2] Research on nanoparticles have recently gained considerable interest in the past few decades due to a wide variety of applications in biotechnological, pharmacological and pure technological use.[2, 3] Surfactants (chemical agents) play an important role in broadening the applications of NPs. In the past decade or so, surfactants have been extensively used to change the surface and interfacial properties of NPs.[2] Coagulation of smaller NPs leads to formation of larger NPs disrupting the surface charges and properties. Using surfactants, NPs have been stabilized against aggregation by

conserving the particle charge and modifying the surface of the particle.[3] The chemical and physical properties of NPs varies with the size of the NPs, whereas bulk materials have comparatively stable or constant physical properties regardless of their size.[1, 3] Properties of NPs change with size as the use of atoms on the surface of a material becomes significant at nanoscale levels. The ease of modification and a vast variety of properties have broadened the applications of NPs using quantum mechanics, fluorescence, chemiluminescence, etc. [3-5]

For NPs, the ratio of surface area to volume present is vastly increased, therefore increasing the surface area greatly making possible new quantum mechanical effects.[4] Optical properties of NPs for e.g. fluorescence also become a function of the particle diameter at nanoscale levels. This optical property does not come into play in the macro to micro dimensions. Zinc oxide NPs are often used in manufacturing sunscreen lotions as they have shown superior UV blocking properties compared to its bulk substitute.[4, 5] The various physical, optical quantum confinement, surface plasmon resonance and superparamagnetism properties have replaced the use of bulk materials with their NPs. Therefore, reducing cost, waste materials, toxicity and manufacturing time.[5] NPs have successfully been used for developing well known applications in the field of biology and medicine.

1.1.1. Gold Nanoparticles (AUNPs)

AUNP colloids are submicrometre sized particles in a fluid, usually water.[1, 2] The size of the particles determine the color of the AUNP suspension. An intense red color is observed for particles less than 100 nm in size. As the particles increase in size the color changes to a dark blue/purple, usually seen in solutions with AUNPs larger than 100 nm in size.[5] Several colorimetric assays take advantage of this phenomenon, usually indicating the presence of the target with a change in the color of the AUNP solution.[5] AUNPs are emerging as the most important candidates

for biomedical applications. Size and shape dependent optical absorption and scattering capabilities make AUNPs useful for detecting targets throughout the visible and near infrared (NIR) region.[6] Another advantage of using AUNPs is little or no long term toxicity allowing their applicability in living systems.[7]

AUNPs are made compatible with biological environments and biomolecules by modification to the solvent accessible surface.[8] Ligand modification, additional coatings and ligand exchange are some of the strategies used for modification of the AUNP surface helping in meeting requirements like biocompatibility, targeting efficacy and chemical stability.[9] These key requirements are important for most of the biomedical applications of AUNPs.[8, 9] Turkevich's method, brust's method, martin's method, citrate reduction and sonolysis are some of the most accurate methods used for the synthesis of AUNPs.[18, 19] These methods used for synthesis of AUNPs have the ability to control the size and shape of the particles broadening their applications to biological imaging and detection, gene regulation, drug delivery and therapeutic tools for treatment of cancer.[4,5,9]

In the current study, AUNPs were synthesized using the citrate reduction method and labeled with aptamers specific for their respective targets. AUNPs ranging from 15 nm to 20 nm in size were also labeled with enzymes for signal amplification purposes, successfully detecting multiple cancer biomarkers.

1.1.2. Silica Nanoparticles (SiNPs)

SiNPs have certain structural properties like tunable pore sizes, high pore volume, high internal surface area, colloidal stability and the ability to modify the inner pore system making them favorable for several biomedical applications.[9] These structural advantages give SiNPs the ability to encapsulate large amounts of antibodies, mediators and enzymes via active functional

group induces modifications.[10] The larger surface area of particles enables loading higher number of delivery agents, antibodies, etc. making the SiNPs an effective drug delivery agent. SiNPs have also been used as biocatalysts for drug release, biosensors, immunoassays, etc.[10, 11]

1.1.3. Magnetic Nanoparticles (MNP)

MNPs are NPs with magnetic properties usually synthesized using iron, nickel and cobalt, ranging from 5 nm to 500 nm. Magnetic fields or magnets are used to take advantage of the magnetic properties, making assay procedures easy, stable and fast. MNPs offer a wide variety of advantages over other NPs. Synthesis with size control; external modification and magnetism are some of the properties that make MNPs the perfect candidate for magnetic resonance imaging (MRI).[12] MNPs have also been used in applications like protein purification, medical imaging and drug delivery. Surface modification and conjugation with antibodies, aptamers, proteins and ligands allow the use of MNPs in various target detection assays and drug delivery mechanisms.[13, 14] MNPs have been used in conjugation with other NPs to synthesize hybrid nanostructures, exhibiting magnetic properties with other properties like chemiluminescence, fluorescence, etc. depending on the hybrid NP.[13] These hybrid nanostructures combine multiple properties of various NPs providing an enhanced platform for medical imaging, drug delivery, and many more assays.[14, 15]

In the current study, MNPs were labeled with aptamers and enzymes for the colorimetric detection of MCF-7 cancer cells. The magnetic properties of MNPs helped in the easy separation and washing steps, reducing the total assay time. With the help of MNPs, the controls for assays showed no signal in the absence of the target.

1.2. Biosensors

Biosensors are analytical devices manufactured using several biological components, used for the detection of one or multiple target analytes.[15] Biosensors have been used for the detection of a broad range of targets like proteins, DNA, RNA, cancerous cells, and many more.[15, 16] Depending on the target the biological component can be nucleic acids, aptamers, enzymes, cell receptors, etc. which interact and bind the detecting target analyte.[16] An important component of the biosensors is the detector element or biotransducers. [16, 17] The biotransducers transform the signal created from the interaction of the biological component and the analyte into detectable signals. These detectable signals are easily readable, quantifiable and reproducible.[14, 15] Pyroelectric biosensors, optical biosensors, gravimetric biosensors, electrochemical biosensors and electronic biosensors are some of the common biotransducers used in biosensors. A good example of transducers would be fluorescent dyes. Fluorescence signals are generated by the fluorescent biotransducers in the presence of the analyte, indicating the successful detection of the target. Another example would be the chemiluminescence signals given out by quantum dots. AUNPs have also been used as the biotransducer component of biosensors. The colorimetric detection assays use the change in color indicated by the aggregation of AUNPs in the presence of the target analytes.[15, 16]

Sensitivity, reproducibility, cost, selectivity and assay time are some of the important factors taken into consideration when designing a biosensor.[16] A suitable recognition element with high selectivity and specificity for the target, a well know target molecule and a detection system with high sensitivity preferred over the standard laboratory based techniques are some of the basic requirements for designing a biosensor.[16] One such well known biosensor is the glucose sensor for monitoring the blood sugar level of diabetic patients.[16, 17] The glucose biosensors are selective and

sensitive toward the change in blood glucose level making them a highly successful biosensor. Other well-known applications of biosensors include; detection of pesticides, proteins, toxins, drug residues, pathogens, etc.

1.3. SELEX

SELEX which is the systematic evolution of ligands by exponential enrichment is *an in vitro* selection technique used for developing single stranded DNA or RNA oligonucleotides used in molecular biology.[18] The single stranded oligonucleotides are termed "Aptamers". SELEX is a process of elimination via exponential exposure of the DNA or RNA pool to the target molecule to find the best binding oligonucleotide sequence for the particular target.[18] Aptamers are highly sensitive and selective target binding oligonucleotides. They are well known for their high binding affinity to targets. Aptamers for the detection of proteins (thrombin, PDGF, etc.), cells, metal ions and small molecules (ATP, adenosine, etc.) have been successfully developed using the SELEX method.

SELEX is a process that begins with a large oligonucleotide library consisting of random sequences of fixed length flanked by constant 3′ and 5′ ends which serve as primers. The target of interest which may be a protein or cell is then introduced into the oligonucleotide library. The sequences that do not bind to the target are removed using affinity chromatography, binding sequences are eluted and amplified via PCR. Subsequent rounds of selection and elution are performed to find the best or tightest binding DNA/RNA sequence for the target.[19] Hundreds of aptamers have been developed for different targets using SELEX. In cancer cell detection, new aptamers can be obtained even without prior knowledge of potential target molecules in the cancer cells. Aptamers for cancer cells, such as liver, ovarian, leukemia and colon have been developed using cell-SELEX based selection methods.[19-21]

1.3.1 Aptamer

First discovered in 1990, aptamers are single stranded oligonucleotides of either DNA or RNA.[1, 2] Aptamers exhibit exceptional binding affinity and selectivity for their target showing several advantages over antibodies. [2] Aptamers offer a wide range of advantages at all stages of production, development and commercial application. As a result antibodies are slowly being replaced by aptamers for conventional detection and diagnosis. The high targeting ability and specificity of aptamers enables a wide range of diagnostic and therapeutic applications. Taking advantage of the aptamer specificity, drug delivery systems targeting cancerous cells have been developed without fear of damaging the surrounding healthy cells.[22] Aptamers have also been extensively compared to antibodies for the binding affinity, in which case, they either exceed or show the same results as antibodies.[19, 20] Another advantage for aptamers over antibodies is the size. Aptamers are a fraction of the size of antibodies making them more acceptable and capable for entering cellular compartments to bind specific targets.[22] Researchers have discovered aptamers that exhibit binding affinities greater than 10,000 folds for theophylline over caffeine, which differ from one another in structure by only a single methyl group.[22, 23] Cross reactivity is not seen in aptamers while antibodies have "false positive" issues.[23] Once dried down, aptamers can be stored at room temperature. When re-suspended in a buffer solution, aptamers can be stored at –20 °C. The structure of the aptamers allow them to be denatures and renatured multiple times, unlike antibodies. These storing flexibilities are far easier to comprehend in comparison to antibodies. Antibodies require to be frozen and have a shelf life of 3 – 6 months once thawed. Also, heat threshold is higher for aptamers in comparison with antibodies.[24]

The availability of automated synthesizers makes the bulk production of aptamers fast, easy and cost effective. Once the aptamer sequence for a particular target has been determined, the

automated synthesizers are used for on demand production of chemically manufactured aptamers at a fraction of the cost of their antibody equivalent.[23]

One of the limitations that aptamers face is the rapid clearance rate from circulation in the body. This is mainly due to the small size and degradation by nucleases for aptamers.[23, 24] Aptamer modifications have been successful in solving this problem, increasing the circulation time of aptamers resulting in a more accurate drug delivery system.[24] Polymers like PEG and various lipids can be conjugated to aptamers to enhance their circulation time. Similarly, nuclease resistance is increased by modifying the nucleotides with altered bases, sugars and also internucleotide linkage.[25]

In this dissertation, ssDNA aptamers were used for the detection of targets like PDGF-BB, Thrombin, CEA and MCF-7 cells. The aptamers showed excellent specificity for their respective targets. The detection limit was well below the cut-off values and the assays show a good linear detection range.

1.4. Cancer

Out of control cell growth is called cancer. There are many types of cancer usually classified by the type of cell it originated from.[26] A group of cells resulted by uncontrolled growth is called tumor. Not all tumors are cancerous, depending on the nature of the cancer cells, tumors are classified into benign and malignant.[27] Benign tumors are local to a region, not spreading to other parts of the body while malignant tumors can spread to different parts thorough the lymphatic system or bloodstream.[27] Studies have indicated that there is an increased risk of cancer with factors such as use of tobacco, certain infections, exposure to radiation, etc. These factors cause cancer by damaging the genes resulting in cancerous mutations.[26 – 28]

The key to improving survival rate for cancer patients is early detection. Early detection improves the odds of successful treatment, provided the cancer is contained and has not spread to different regions of the body. Cancer detection techniques such as X-rays, CT scans, PET scans, etc. are imaging techniques that help detect tumors.[30, 31] Once the tumor is located in an organ, the cells are extracted and observed to confirm whether they are malignant or benign. This procedure is called a biopsy.[32] Physicians also analyze sugar, protein, fat levels for any indication of cancer in the body. The presence of cancerous prostate cells in the body results in a higher level of prostate-specific antigen (PSA).[31] Physicians perform blood test and analyze the PSA levels to detect cancer. Combining the power of biopsies and cellular imaging, early detection of cancer is now possible.[30-32]

1.4.1. Cancer Biomarkers

Cancer biomarkers are substances that indicate the presence of cancerous cells in the body. A biomarker may not only be a molecule released from cancerous cells, but it could also be a phenomenon observed in the body.[32, 33] Currently cancer diagnosis and prognosis are dependent on genetic, epigenetic and imaging biomarkers. These biomarkers are present in the blood, plasma and/or serum in an elevated level in the presence of cancerous cells.[35 – 37] Biomarkers are widely used in cancer research to determine the seriousness of cancer in a patient, usually determined by the level of cancers cells in the body.[35] They are also helpful in determining the patient response to a particular treatment helping physicians to plan out the best phases of treatment.[36-38] Biomarkers also help to monitor the effect of the treatment for patients, indicating the effectiveness of the treatment over time.[39, 40] The current image based tests such as CT and MRI are highly costly.[39] Biomarkers are gaining a lot of interest as it has the ability to detect cancerous cells at an early stage, resulting in lower cost for patient care and improving survival rates.[39-41]

1.4.2. Thrombin

Thrombin plays an important role in blood clotting and stopping bleeding in the human body. A serine protease, encoded by the f2 gene in the human body, thrombin is formed by the proteolytic cleaving of prothrombin in the coagulation cascade.[42] Thrombin plays an important role in the conversion of soluble fibrinogen into insoluble strands called fibrin. It is also known to catalyze many other coagulation related reactions that cause clotting of the blood.[42] During the coagulation process, thrombin concentration in blood increases to nM to low μM levels.[42]

Detection of elevated levels of thrombin in blood serum is important for the early detection of abnormal coagulation. Techniques like electrochemistry, colorimetry, fluorescence and various aptasensors have been developed for the detection of thrombin.[39-42] Thrombin specific aptamers have shown high specificity and selectivity with detection limits matching or even exceeding that of the thrombin antibody.[43]

In this study, we detect Thrombin using aptamers, gold nanoparticles and lateral flow biosensors. The lateral flow biosensors were also tested in serum, showing a linear detection range with a sensitive detection limit.

1.4.3. PDGF

PDGF, present in three forms, PDGF-AA, PDGF-BB and PDGF-AB, stimulates cell division and proliferation through binding to receptors on cell membranes.[45] The protein product of the *sis* oncogenes of simian saroma virus has an amino acid sequence identical to the B chain of PDGF. PDGF-BB has been proven to have a direct correlation with angiogenesis, which is the formation of new blood vessels from existing ones.[45] Uncontrolled angiogenesis is seen in cancer patients with overexpressed concentrations of PDGF-BB. Many research studies have found a direct correlation of cancer with overexpression of PDGF-BB. [46]

PDGF-BB is expressed at very low, undetectable levels in normal cells, but have been found to be overexpresses in human tumors such as sarcomas and gliboblastomas.[47] Several antibody based detection methods have been developed for the detection of PDGF. Techniques like ELISA and radio isotropic methods have been successful in detecting PDGF, but need improvement as they are expensive, time consuming, complex and suffer from bad sensitivity. [48, 49]

In this dissertation, PDGF-BB was detected using lateral flow biosensors with gold nanoparticles and aptamers specific for PDGF-BB. We were successful in developing a lateral flow biosensor which can detect PDGF-BB and Thrombin simultaneously. The two aptamers used showed high specificity and sensitivity for their respective targets.

1.4.4. Breast Cancer

Breast cancer is the second most common type of cancer affecting both males and females usually occurring in the inner lining of the milk ducts. Metastasis is one of the major reasons for deaths. Detection of breast cancer at early stages of development is highly important for improving the chances of survival of the patient.[51, 52] Conventional detection methods are time consuming, inaccurate and lack efficiency. Therefore, the development of new techniques for the rapid, easy and sensitive detection of breast cancer is needed.[53] To breast cancer, human mucin-1(MUC1) and carcinoembryonic antigen (CEA) are the most common markers to monitor the metastatic breast tumors.[54]

1.4.5. CEA

CEA antigen belongs to a set of glycoproteins involved in cell adhesion. During fetal development CEA levels increase in the body and levels are back to normal before birth.[55] CEA is usually present at very low, undetectable levels in the human body. Studies have indicated high

levels of CEA in serum of cancer patients and therefore have been used as cancer biomarkers for early detection.[56] The limit of detection for CEA has been determined to be approximately 2.5 ng/mL in serum samples from colorectal cancer patients.[56, 57] CEA levels have also seen to be elevated in pancreatic, lung, breast and gastric cancers.[57-59]

1.4.6. MUC1

Mucins are glycoproteins bound to cells by integral transmembrane domain via the formation of a gel matrix.[60] It is overexpressed in breast, lung, colorectal, lung, prostate, ovarian and many other types of carcinomas.[61] MUC1 levels in many cancer patients are overexpressed to a point that traces of the glycoprotein are found in the blood stream. Generally found on cell surfaces, MUC1 have been used extensively as cancer biomarkers.[62]

For breast cancer detection, CEA and MUC1 are the two most important cancer biomarkers. They have been studied extensively and have shown high selectivity and sensitivity for detection of breast cancer cells. Highly overexpressed MUC1 have been found in breast cancer patients showing elevated levels of the glycoprotein in the blood serum.[61, 62] Combining the detection of CEA and MUC1 targeted for the diagnosis of breast cancer have proven to be much more accurate than targeting individual biomarkers.[63] The 5 year and 10 year survival rate for breast cancer patients with indication of elevated CEA levels are worse than patients with normal CEA levels.[64] Therefore, the detection of these two well-known cancer biomarkers in conjugation promises a more accurate prognosis and better sensitivity toward detection of breast cancer.[64, 65]

In this study, we developed a colorimetric system using magnetic beads, aptamers, horseradish peroxidase and TMB. The colorimetric system showed good detection limits for both the CEA and MUC1 targets. The detection limit was lower than the cut-off values in healthy

people. Blood spiked with the cancer biomarkers were also tested, showing good response with minimal interference from the biological matrix.

1.5. Colorimetric Detection

An assay developed for the detection of a target molecule, indicating the presence of the target with a color change phenomenon is called colorimetric detection. The target molecule can be anything ranging from a protein, DNA, cell to even metal ions. [65] Most colorimetric detection methods depend on enzymatic reactions. Enzymes react specifically to their substrates making the colorimetric reaction more accurate and specific. The reaction is usually carried out at a specific temperature in a buffer solution to provide optimal conditions for the enzyme.[65]

For the colorimetric detection system developed during this study, Horseradish peroxidase (HRP) was incorporated into the system. 3, 3', 5, 5'-Tetramethylbenzidine (TMB) was used as a substrates detect horseradish peroxidase (HRP) activity, yielding a blue color (Amax = 370nm and 652nm) that changes to yellow (Amax = 450nm) upon addition of a sulfuric or phosphoric acid stop solution. TMB is the most popular chromogenic substrate for HRP detection in ELISA.

1.6. Signal Amplification

Target detection assays used for detecting proteins, DNA, etc. rely on various signal amplification techniques to make the assay more sensitive towards their target molecules. Over the past few decades, signal amplification has gained a lot of interest as this method amplifies the detection signal at least 10 folds, lowering the detection limit of the whole assay.[66] An enzyme reacting with its substrate in the presence of the target amplifies the detection signal which usually is chemiluminescence, fluorescence, an electromagnetic signal, or other detection signals enhancing the sensitivity of the whole assay.[67] The signal amplification is currently being used in areas like food safety, drug detection, clinical diagnosis, etc.[66, 67] Polymerase chain reaction and

mass spectrometric techniques are two well-known amplification techniques used for ultrasensitive single molecule detection.

Some drawbacks pertaining to extra time consuming steps, increasing the complexity of the assay, high cost, wider linear correlation range, etc. are associated with the signal amplification methods.[68] But, the increase in sensitivity leading to lower detection limits and a more sensitive assay allows the detection of the target molecule at about 50 folds lower.[68] The two main strategies for signal amplification used in this study were enzyme labeling and cross flow amplification.

1.6.1. Enzyme Labels

Enzyme labels play an important role in the signal amplification reactions that make the target detection assays more sensitive by amplifying the detection signal. Horseradish peroxidase (HRP) is used extensively in biochemistry applications for its ability to produce signal amplifying byproducts by reacting to its substrates.[69] Substrates like TMB, DAB and ABTS in the presence of hydrogen peroxide oxidize HRP to produce a characteristic change that is detectable using spectrometric methods.[70] HRP catalyzes the reaction converting chromogenic substrates to colored products, which emit light when acting on chemiluminescent susbtrates.[71, 72] The amplified signal in some cases is also visible to the naked eye.[73]

Streptavidin-HRP was used in conjugation biotin-aptamers for the detection of CEA and MUC1 using the colorimetric system developed in this study. The color output from the HRP and TMB reaction in the presence of the target indicated a successful detection system. HRP was also labeled onto gold nanoparticles for the amplification of signal in the presence of thrombin; AEC substrate was used in this method. The amplification using HRP as label resulted in more sensitive assays, lower the detection limit by several orders.

1.6.2. Cross Flow

Cross flow is another technique used for the amplification of the detection signal. Lateral flow biosensors with the cross flow design have been developed in which the signal amplifying component is introduced after the target is captured onto the test zone. Usually, the captured nanoparticle are labeled with enzymes or complementary oligonucleotides to which the substrate or complementary probes bind to increase the detection signal.

In this study, we labeled gold nanoparticles with ssDNA oligonucleotides and aptamers specific for MCF-7 cells. Once the MCF-7 cells were captured on the test zone, complementary DNA probes labeled onto another set of gold nanoparticles were introduced onto the biosensor. The complementary DNA probes form dsDNA and capture the gold nanoparticles introduced via cross flow, therefore increasing the intensity of the red color on the test zone. The cross flow amplification introduced for the detection of MCF-7 cells reduced the detection limit 10 folds, increasing the sensitivity of the biosensor.

CHAPTER 2. EXPERIMENTAL TECHNIQUES

A variety of techniques and instrumentations were used in the manufacturing and development of the lateral flow biosensors. Gold nanoparticles were prepared using the citrate reduction method. Biosensor strips were prepared using the BioDot XYZ dispensing platform along with the AirJet dispenser (for immobilizing the gold nanoparticle-aptamer conjugates) and the BioJet dispensers (for immobilizing the thiolated-aptamers). A portable strip reader was used to readout the intensity of the test zone and control zone giving a quantitative analysis for each assay. During the conjugate preparation steps, pH meters and pH papers were used to check the pH of the AUNP-aptamer conjugates prior to HRP conjugation. Conjugates were also labeled with HRP for signal amplification purposes. For the colorimetric detection method UV-Vis absorbance spectroscopy was used to observe the concentration of target proteins present in the samples. In addition, we also collaborated with the core facility to culture MCF-7 breast cancer cell lines along with control cell line (CCL-2, CCL-119 and CCL-185). A description of each technique that was used in this research project is presented here after.

2.1. Gold Nanoparticle Preparation

AUNPs are been used extensively for various detection assays. AUNPs show numerous advantages over other NPs broadening their application in detection assays. Ease of surface modification, controllable size, stability, color, conjugation with oligonucleotides and antibodies are only some of the advantageous properties for AUNPs.

Several techniques have been developed for the synthesis of AUNPs. Turkevich et al. developed AUNPs b treating $HAuCl_4$ (hydrogen tetrachloroaurate) with citric acid in boiling water.[19] Using this method we could control the size of the AUNPs by changing the ratio of the $HAuCl_4$ in the solution.

We prepared gold nanoparticle using the citrate reduction method with slight modifications. The glassware was thoroughly cleaned with aqua regia (three parts HCl, one part HNO_3), rinsed with double distilled H_2O, and oven-dried prior to use. A 250 mL aqueous solution of $HAuCl_4$ (0.01%) was brought to a boil with vigorous stirring in a 500mL round bottom flask. Trisodium citrate 1% (4.5 mL) was then added quickly to the boiling $HAuCl_4$ solution. A series of color changes from dark purple to wine red indicated the reduction reaction which results in the formation of AUNPs. The reaction was allowed to run until the solution became wine red in color. After removing it from the hot plate the solution was cooled to room temperature with continuously stirring. The gold colloids were then stored in dark bottles at 4 °C. Different sizes of AUNPs were prepared by changing the ratio of the $HAuCl_4$ and sodium citrate. AUNPs with diameters ranging from 15 nm to 100 nm were prepared and tested for conjugate preparation. Nanoparticles with size greater than 50 nm were found to be less stable and these citrate-stabilized AUNPs showed irreversible aggregation during functionalization with thiolate ligands. Figure 1 shows the color associated with different sizes of AUNPs. As the size increases the color changes from wine red to dark purple. AUNP with a size range of 15 ± 3.5-nm-diameter showing good stability and reproducibility were chosen for this study. Small sized nanoparticle have several advantages like large surface area, stability and good reproducibility as compared to larger nanoparticles.

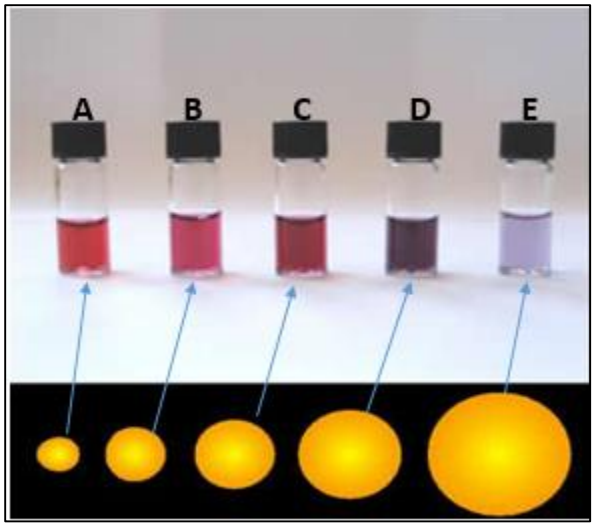

Figure 1. Image showing different sizes of AUNPs and the color associated with their respective sizes.

2.2. Conjugate Preparation

AUNP surfaces can easily be modified with citrates, thiols, or other adsorbed ligands via the displacement of the labile capping ligands by thiols through a place ligand exchange reaction, synthesizing monolayer protected AUNPs.[18, 19] The loading efficiency can be controlled through the reaction time and the ratio of the functional ligand to be conjugated.[20] Adding one or more functional groups during the conjugation procedure can provide mixed monolayer protected AUNPs for multiple detection.[18] A simpler way for surface modification of AUNPs is non-covalent conjugation, as they attach via different interactions like electrostatic interactions, hydrophobic interactions or specific binding affinity.[21]

AUNPs in this study were modified with aptamers specific for different analytes. Dual labeled AUNPs were also prepared in which the nanoparticles were labeled with aptamers as well as HRP for signal amplification purposes. In the early stages of development, conjugate preparation took about sixty hours. Later on as the optimizations and new techniques were researched and implemented, we managed to reduce the conjugate preparation time to about six

hours. Mentioned below are the traditional (method 1) and new methods (method 2) for conjugate preparation and a transition from a 60 hour procedure to a 6 hour procedure.

AUNPs were labeled with aptamers with a thiol (-SH) modification at the 5′ end. For method 1, Thiolated aptamers (20 μL; 2.0 OD) were mixed with 80 μL Nuclease free water, 2 μL of TEA and 7.7 mg DTT and incubated for 60 minutes at room temperature. The excess DTT was removed by extraction with 400 μL ethyl acetate solution, four times. The activated aptamer was then added to a 1 mL portion of 5-fold concentrated AUNP solution in a vial. After a 24 h incubation period at 4 °C, the solution was subjected to aging by the addition of NaCl (150 mM) and a certain quantity of 1% SDS (final concentration 0.01%). The solution was allowed to stand or another 24 h at 4 °C, excess reagents after the completion of the incubation period were removed by centrifugation (12 min at 12,000 rpm), 3 times. The supernatant was discarded and the pellet was redispersed in 1mL of the eluent buffer (20 mM Na3PO4, 5% BSA, 2.5% Tween-20, and 10% sucrose).

Compared to the old method the incorporation of dATP in the procedure reduced the conjugate preparation time remarkably. For method 2, the conjugates were prepared by the reported method[28] with slight modifications. Briefly, 1mL 5-fold solution of AUNPs were prepared using the centrifuge. To the 5-fold AUNP solution, 7.05µM dATP was added and incubated for 15minutes. SDS (1%) with a final concentration of 0.01% was then added to the solution and incubated for about 10 min. SDS stabilizes the AUNP solution and prevents unwanted aggregation in the next step, which is the addition of NaCl (2M) with a final concentration of 0.01M in the 1mL AUNP solution. After addition of salts, thiolated aptamer 0.3 OD was added, the solution was kept on a shaker at RT for 3 h. Unbound thiolated aptamers were removed from the AUNP-aptamer conjugate solution by centrifugation (12,000 rpm; 20 min) and washing using

PBS, this was done three times. After the final wash the pellet was resuspended in 1mL eluent buffer (20 mM Na3PO4 · 12H2O, 5% BSA, 0.25% Tween 20, and 10% sucrose).

Figure 2 shows the two methods for conjugate preparation. Compared to method 1, method 2 was more efficient in binding the thiolated aptamers onto the AUNP surface. Rapid addition of the NaCl causes the AUNPs to aggregate forming larger sized nanoparticles which are unstable for conjugate preparation. The dATP incorporated in method 2 forms a monolayer of adenosine around the AUNP protecting it from aggregation due to salt addition. dATP also reduced the preparation time as well as the amount of thiolated aptamer used in the conjugate preparation. Out of the four different mononucleotides, dATP covered AUNPs were found to have a higher salt tolerance than AUNPs protected by other mononucleotides. The controlled salt concentration and dATP monolayer on the AUNPs facilitate the ligand exchange reaction between the incoming thiol-aptamer and the outgoing dATP. Studies have shown that mononucleotide mediated conjugation approaches enables the loading of about 80 oligonucleotide strands per nanoparticle, prepared in salt solution. This ability of modifying the nanoparticle surface with various biomolecules in a rapid and controlled manner provides endless opportunities in nanobiotechnology.

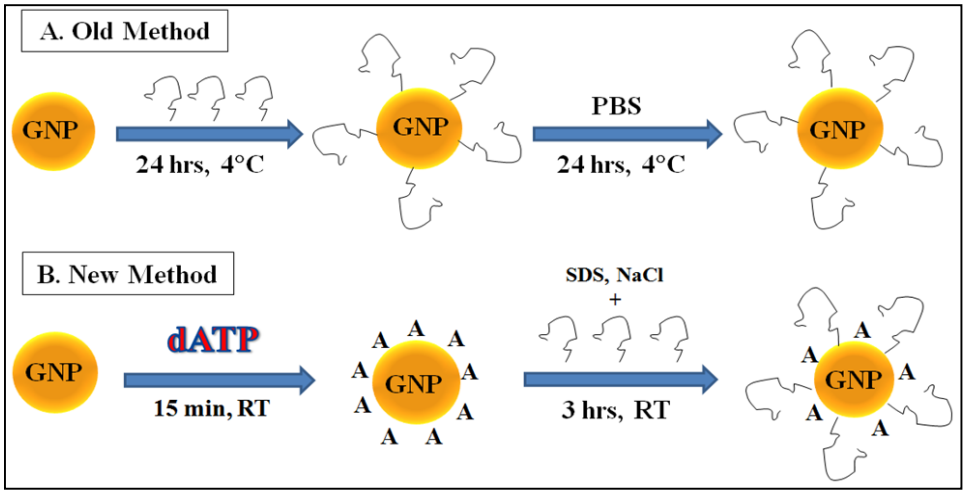

Figure 2. A comparison of the old method and new method of conjugate preparation.

2.3. Biosensor Manufacturing

A lateral flow strip consists of five main components: sample application pad, conjugate pad, nitrocellulose membrane, absorption pad, and a plastic backing layer. A schematic diagram of the biosensor is shown in figure 3. The sample application pad which is made of cellulose fiber (CFSP001700, Millipore) was pretreated with a buffer containing 0.25% Triton X-100, 0.05M Tris-HCl, and 0.15 mM NaCl; pH 8. After pretreatment the sample pad was dried in an incubator oven for 60 min and stored in desiccators at RT. Sample pads are pretreated to ensure the movement of the target analyte onto the conjugate pad. Without pretreatment, the target analytes might get stuck in the pores of the cellulose fiber and not move onto the conjugate pad. Assays without pretreating the sample pad have shown poor sensitivity and reproducibility. Conjugate pad is prepared by dispensing a desired volume of AUNPs conjugated with an aptamers. They are made up of glass fiber material and hold the nanoparticles until the analyte solution from the sample pad comes in contact. The conjugate pads are good for the release of the AUNP conjugates, larger nanoparticles like silica nanoparticles, magnetic nanoparticles and even magnetic beads have shown good movement or release from the conjugate glass fiber pads.

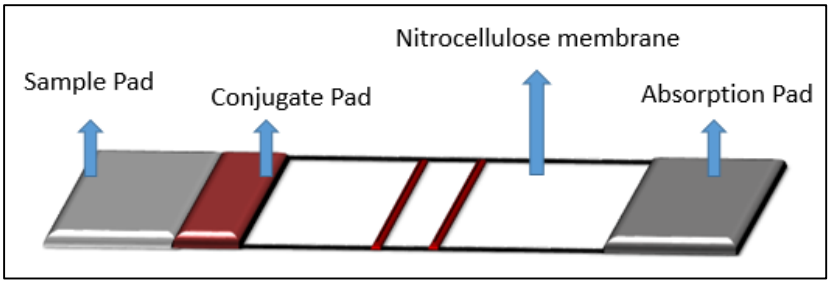

Figure 3. Image showing the components of the lateral flow strip.

The third important component of the lateral flow strips are the nitrocellulose membrane. These are made up of nitrocellulose and are used to trap proteins into the pores of the membrane. Test zone, generally consisting of a streptavidin-biotinylated-aptamer conjugate are dispensed onto the nitrocellulose membrane. The streptavidin binds to the nitrocellulose membrane and in turn immobilizes the biotinylated aptamer, which acts as the test zone. After dispensing the test zone, the nitrocellulose membranes are dried in an incubator oven and stored at 4˚ C. Another way of immobilizing unmodified aptamer or DNA onto the nitrocellulose membrane is UV linking. We used a UV-strataliker 1800 (Figure 4), which is designed to crosslink DNA or RNA to nitrocellulose membrane. The crosslinking process takes about 25 – 50 seconds, as compared to the traditional baking method which took about 2 hours. When crosslinking, a covalent bond forms between the thymine of the DNA probe or uracil of RNA and the amino group of the nitrocellulose membrane at an energy of 120,000 µJ, utilizing a 254 nm light source.

The absorption pad is exactly the same as the sample pad, except that it is not pretreated. The main function of the absorption pad is to absorb all the excess buffer containing the AUNP conjugates and target analyte that do not bind to the test zone. The absorption pad also prevents the excess solution from flowing back onto the lateral flow strips and preventing false control signals which might occur due to nonphysical adsorption. The plastic backing layer is used to assemble all the four components and stick them together.

Figure 4. Photograph showing the UV strata linker

2.3.1. Dispensing

The AUNP-aptamer conjugates and the Streptavidin-Biotin aptamer test line are dispensed onto the nitrocellulose membrane using the XYZ3060 dispensing platform shown in figure 5. The XYZ series from BioDot is a powerful production tool for rapid test development and manufacturing. It has a flexible XYZ system which is fully programmable to dispense lines of desired width and intensity onto the nitrocellulose membrane and the glass fiber membrane.

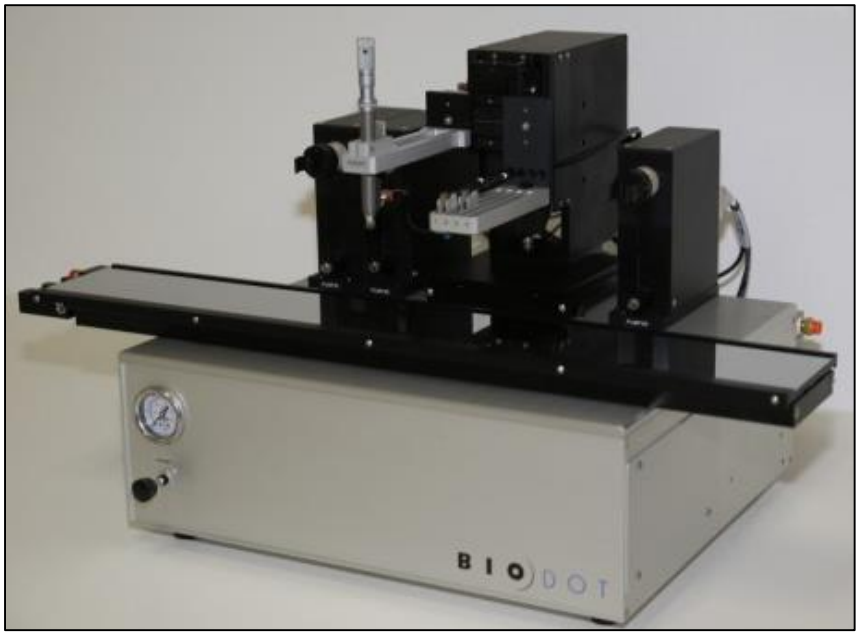

Figure 5. Photograph showing the XYZ 3060 dispensing platform.

2.3.1.1. Dispensing AUNP-Aptamer Conjugates

The AUNP-aptamer conjugates prepared are dispensed onto the conjugate pad using the AirJet dispenser attachment on the XYZ3060 dispensing platform. The AirJet dispenser is a non-contact, quantitative aerosol dispensing technology that uses pressurized air to atomize the fluid passing through its nozzle creating a quantitative spray format. The AirJet is capable of dispensing volumes ranging from 0.5 µL – 34 µL/cm consisting of multiple droplets. Figure 6 shows the image for the AirJet dispenser.

Figure 6. Image showing the AirJet dispenser.

2.3.1.2. Dispensing Test and Control Zones

The test zone and control zone on the nitrocellulose membrane (25 mm × 30 mm) were prepared by dispensing the secondary aptamer and biotinylated DNA (control probe, complementary with the primary aptamer) solutions, respectively. The distance between two zones was around 0.2 cm. To facilitate the immobilization of the probes, streptavidin was used to react with the biotinylated aptamer (secondary aptamer) and biotinylated DNA. The solution was dispensed using the BioJot dispenser attachment onto the XYZ3060 dispensing platform. The BioJet is a non-contact liquid dispensing system which is a low cost dispensing approach. It can dispense a wide range of reagent types (e.g. aqueous, organic, cells) as well as highly viscous reagent. Dispensing volumes range from 60-500 pL as a single drop in the line dispensing mode. Figure 7 shows an image of the BioJet dispenser attachment.

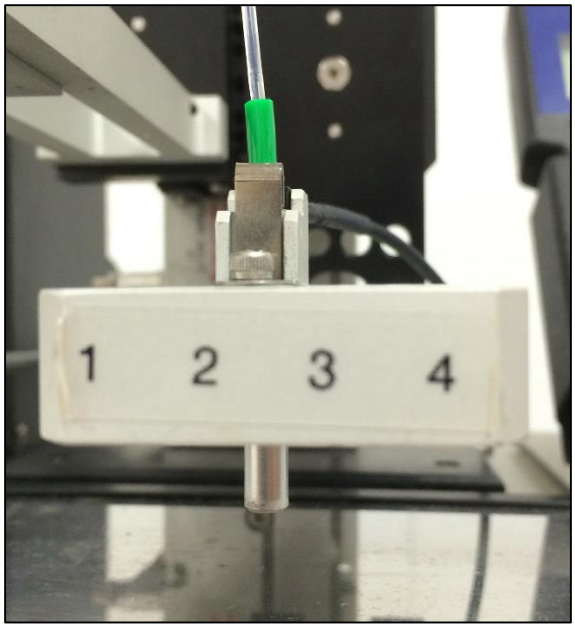

Figure 7. Photograph showing the BioJet dispenser.

2.3.2. Assembly of the Lateral Flow Biosensor

Once all the components are prepared the strips are put together using the LM5000 Clamshell. The plastic backing layer has a sticky surface that holds the sample pad, conjugate pad, nitrocellulose membrane and the absorption pad together. LM5000 clamshell is designed to assemble the lateral flow strip comprised of multiple components onto the adhesive backing layer. It consists of a top and bottom vacuum nets that hold the strip materials in place. Vacuum pressure is applied onto the lateral flow strips to ensure that all the components are stuck together and laminated. A pump is used to apply pressure of about 20 psi. Figure 8 shows the LM5000 clamshell used in this study.

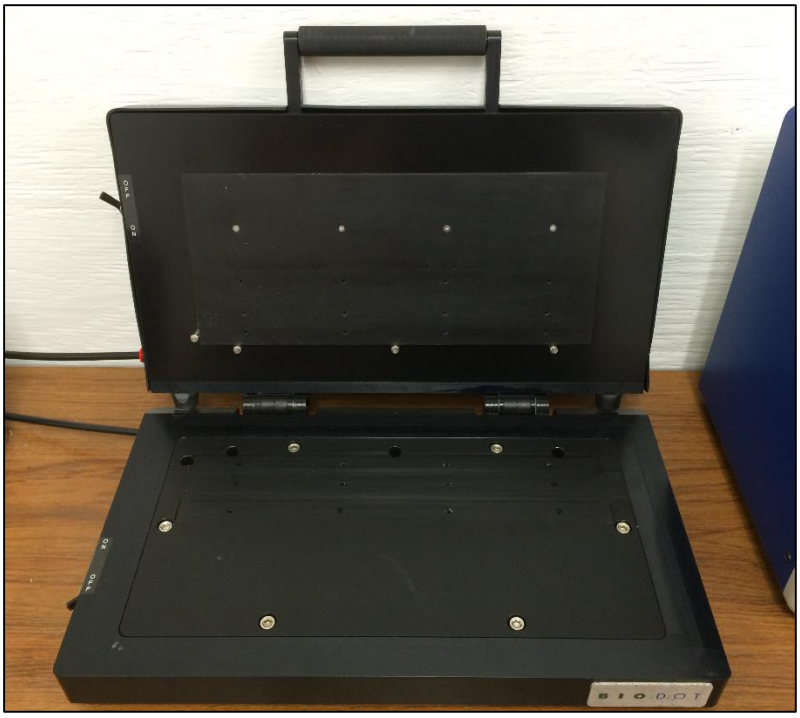

Figure 8. Image showing the LM5000 Clamshell.

2.3.3. Cutting the Lateral Flow Strips

Once all the components are assembled and the strips are vacuum laminated, the CM4000 Guillotine Cutter (figure 9) is used to cut the strips into 3mm x 50mm small lateral flow strips. The width of the strips can be controlled and the desired width can be cut using the cutter. The CM4000 is a fully automated cutter that provides high quality precision cuts. The blades are made from hardened steel, and specially coated for the ejection of cut strips, preventing glue build up. Cut widths and quantities are easily programmed through a hand held remote, which can also store several programs for future use.

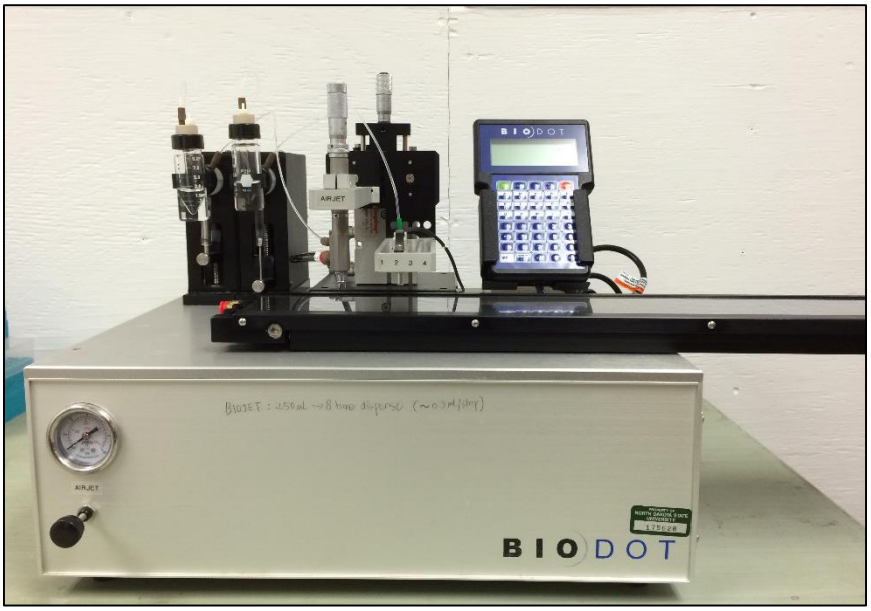

Figure 9. Image showing the CM4000 Guillotine Cutter.

2.4. Strip Reader

We used a DT1030 strip analyzer for the analysis of lateral flow strips after the assay was completed. Analyzer DT1030 is a sensitive image analyzer which reads the color intensity of the captured AUNPs on the test and control zone. The analyzer software was also used giving us the peak height, line distance and area integral depending on the intensity of the red line. Figure 10. Shows the strip reader along with an image taken using the software. Using the strip reader we performed many optimizations like the conjugate amount, aptamer concentration, etc. and also tested the analytical performance of the strips. The peak height and area increased with the increase in intensity of the red band corresponding to the concentration of the analyte being tested. The strip reader showed a good control signal with zero to negligible readings for plain strips during the control experiments.

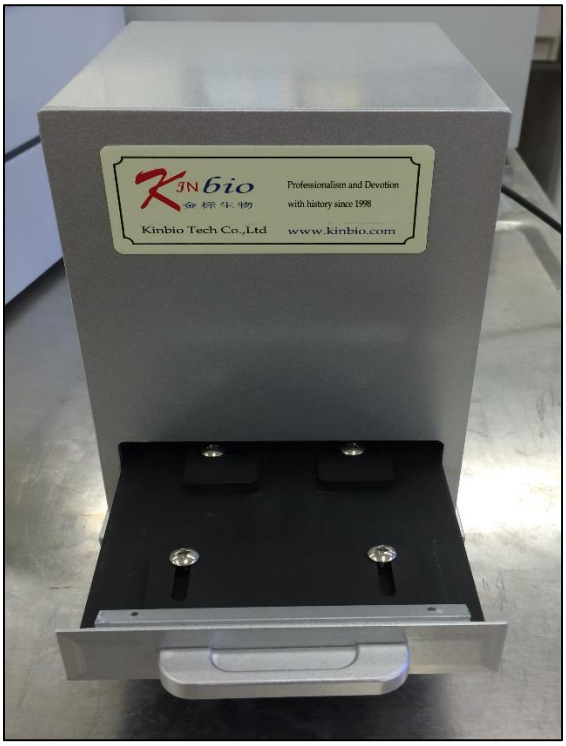

Figure 10. Photo image of the portable strip reader.

2.5. UV-Vis Spectroscopy

Absorption spectroscopy in the ultraviolet-visible region refers to Ultraviolet-visible spectroscopy (UV-Vis). UV-Vis measures the electronic transition from the ground state to the excited state. Fluorescence spectroscopy is opposite; it measures the electronic transition from the excited state to the ground state.[75]

In this study we use UV-Vis spectroscopy to measure the concentration of the CEA and MCF-7 cells in our sample solution. Figure 11 shows the absorbance readout for the detection of MCF-7 cells. As the number of cells increases, more HRP molecules trapped in the sandwich assay react with the substrate (TMB + Stopping solution), therefore giving higher absorbance readings at 450 nm. UV-Vis spectroscopy was used for various optimizations like, aptamer concentration, magnetic bead amount, HRP concentration and substrate amount. We also tested the assays for analytical performances like, specificity, reproducibility, interference, and calibration curve. A

good detection limit and an excellent dynamic linear range for the target analyte was achieved using the Cary 100 UV-Vis spectrophotometer shown in Figure 12.

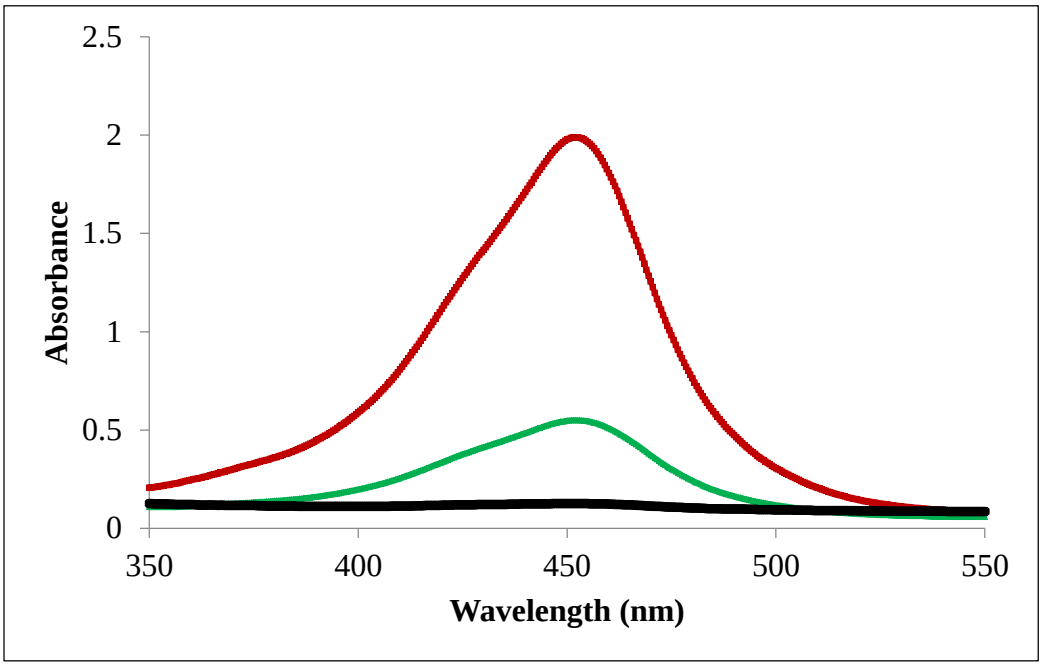

Figure 11. Graph showing the absorbance readings using the Cary 100 UV-Vis spectrophotometer.

Figure 12. Image showing the Cary 100 spectrophotometer.

2.6. Cell Culture

Growing cells under controlled optimal conditions, generally in an incubator is called cell culture. In this study, we cultured the MCF-7 breast cancer cells along with other cell lines like HeLA cells (CCL-2), CCRF-CEM (CCL-119) and A549 (CCL-185). Our target were the MUC1 proteins that are overexpressed on the MCF-7 cell surface in metastasis breast cancer. Other cell lines which were used as control cell lines were related to lung cancer and leukemia. Laminar flow hoods (Figure 13) at the Core Biology facility, NDSU were used for culturing the cells in a contaminant free environment. We successfully developed lateral flow biosensors and colorimetric assays for the detection of MCF-7 cells, distinguishing them from other control cell lines.

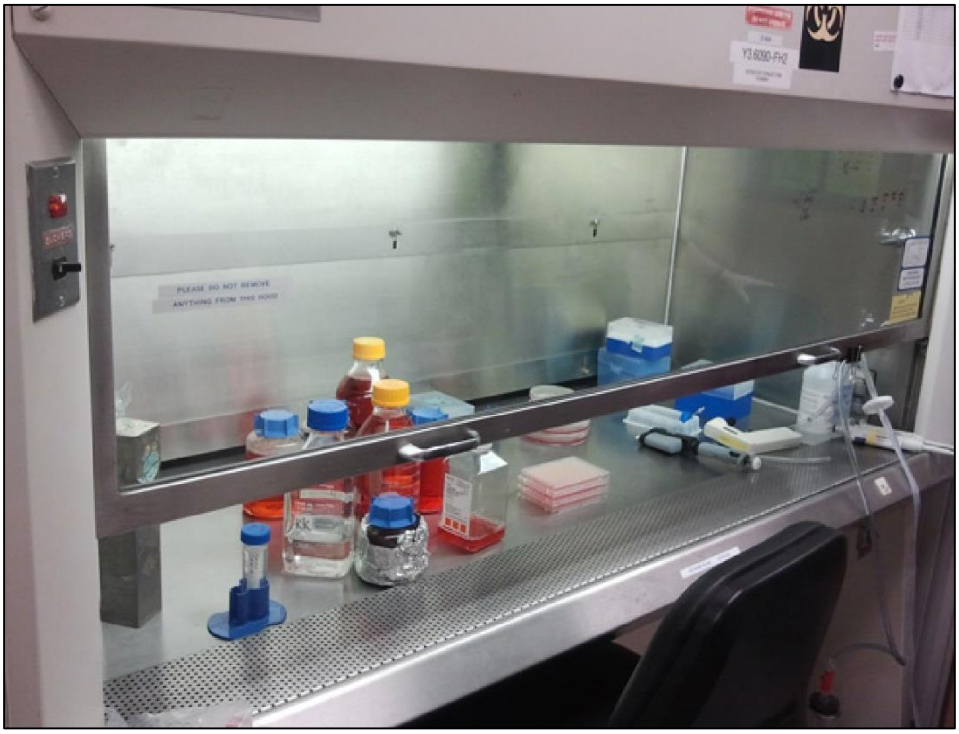

Figure 13. Image showing Laminar flow hood.

CHAPTER 3. AUNP-APTAMER BIOSENSORS FOR THE DETECTION OF THROMBIN AND PDGF-BB[1]

This chapter includes the development of a Lateral Flow Biosensor for the detection of multiple proteins. This project tests the high specific molecular recognition properties of aptamers for their respective targets, PDGF-BB and Thrombin. Taking advantage of the unique surface modification properties of AUNPs, different conjugation techniques are studied for the modification of thiolated aptamers on their surfaces. In addition, the lateral flow strips are also tested for analytical performances like reproducibility, interference, calibration curve and detection limit. We could clearly show that the aptamer functionalized AUNP were successfully incorporated with the lateral flow strips for the simultaneous detection of proteins.

Firstly, an introduction on the importance of detecting Thrombin and PDGF-BB, and why we need a low cost, fast, simple and accurate point-of-care detection method. It is followed by a discussion on the steps for manufacturing a lateral flow biosensor based on AUNPs and aptamers, along with the various optimizations performed to make the biosensors sensitive and selective for the protein targets. A combined result and discussion section about the analytical performance of the biosensor is presented next, followed by a summary of this study at the end.

---

[1] The material in this chapter was co-authored by Xun Mao, Hui Xu and Guodong Liu. Hui Xu first proved the working principle by using Thrombin as the detection Target. Guodong Liu and Xun Mao served as proofreaders and approved the statistical analysis of the results.

3.1. Introduction

The detection and quantification of extremely low concentration of proteins play an important role in the clinical application and research. Thrombin, a blood coagulant was one of the first targets used for the development of aptamers using SELEX. Thrombin plays an important role in thrombosis and hemostasis by catalyzing the conversion of fibrinogen to clottable fibrin.[80, 81] In healthy individuals, thrombin concentrations in blood are very low and in some are completely absent.[82-84] However, during the coagulation of blood, thrombin concentration spikes up to low-μM levels.[86, 87] Thrombin has been recognized as an important cancer biomarker. Therefore, the detection of thrombin in blood serum at sensitive low concentrations is important for the early detection and diagnosis of cancer patients.

PDGF is an important component for healing injuries and wounds. A stimulator of collagen via fibroblasts, PDGF is a potent mitogen contributing to tissue repair and recovery.[89] Diseases like cancer; atherosclerosis, etc. have been directly linked to elevated levels of PDGF in the human body.[90] Three basic isoforms of PDGF: PDGF-BB, PDGF-AA and PDGF-AB exist. PDGF-BB out of the three has been implicated in the tumor growth and progression.[91] In healthy individuals PDGF-BB is found in low or undetectable levels while a spike in PDGF-BB levels is seen in the presence of tumor, including sarcomas and glioblastomas.[92]

Fluorescence, radioimmunoassay, enzyme-linked immunosorbent assay and surface-enhanced Raman spectroscopy are the common techniques being currently used for protein detection.[94-96] Although these techniques are accurate, selective and sensitive, they suffer from drawbacks like; incorporation of radioactive substances, extra washing steps, time consuming experimental setup, sample pre-treatment, incubation and the need of technically expert scientists along with complicated instrumentation. Recently, lateral flow biosensors which combine

chromatography with conventional immunoassay have gained a lot of interest for protein detection and analysis. They provide a platform for protein detection with advantages like easy usability, short assay time, long-term stability, low cost and reproducible results. One excellent example of lateral flow biosensors are pregnancy strips.[97] Pregnancy tests rely on the detection of human chorionic gonadotropin (hCG). The hCG is present in the body after six to twelve days of fertilization. The detection of early pregnancy factors (EPF) is a faster method for the detection of pregnancy. EPF is present within a few hours of fertilization.[98] These pregnancy factors are biomarkers for the detection of pregnancy at a very early stage. Antibodies specific for these biomarkers are immobilized on nitrocellulose membranes and on AUNPs. The sandwich type hybridization captures the AUNPs on the nitrocellulose membrane indicating a red line in the presence of the target analyte, indicating pregnancy. Absence of the red line indicates a negative test result. The simple principle of sandwich type assay is used here to trap the biomarkers and indicators like AUNPs are used for the visual detection of the take home pregnancy tests. Other groups like, Sithigorngul et al. developed biosensors for the detection of pathogenic isolates and Shim et al. developed the atrazine detecting biosensor for testing in water samples from lakes and rivers.[127, 128] These scientists that have proven the concept of detecting biomarkers, molecules and other target analytes have shown that biosensors are sensitive, selective and reliable.

Even though antibody based biosensors have shown good sensitivity and selectivity for their targets, they face some problems related to antibodies.[98] Drawbacks like stability, storage, cross contamination, cross linking, false positives and many more make the antibody based biosensors costly to manufacture. Moreover, it takes about seven to fifteen years from the lab to the pharmacy and costs billions of dollars for the development of antibody based bisosensors.[99, 100] Now, aptamer based biosensors on the other hand do not suffer from all these drawbacks.

First discovered in 1990, these artificial nucleic acid ligands are well known for their sensitivity and specificity toward a particular target. Advantages like low cost of production, easy modification and high selectivity have created great interest in the research community for discovering unknown aptamers using SELEX.[1, 2] Researchers spend several years studying the binding sites of antibody and antigens before moving onto the drug discovery phase. One major advantage of using aptamers is that it is unnecessary to know the exact binding site of the aptamer to the target. Therefore, drug discovery and development phase does not take several years. Another advantage is the availability of automated synthesizers. These automated synthesizers enable on demand chemical based production of aptamers once the sequence is discovered for a particular antigen, using SELEX.[99] The production of the antibody equivalent on the other hand is far more complex, costly and time consuming. Aptamer modification using the inverted thymidine, polyethylene glycol (PEG), 2'-O-methyl, biotin or fluorescent tags broaden the applications for aptamer based biosensors. Antibody modifications are again, costly and time consuming.[100]

In this study we have incorporated the lateral flow biosensors with aptamers and AUNPs, taking advantage of all the positive aspects of each component and developing a lateral flow biosensor which can simultaneously detect Thrombin and PDGF-BB.

3.2. Material and Methods

The following reagents and materials were used in the development of the lateral flow biosensor: The AirJet AJQ 3000 dispenser, BioJet BJQ 3000 dispenser, clamshell laminator and the guillotine cutting module CM 4000 were from Biodot LTD (Irvine, CA). The Portable strip reader, DT1030, was purchased from Shanghai Aubio Tech. Co., LTD (Shanghai, China). Streptavidin from Streptomyces avidinii, dithiothreitol (DTT), triethylamine (TEA), ethyl acetate, $Na_3PO_4 \cdot 12H_2O$, $HAuCl_4$, trisodium citrate, sucrose, Tween 20, Triton X-100, sodium chloride-

sodium citrate (SSC) buffer (pH 7.0), phosphate buffer saline (PBS, PH 7.4, 0.01 M), bovine serum albumin (BSA), human serum albumin (HSA) thrombin (from human plasma) and PDGF-BB were purchased from Sigma-Aldrich. Glass fibers (GFCP000800), cellulose fiber sample pads (CFSP001700), laminated cards (HF000MC100) and nitrocellulose membranes (HFB24004) were provided by Millipore (Bedford, MA). The serum, aptamers and oligonucleotide probes used in this study were obtained from Integrated DNA Technologies, Inc. (Coralville, IA) and have the following sequences:

Primary Aptamer for Thrombin: 5′-/5ThioMC6-D/TT TTT TTT TTT TTT TTT TTT GGT TGG TGT GGT TGG-3′

Secondary Aptamer for Thrombin: 5′-AGT CCG TGG TAG GGC AGG TTG GGG TGA CT-/3BioTEG/-3′

Primary Aptamer for PDGF-BB: 5′-/5ThioMC6-D/TAC TCA GGG CAC TGC AAG CAA TTG TGG TCC CAA TGG GCT GAG TAT -3′

Secondary Aptamer for PDGF-BB: 5′- TAC TCA GGG CAC TGC AAG CAA TTG TGG TCC CAA TGG GCT GAG TA/3BioTEG/ -3′

DNA oligonucleotide (control probe): 5′-ATA CTC AGC CAA TTG GGA CCA CAA TTG CTT GCA GTG CCC TGA GTA AAA AAA AAA AAA AAA AAA AA-biotin-3′

All buffer solutions were prepared using ultrapure (>18MΩ cm) water from a Millipore Milli-Q water purification system (Billerica, MA).

3.2.1. Preparation of AUNP-Aptamer Conjugates

For this study AUNP were prepared using the citrate reduction method mentioned in the experimental section, 15 ± 3 nm sized nanoparticles were chosen as they showed good stability with no aggregation while adding salts to the conjugate. Roughly 40-50 aptamers were labeled

onto each AUNP. Conjugates were prepared using method 1 mentioned in the experimental section. Different approaches were tested for conjugate preparation. First, a five-fold concentrated AUNP solution was prepared by centrifuging five 1 mL portions of AUNP at 12,000 rpm for 12 minutes. After centrifugation the AUNP being heavier formed a pellet at the bottom of each tube, leaving a transparent water solution as the supernatant. After discarding the supernatant the AUNP pellets were collected from each tube and concentrated into one tube with a final volume of 1 mL using nuclease free water.

Two approaches were studied for the preparation of the AUNP conjugates. Since we had two thiolated aptamers (one specific for Thrombin and the other specific for PDGF), the 1st approach was to add equal amounts of thiolated aptamers for each target to the same five-fold AUNP solution for conjugation. Briefly, 2.0 OD concentrations of the primary thiolated aptamer for both PDGF and thrombin were activated using TEA and DTT, excess DTT was removed by extraction using ethyl acetate solution. Both the activated primary thiolated aptamers were added in equal ratios to the five-fold AUNPs and kept at 4˚ C for 24 hours. Salts were then added for aging and stabilizing the AUNP-Aptamer (PDGF and Thrombin aptamers) conjugates. After incubating the conjugates for another 24 hours, excess unbound aptamers were removed via washing the conjugates three times using PBS. The conjugates after the final wash were re-dispersed in 1 mL of the eluent buffer (20 mM $Na_3PO_4 \cdot 12H_2O$, 5% BSA, 0.25% Tween 20, and 10% sucrose).

The 2nd approach was to make the AUNP-aptamer conjugates separately for each primary thiolated aptamer, then mixing equal volumes of the AUNP-aptamer conjugate for thrombin and the AUNP-aptamer conjugate for PDGF at the end. Briefly, two separate five-fold AUNP solution were prepared. Activated primary thiolated aptamers for PDGF and Thrombin were added into

separate five-fold AUNP solutions. Once the conjugation procedure was complete we combined the two conjugates giving us a mixture of AUNP-aptamer (thrombin) and AUNP-aptamer (PDGF) in the same tube.

3.2.2. Preparation of Aptamer-Based Lateral Strip Biosensor

The lateral strip biosensor has five main components: sample pad, conjugate pad, nitrocellulose membrane, absorption pad and the plastic backing layer. For this study the strips were prepared for the multiple detection of proteins i.e. Thrombin and PDGF-BB. We dispensed two test zones on the nitrocellulose membrane, one for capturing PDGF-BB and the other for capturing Thrombin. A control zone was also dispensed to check the working of the biosensor and the quality of the conjugates. Sample pads were pretreated with a buffer (pH 8.0) containing 0.25% Triton X-100, 0.05 M Tris-HCl, and 0.15 mM NaCl. This was done to ensure the proper movement of the analytes onto the conjugate pad. AUNP-Aptamer conjugate mixture for PDGF-BB and Thrombin was dispensed onto the glass fiber conjugate pad. AirJet dispenser was used for dispensing, we also optimizing the dispensing times onto the conjugate pad. The dispensed conjugate pads were then dried for 1h at 37 °C and stored at 4 °C until further use.

For the nitrocellulose membrane, we first prepared the secondary biotinylated aptamer conjugated with streptavidin for immobilization onto the membrane. Briefly, 50 nmoles of the secondary biotinylated aptamer for PDGF-BB was mixed with 250 µL of 2mg/mL streptavidin. After incubating it for 1h at RT, 400 µL of PBS was added for the washing step. Excess unbound biotinylated aptamer was removed by centrifugation for 20 minutes with a millipore filter (cutoff 30,000 D) at 6000 rpm. The conjugates were washed twice again and finally diluted to a volume of 500 µL with PBS. Following the same procedure, the biotinylated secondary aptamer for thrombin was used to prepare the streptavidin-biotinylated aptamer conjugate. Using the BioJet

dispenser both the streptavidin-biotinylated aptamer conjugates were dispensed onto the nitrocellulose membrane. The distance between each zones was around 0.2 cm and there were a total of three zones on the biosensor (test zone 1: PDGF-BB, Test zone 2: Thrombin and control zone). The control zone was a biotinylated DNA probe complementary to the primary PDGF aptamer, prepared using the same technique as above. After dispensing the nitrocellulose membrane was dried at RT for 1h and stored at 4 ˚C.

A plastic backing layer was used to assemble all the components together, using a clamshell laminator. All the membranes overlapped each other by 2mm, which made the migration of solution from one pad to the other fluent and smooth during the assay. Biosensors with a width of 3 mm were cut using the guillotine cutting module CM 4000.

3.2.3. Assay Procedure

A total volume of 80 μL, with the desired concentration of PDGF-BB and Thrombin in running buffer (PBST containing 1%BSA) was added onto the sample application pad. The solution through capillary action then migrated onto the conjugate pad, where the AUNP-aptamer conjugates captured their specific targets. The AUNP-aptamer-target complex then migrated onto the nitrocellulose membrane where they were captured by the Biotinylated aptamers on the test zones. The biosensor was washed with 15 μL buffer (PBST containing 1%BSA), two times at intervals of 5 minutes each. The test zones and the control zone were evaluated visually within 10 min. For the quantitative measurements, the optical intensity of the red band was observed using the portable "strip reader" combined with the "AuBio strip reader" software. For the detection of PDGF-BB and Thrombin in complex biological matrixes, 15 μL of plasma spiked with different quantities of PDGF-BB and Thrombin was tested on the biosensor. The solutions were made using

PBST (1%BSA) with a total volume of 80 μL. Results were obtained by recording the optical responses with the strip reader after 10 min of assay time.

3.3. Results and Discussion

Figure 14 shows the biosensor with its four major components: sample pad, conjugate pad, nitrocellulose membrane, and absorption pad. All these four sub- pads are mounted on a common backing layer (typically, an inert plastic, e.g., polyester). PDGF-BB and Thrombin were used as model targets to demonstrate the working principle of the lateral flow strips. The test zones dispensed using the BioJet dispenser, consisted of the biotinylated aptamers specific for their respective targets while the control zone consisted of the biotinylated control probe complementary to the PDGF and thrombin aptamer. The primary biotinylated aptamers for PDGF-BB and Thrombin were conjugated with AUNPs and dispensed on the conjugate pad using the AirJet dispenser.

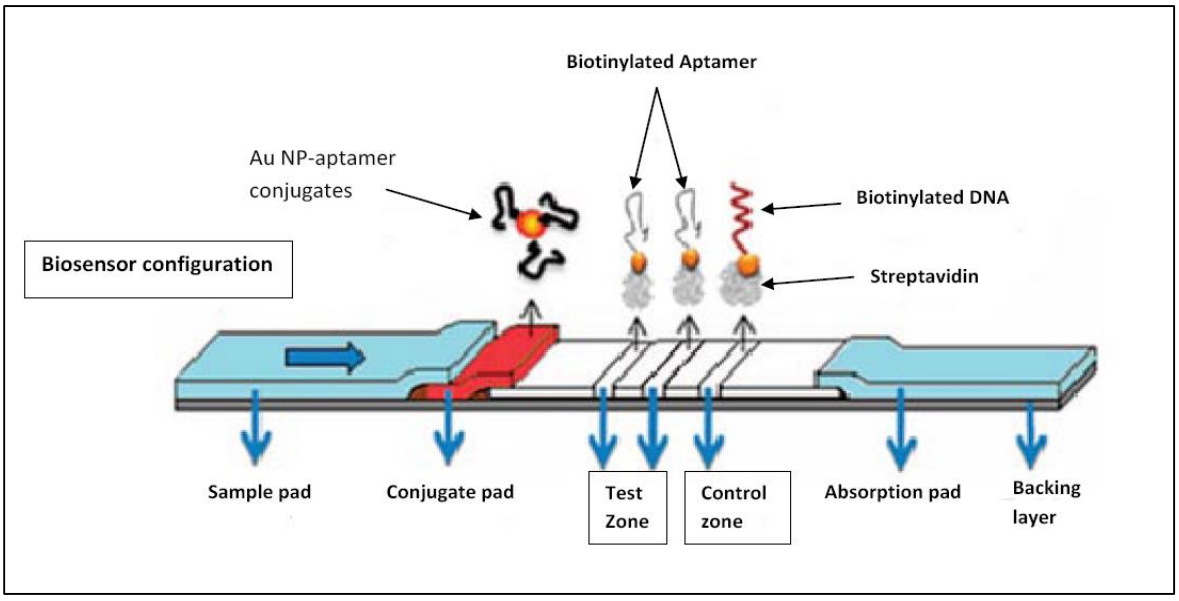

Figure 14. Schematic representation of the biosensor.

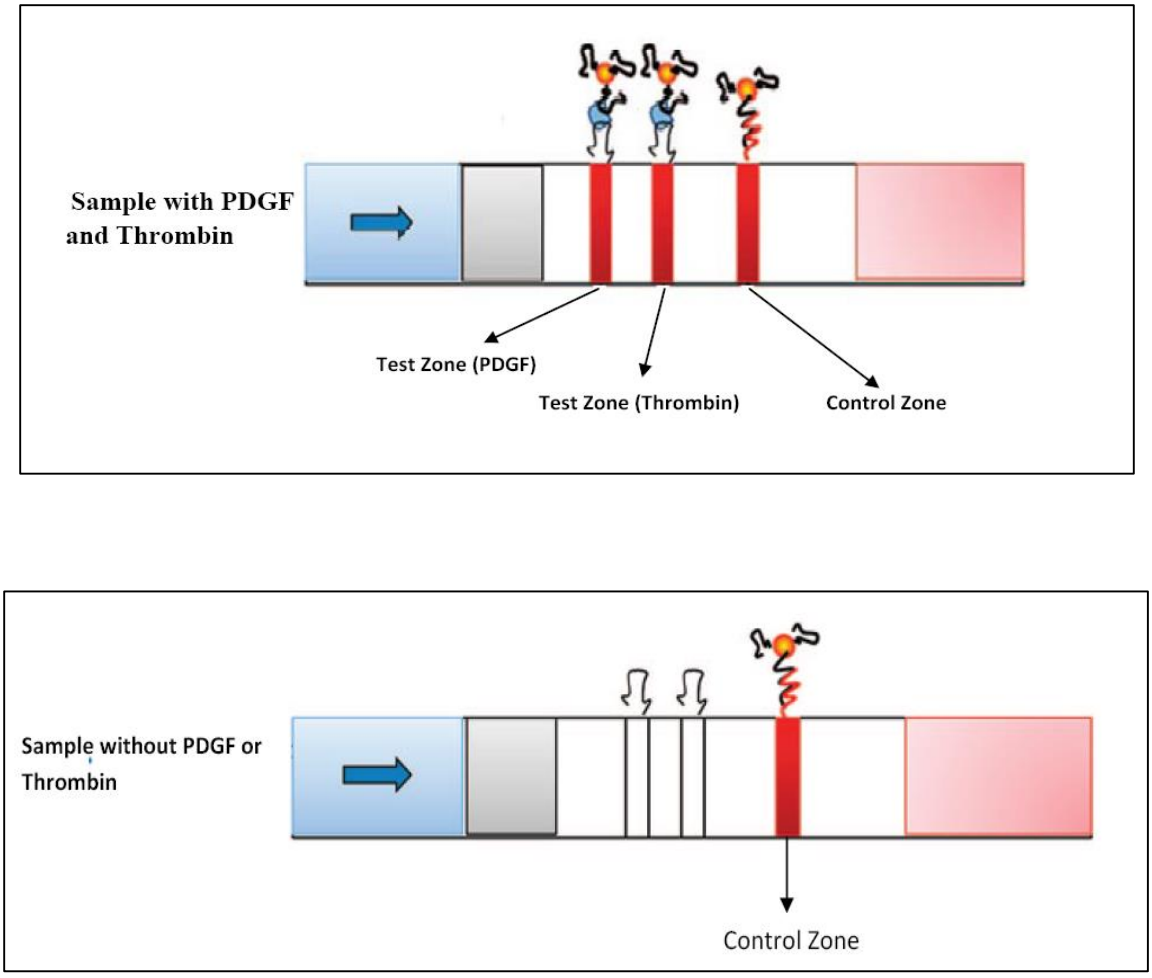

Figure 15. Schematic representations showing the qualitative detection with the LFS.

Figure 15 shows the working principle of the lateral flow strips. Briefly, 80 µL buffer solution (PBST with 1%BSA) containing the desired concentration of PDGF-BB and Thrombin were loaded onto the sample pad. The solution which migrates due to the capillary action moves onto the conjugate pad, coming in contact with the AUNP-aptamer conjugates. The aptamers being specific for the targets (PDGF and Thrombin) capture them onto the AUNP-aptamer complex forming the AUNP-aptamer-target complex. The solution then moves onto the test zones where the biotinylated secondary aptamers bind their respective targets, immobilizing the whole AUNP-aptamer-target complex on the nitrocellulose membrane. AUNPs trapped on the test zone via the sandwich type hybridization gives the two red bands in the presence of both the targets. The excess

AUNP-aptamer conjugates were captured on the control zone via the hybridization between the control DNA probes (which were pre-immobilized on the control zone) and the primary aptamers, thus forming a third red band. In the absence of PDGF-BB and Thrombin the red band is observed only on the control zone, indicating that the biosensor is working properly. For the control zone we designed a sequence which was complementary to both the primary aptamer sequences of PDGF-BB and Thrombin. The first part of the sequence is complementary to the PDGF-BB primary aptamer while the second part is complementary to the Thrombin primary aptamer. Qualitative analysis is simply performed by observing the red color on the test zone, and quantitative analysis is measured by reading the optical intensities of the red bands with a portable strip reader (figure 16). The peak area is proportional to the amount of the captured AUNPs on the test zone, which is proportional to the concentration of PDGF-BB and Thrombin in the sample solution.

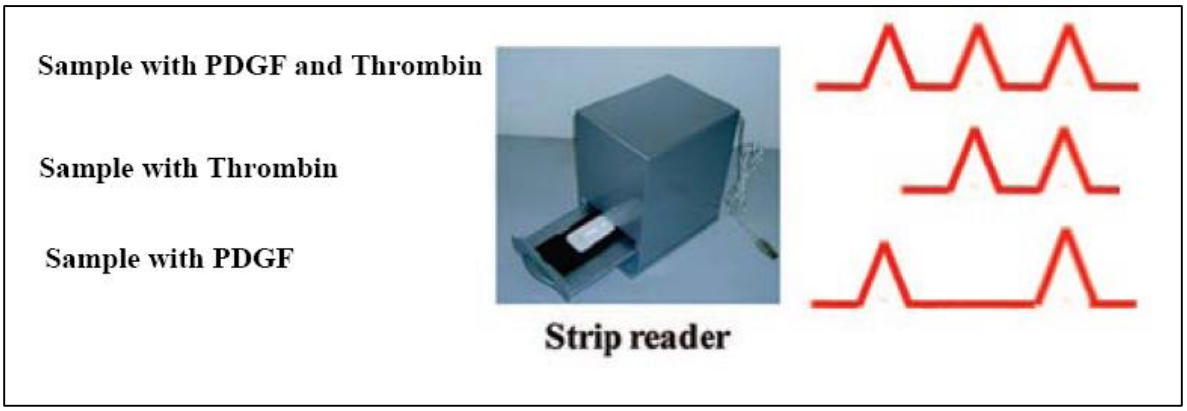

Figure 16. Schematic representation of the Portable strip reader showing the signal output.

The lateral flow strips were also tested for interference with other components like IgG, IgM, Casein, HSA, and their mixtures with PDGF-BB and Thrombin. There was no interference from these components showing that the biosensor is specific and sensitive only for PDGF-BB and Thrombin. Figure 17 shows the photo images and the responses recorded using a portable strip

reader. It indicates that the biosensor is selective and PDGF-BB or Thrombin do not cause interference for each other. Therefore, can be detected on the same biosensor individually. Two red lines (one for test zone and one for the control) were observed when PDGF-BB or Thrombin was present along with the interference component while three red lines were observed (two for test zones and one for control zone) when both PDGF-BB and Thrombin were present in the target solution with the interference components.

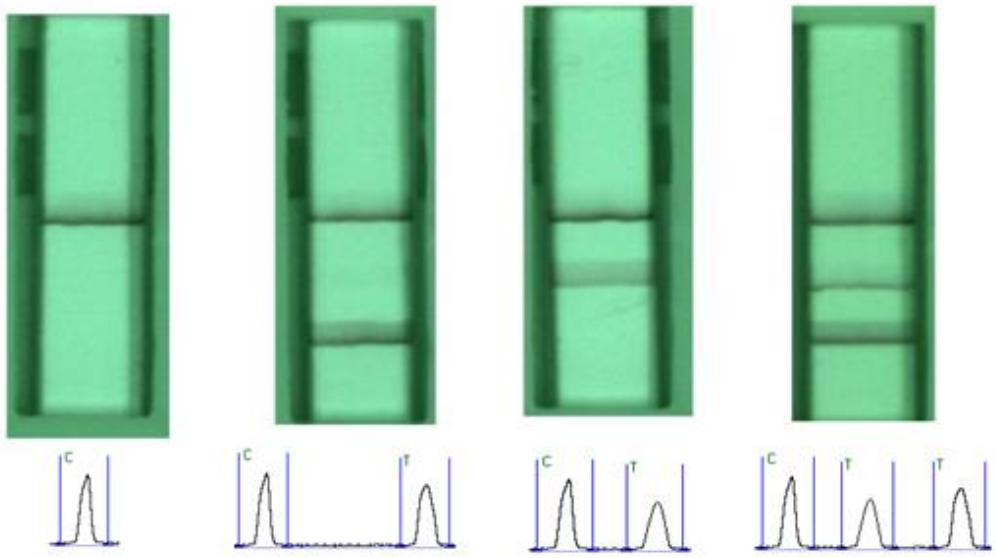

Figure 17. Photo images and responses from the strip reader.

3.4. Optimization of Parameters

To obtain the best results, the analytical parameters including the components of the running buffers, dispensing cycles of the AUNP-aptamer conjugates and the amount of capturing secondary aptamers on the test zones were optimized. The amount of AUNP-aptamer conjugates loaded on the conjugate pad affects the intensities of both test and control zones greatly. It was determined by the dispensing volume of the conjugate solutions on the conjugate pad. The histogram of the Peak Area for thrombin and PDGF-BB is shown in Figure 18. The Signal was

found to be the highest for dispensing the AUNP-aptamer conjugates (PDGF and Thrombin) four times on the conjugate pad. The decrease in signal with more dispensing cycles is ascribed to the increased background signal. Therefore, dispensing four times, was selected as the optimal dispensing time in this study.

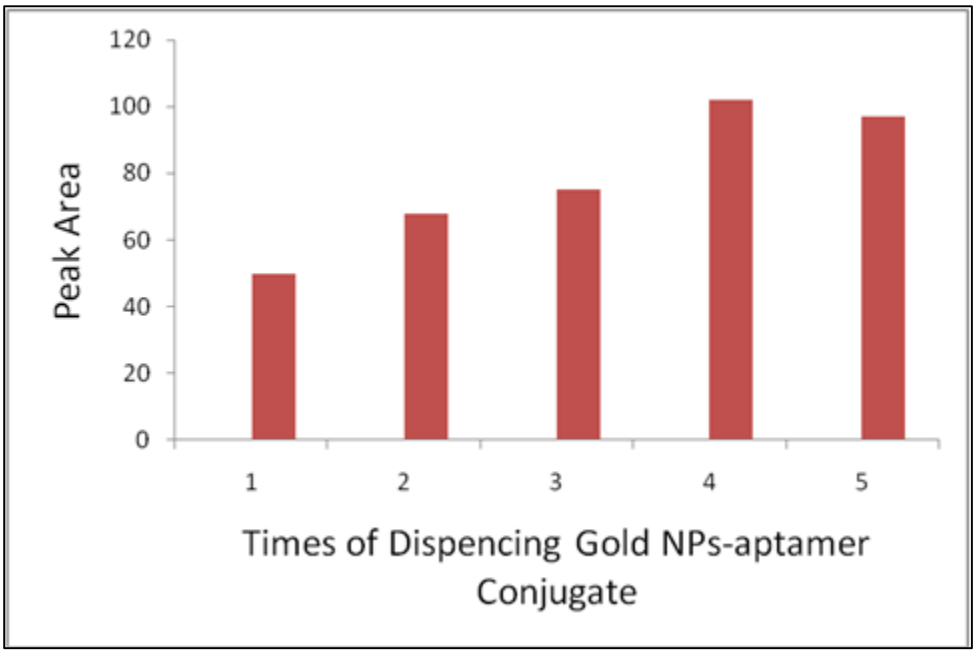

Figure 18: Image showing optimization for amount of AUNP-aptamer conjugates.

The biosensor is also sensitive towards the amount of secondary immobilized on the test zones. Figures 19A and 19B indicate that the signal of the biosensor increased with an increase of the secondary aptamer concentration from 1 OD/mL to 4 OD/mL for PDGF-BB and Thrombin respectively. After 4 OD/mL the Signal saturated and gave almost the same readings. Thus, an aptamer concentration of 4 OD/mL was used to prepare both the test zones of PDGF-BB and Thrombin.

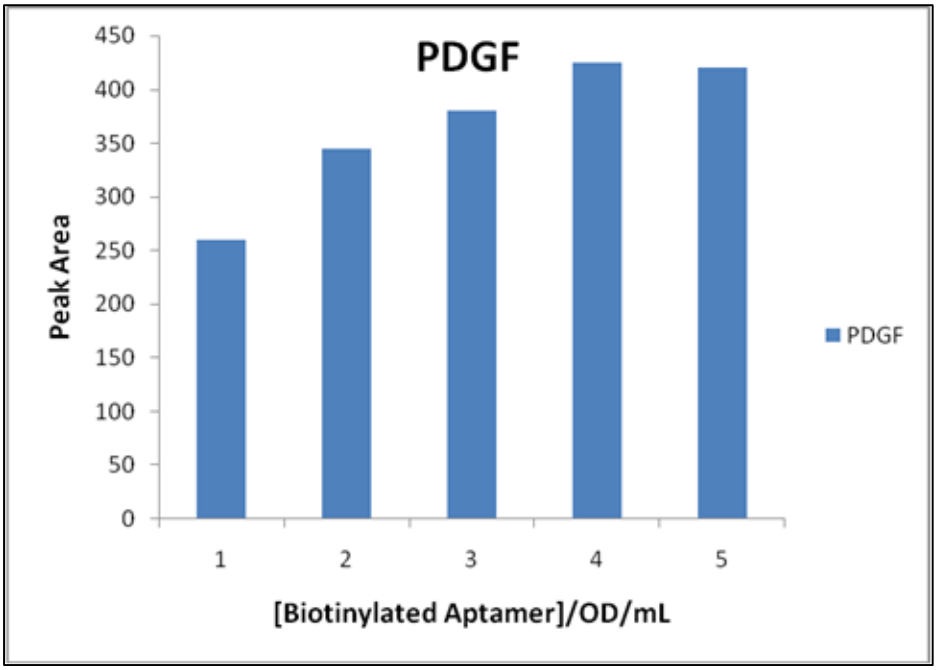

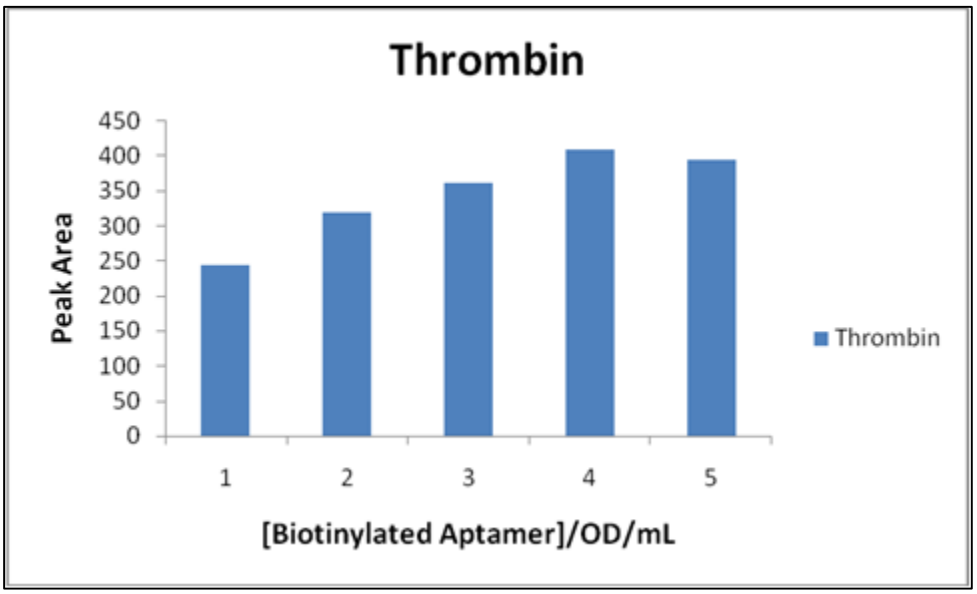

Figure 19. Images showing the optimization for the biotinylated aptamer concentration.

Buffers play an important part in the development of an assay. Four kinds of buffers are used for the fabrication and assay on the biosensor. (A) 0.05M Tris-HCl buffer containing 0.25% Triton X-100, 5% tween and 0.15 M NaCl (pH 8.0) was used to saturate the sample pad. This treatment facilitates the transportation and reduces the amount of PDGF-BB and Thrombin trapped

on the sample pad. (B) A buffer containing 20 mM Na_3PO_4, 5% BSA, 0.25% Tween, and 10% sucrose was used to disperse the pellets of the AUNP-aptamer conjugates (both PDGF-BB and Thrombin). This buffer stabilizes the nanoparticles, reduces the nonspecific adsorption of conjugates on the nitrocellulose pad and facilitates the release of the conjugates from the conjugate pad. (C) PBS (0.01 M, pH 7.4) was used to prepare the streptavidin-biotinylated aptamer solution. (D) The composition of the running buffer has a significant effect on the performance of the biosensor. Several buffers, including Tris-HCL, PBS, 1/15 SSC, 1/15 SSC (1% BSA), PBS (1% BSA), PBST, and PBST (1% BSA) were tested on the biosensor. While SSC, PBS and PBST showed good response, the best performance (signal) of the lateral flow strips was observed with the PBST (1% BSA) (Figure 20). Therefore, PBST (1% BSA) was chosen as the optimal buffer for this study.

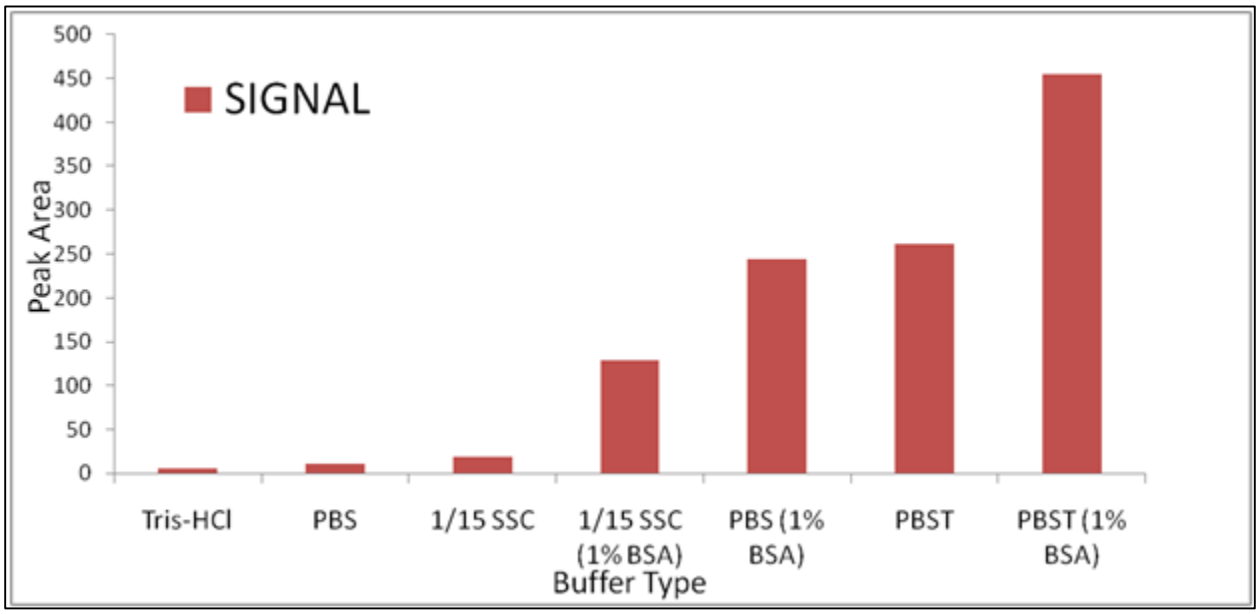

Figure 20. Optimization for running buffers.

3.5. Analytical Performance

To investigate whether the biosensor could provide quantitative detection of PDGF-BB and Thrombin, different concentrations of targets were tested on the biosensor. The intensities of the test zones were measured and plotted as a function of different concentrations of PDGF-BB and Thrombin (figure 21). Well-defined peak areas were observed for each concentration of the target. As the concentration of the target analytes increased in the sample solution, the peak area increased showing a linear relationship between the target and the signal intensity. Using the lateral flow strips a detection limit of 1 nM for PDGF-BB and 1.5 nM for Thrombin was determined. The useful analytical range extended from 2 nM to 200 nM (figure 22A and 22B), while a plateau was observed above 200 nM for the peak intensity of both the targets.

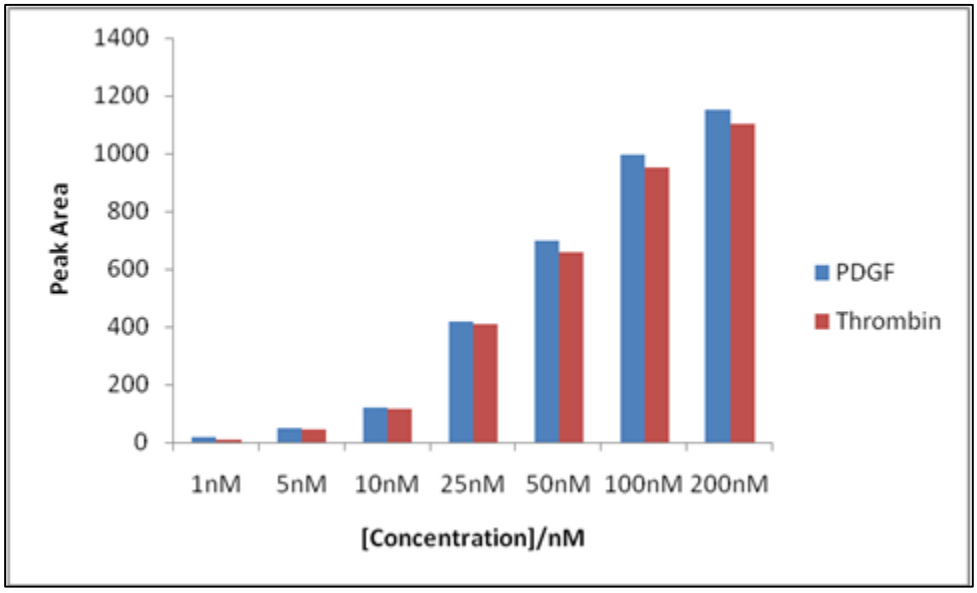

Figure 21. Graph for the different concentrations of PDGF-BB and Thrombin.

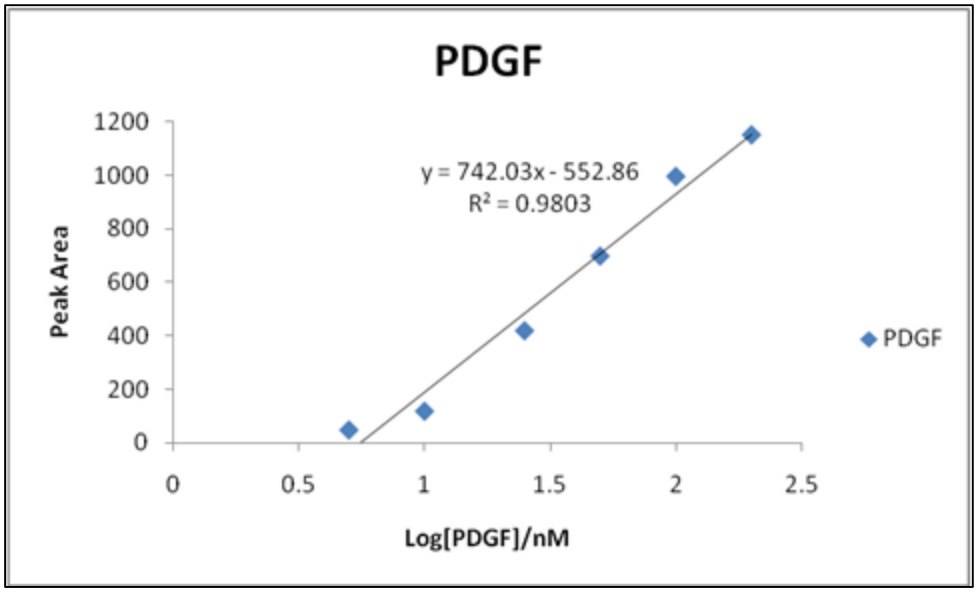

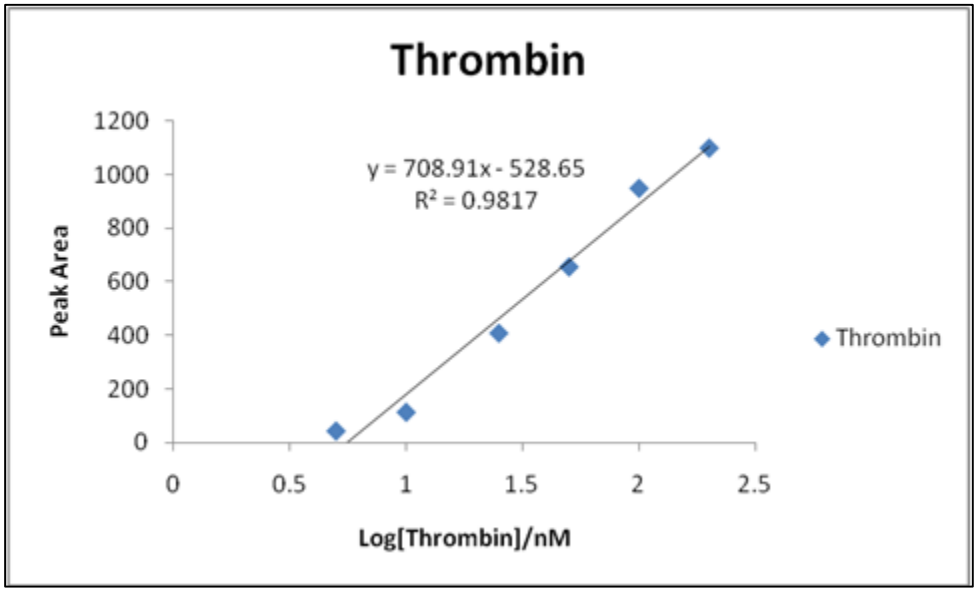

Figure 22. Calibration curves for the detection of PDGF and Thrombin.

Since quantitative analysis relies on the stability of the analyte signal and reproducibility of the assay, six different biosensors were tested with 25 nM concentrations of PDGF-BB and Thrombin to determine the reproducibility of the biosensor. The relative standard deviation (RSD) for PDGF-BB and Thrombin were 8.9% and 8.6%, respectively.

3.6. Conclusion

In this study, a lateral flow biosensor based on the gold nanoparticle-aptamer conjugates was developed for the multiple detection of proteins. PDGF-BB and Thrombin along with two pairs of aptamers, each specific for its particular target were used to show the working principle of the biosensor. Under optimal conditions, a linear dynamic relationship between the peak area and the concentration of the target analytes was observed giving us a detection range of 2 nM to 200 nM. The detection limit was determined to be 1 nM for PDGF-BB and 1.5 nM for thrombin, which is below the cut-off values for healthy subjects. The biosensor developed in this study is also capable of detecting the two targets (PGDF-BB and Thrombin) in human plasma samples with a detection limit of 1 nM for PDGF-BB and 2 nM for Thrombin. Other proteins like HSA, casein, IgG, and IgM did not cause any interference, nor showed any background signal, proving that the biosensor is selective and sensitive particularly for the two protein biomarkers. The lateral flow biosensor shows great promise for the development of aptamer-based dry-reagent strip biosensors for point-of-care or infield detection of proteins.

The promising results shown with the development of the lateral flow biosensors, detecting PDGF-BB and Thrombin successfully has been the main motivation for the next study. The PDGF-BB is expressed at undetectable levels in normal cells, but is found to be the overexpressed in some human tumors. To study the progression of the tumor it is important to detected PDGF-BB at even lower levels compared to the standard cut-off value. The next chapter includes the study for making the detection of PDGF-BB even more sensitive, using signal amplification techniques.

CHAPTER 4. AUNP-APTAMER-HRP FOR THE ULTRASENSITIVE DETECTION OF PDGF-BB[2]

This chapter focuses on the development of a lateral flow biosensor incorporating signal amplification for the ultrasensitive detection of PDGF-BB. This project tests the high specific molecular recognition properties of aptamers along with the signal amplification capabilities of the enzyme, Horseradish Peroxidase (HRP). We optimized various different conjugation techniques for the dual modification of AUNP surfaces with aptamers and HRP molecules. This study shows that the dual labeled AUNPs were successfully used to detect and amplify the signal, reducing the detection limit and therefore increasing the sensitivity of the lateral flow biosensors for PDGF-BB detection.

4.1. Introduction

Cell growth and cell division are regulated by Growth factors known as PDGF. PDGF-BB and PDGFR-β help in angiogenesis which is the formation of new blood vessels. Uncontrolled angiogenesis is one of the leading causes for canner.[101] Usually PDGF is expressed at undetectable or very low levels in the human body. But, in cancer patients PDGF is overexpressed and seen in higher concentrations in the blood stream. PDGF have directly been correlated to breast cancer, lung cancer, esophageal cancer and colorectal cancer.[102]

---

[2] The material in this chapter was co-authored by Xun Mao, Hui Xu and Guodong Liu. Hui Xu first proved the working principle by using Thrombin as the detection Target. Guodong Liu and Xun Mao served as proofreaders and approved the statistical analysis of the results.

The detection of PDGF was shown in the previous chapter, proving the concept of lateral flow biosensors based on AUNP aptamers. A sensitive detection limit of 1 nM for PDGF was achieved, although sensitive we aim to make the lateral flow biosensors even more sensitive by amplifying the detection signal using HRP.

HRP, a 44 kDa glycoprotein can be conjugated or labelled to AUNPs via the 6 lysine reside. In reaction with substrates like TMB, DAB and AEC, HRP is known to amplifying the detectable signal, increasing the sensitivity of the assay.[104-106] Hydrogen peroxide is used as the oxidizing agent, yielding detectable characteristic change in color, electrochemical signal and fluorescence, depending on the type of assay being used. Western blot is one such technique that uses antibodies labelled with HRPs to amplify the detection signal.[107] The antibody specifically binds to the target antigen, while the HRP in reaction with its substrate and hydrogen peroxide produces a detectable signal.[108] Other techniques like ELISA, chemiluminescence based detection and Immunohistochemistry are also know for the use of HRP for protein detection.[109] Small size, low cost of manufacturing, and stability are some of the advantages that make HRP an ideal molecule for target detection and signal enhancement. The signal amplification properties of HRP is also used in Enhanced chemiluminescence (ECL) to enhance the emitted light up to 1000 folds. HRP is catalyzed by the oxidation of luminol to 3-aminophralate emitting light at 428 nm. In presence of p-idophenol, the intensity is amplifies 1000 folds increasing the sensitivity of the assay.[110-113]

4.2. Materials and Methods

The following equipment and reagents were used in this study: The Airjet AJQ 3000 dispenser, Biojet BJQ 3000 dispenser, clamshell laminator and the guillotine cutting module CM 4000 were bought from Biodot LTD (Irvine, CA). The Portable strip reader, DT1030, was purchased from Shanghai Aubio Tech. Co., LTD (Shanghai, China). Horseradish peroxidase

(HRP), human serum albumin (HSA), Streptavidin from Streptomyces avidin, ethyl acetate, AEC, Sodium acetate, hydrogen peroxide, $Na_3PO_4 \cdot 12H_2O$, $HAuCl_4$, trisodium citrate, sucrose, Tween 20, Triton X-100, sodium chloride-sodium citrate (SSC) buffer (pH 7.0), phosphate buffer saline (PBS, PH 7.4, 0.01 M), bovine serum albumin (BSA), and PDGF-BB were purchased from Sigma-Aldrich. Glass fibers (GFCP000800), cellulose fiber sample pads (CFSP001700), laminated cards (HF000MC100) and nitrocellulose membranes (HFB24004) were provided by Millipore (Bedford, MA). The serum, aptamers and oligonucleotide probe used in this study were obtained from Integrated DNA Technologies, Inc. (Coralville, IA) and have the following sequences:

Primary Aptamer for PDGF-BB: 5′-/5ThioMC6-D/TAC TCA GGG CAC TGC AAG CAA TTG TGG TCC CAA TGG GCT GAG TAT -3′

Secondary Aptamer for PDGF-BB: 5′- TAC TCA GGG CAC TGC AAG CAA TTG TGG TCC CAA TGG GCT GAG TA/3BioTEG/ -3′

DNA oligonucleotide (control probe): 5′-/ 5Biosg/ ATA CTC AGC CCA TTG GGA CCA CAA TTG CTT GCA GTG CCC TGA GTA- 3′

All buffer solutions were prepared using ultrapure (>18MΩ cm) water from a Millipore Milli-Q water purification system (Billerica, MA).

4.2.1. Preparation of AUNP-Aptamer-HRP Conjugates

For the preparation of dual labeled AUNPs, we experimented with several techniques. The best method showing stable conjugates and good amplification required the monitoring of pH and a proper sequence for the addition of various components. Method 1: Briefly, thiolated aptamer 4 OD (primary aptamer) for PDGF-BB was added to a 1 mL portion of 5-fold concentrated AUNP solution. After incubating it for 24 h, the pH of the solution was adjusted to 9.0 and HRP 10 mg/ml

was added to the AUNP-aptamer solution which was kept at 4 ˚C for another 3 hours. The solution was then aged with 20 μL 1% SDS (incubation for 15 minutes) and 75 μL NaCl 2M which was added slowly to prevent aggregation of the AUNPs. The AUNP-aptamer-HRP conjugates were incubated for another 24 h at 4 °C, followed by centrifugation for 20 min at 12 000 rpm to remove the excess reagents along with the unbound aptamers and HRP molecules. After discarding the supernatant, the red pellets were washed twice with PBS and re-dispersed in 1 mL of an aqueous solution containing 20 mM $Na_3PO_4 \cdot 12H_2O$, 5% BSA, 0.25% Tween 20, and 10% sucrose. The conjugates were then stored at 4 °C until further use.

We also tried a number of other methods which included adding the HRP molecules to the 5-fold AUNPs before the thiolated primary aptamers (method 2). Although this method showed a response for the detection of PDGF, the conjugates could not amplify the signal, indicating that the HRP molecules were not labelled successfully (figure 23). Also the sensitivity of the conjugates were not good compared to the method illustrated above. Adjusting the pH, before adding the HRP molecules is another factor important for the production of sensitive and stable conjugates. Different pH settings were tried and optimized, pH 9 showed the best sensitivity and amplification for the detection of PDGF-BB, shown in figure 24.

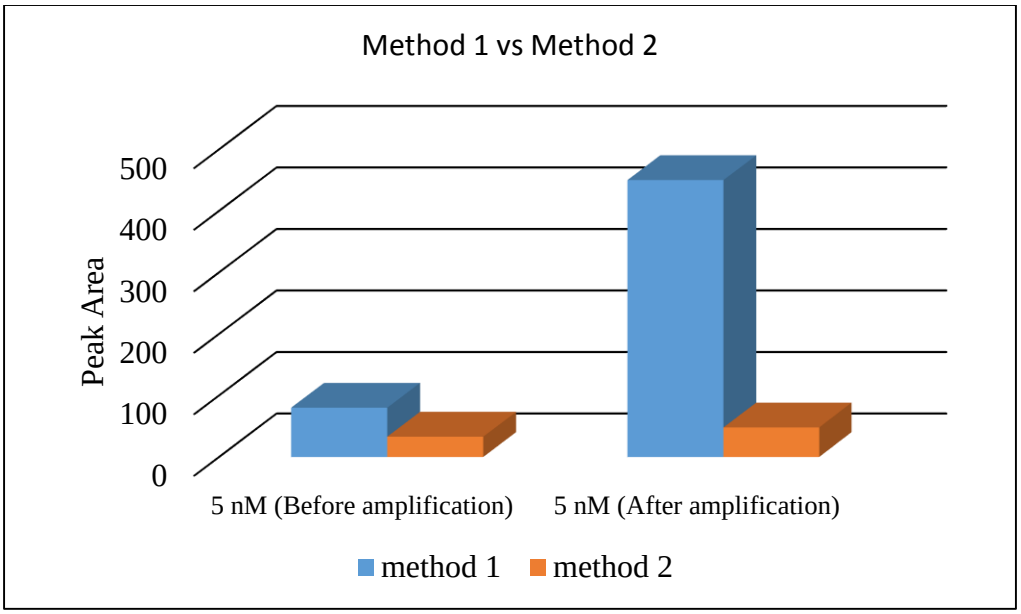

Figure 23. Graph showing a comparison of methods for the preparation of dual labeled conjugates.

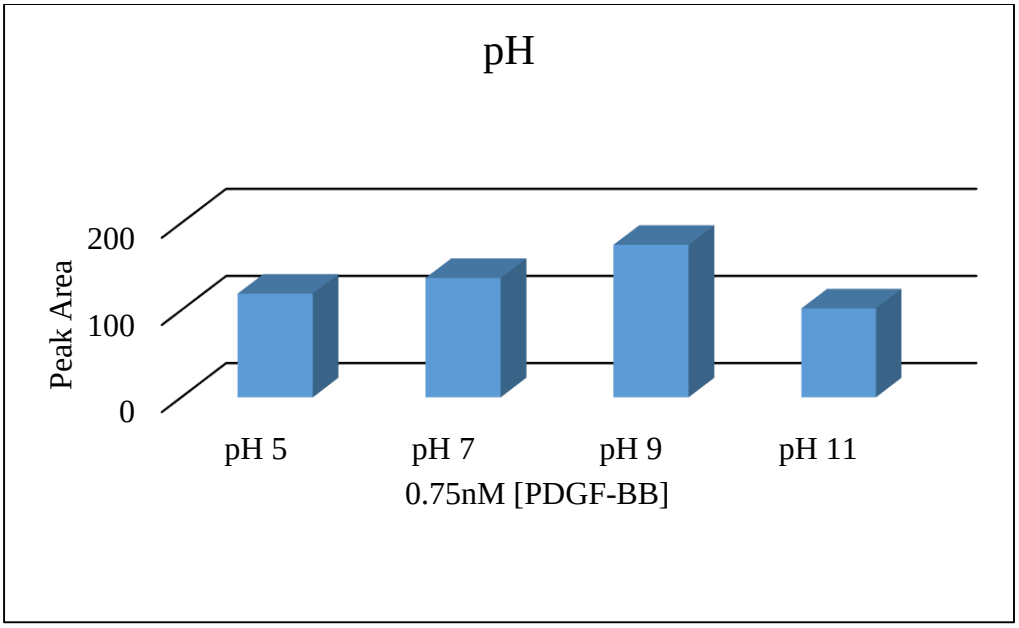

Figure 24. Graph showing optimization with different pH.

4.2.2. Preparation of Aptamer-Based Lateral Flow Strips

The lateral flow biosensor in this study had one test zone and one control zone. Briefly, 50 nmoles of the secondary biotinylated aptamer for PDGF-BB was mixed with 250 µL of 2mg/mL

streptavidin. After incubating it for 1h at RT, 400 µL of PBS was added for the washing step. Excess unbound biotinylated aptamer was removed by centrifugation for 20 minutes with a Millipore filter (cutoff 30,000 D) at 6000 rpm. The conjugates were washed twice again and finally diluted to a volume of 500 µL with PBS. Following the same procedure, biotinylated DNA with a concentration of 10 OD was used to prepare the streptavidin-biotinylated DNA conjugate (control line). Using the BioJet dispenser, streptavidin-biotinylated aptamers and streptavidin-biotinylated DNA were dispensed on the nitrocellulose membrane to form the test zone and control zone, respectively. The nitrocellulose membrane was then dried at room temperature for 1 h and stored at 4 °C. The distance between the control and test zones was 0.2 cm and the control zone was a biotinylated DNA probe complementary to the primary PDGF aptamer. The sample application pad (17 mm × 30 cm) made from cellulose fiber (CFSP001700, Millipore) was soaked with a buffer (pH 8.0) containing 0.25% Triton X-100, 0.05 M Tris-HCl ,and 0.15 mM NaCl. It was then dried at 37°C for 1 h and stored in desiccators at room temperature. The conjugate pad was prepared by dispensing a desired volume of AUNP-aptamer-HRP conjugate solution onto the glass fiber pad (8 mm × 30 cm) using the AirJet AJQ 3000 dispenser. The pad was then dried at 37 °C for 1 h and stored at 4 °C. Finally, all of the components of the lateral flow strip were assembled on a plastic adhesive backing layer (typically, an inert plastic, e.g., polyester) using the clamshell laminator (Biodot, CA). Each component overlapped each other by 2 mm to ensure the solution migrated smoothly through the biosensor during the assay. After the assembly, strips with a 3 mm width were cut using the guillotine cutting module CM 4000.

4.2.3. Assay Procedure

A total volume of 80 μL containing the desired concentration of PDGF-BB in the running buffer PBST (1%BSA) was added onto the sample application pad. The solution from the sample

pad then migrated towards the absorption pad which absorbed all the excess buffer on the strip. After 10 minutes the biosensor was washed twice with 15 μL PBST (1%BSA) at intervals of 5 minutes to move all the excess unbound conjugates onto the control zone and finally onto the absorption pad. The test zones and the control zone were evaluated qualitatively and quantitatively after the washing step. After the assay, 60 μL of the AEC substrate was added onto the lateral flow strips amplifying the intensity of the test zone and control zone. The amplified signal of the test zone was then measured quantitatively using the portable "strip reader" combined with the "AuBio strip reader" software. The intensity of the test zone for PDGF-BB was evaluated after 10 min of adding the substrate, which is the optimal time for the HRP to react completely with the AEC substrate. Results show clear amplification of the signal after 10 min of adding the AEC substrate with a total assay time of 20 minutes. AEC substrate was prepared by mixing 1% AEC, 0.3% H2O2, and 0.05M sodium acetate in a 1mL vial.

4.3. Results and Discussion

Figure 25. Shows the schematic illustration for the working principle of the AUNP-Aptamer-HRP biosensor. The aptamer pair used in the biosensor are specific for PDGF-BB, trapping the target analyte in a sandwich type hybridization assay. As a result the AUNP in the presence of the PDGF-BB get immobilized on the test zone giving a red band. Excess conjugates move onto the control zone and bind via the complementary binding between the primary biotinylated aptamer and the complementary DNA probe immobilized on the control zone. Once the assay is complete, the substrate AEC is added onto the lateral flow strips. HRP reacts with its substrate and produces a red insoluble product which accumulates on the test zone and control zone. The red product accumulated on the test zone and control zone further enhance the red color of the bands, therefore increasing the intensity for easy detection using the portable strip reader.

The “AuBio strip reader” measures the intensity of the red bands giving the peak height and peak area corresponding to the concentration of the analyte target captured on the test zone. The signal amplification aspect of the ultrasensitive biosensor developed reduced the detection limit of PDGF-BB from 1 nM to 0.05 nM, which is a 20-fold increase in the sensitivity of the biosensor.

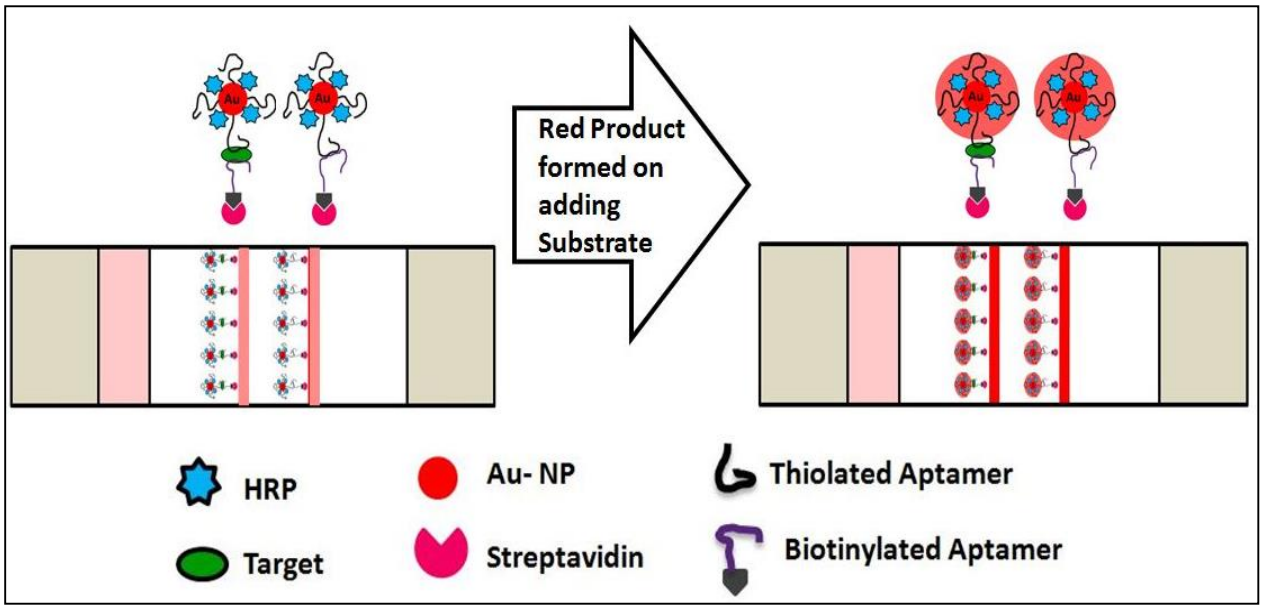

Figure 25. Schematic representation of the working principle for the detection of PDGF-BB.

Figure 26 presents the typical photo images and corresponding responses of the biosensor for 0.075 nM PDGF-BB detection. The biosensor strips clearly shows the amplification of the red bands on the control zone and test zone for both the control and sample strips. The biosensor before amplification are not sensitive enough to detect 0.075 nM concentration of PDGF-BB. But after the introduction of the AEC substrate, amplification takes place and the bound HRP molecules on the test zone amplify the signal (red band) making the 0.075 nM test line visible to the naked eye. The intensity of the control line also increases as a result of the amplification process.

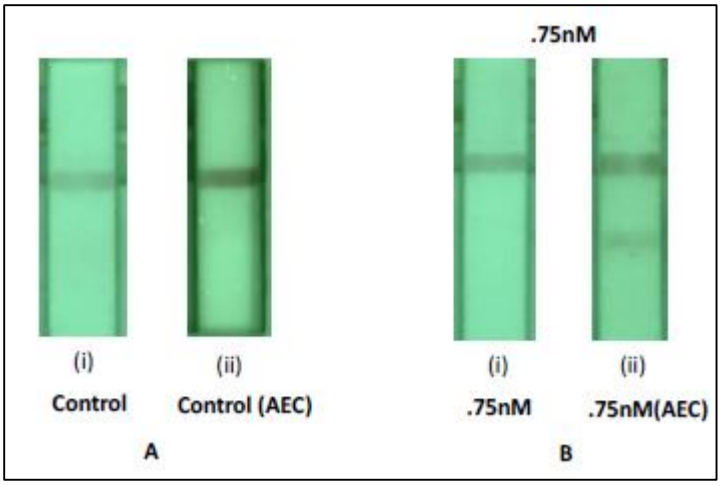

Figure 26. Images of the AUNP-Aptamer-HRP Biosensor showing the amplification effect.

For the optimization experiments, we tested the dispensing times for the: AUNP-Aptamer-HRP conjugates on the conjugate pad, the streptavidin-biotin conjugates on the test zone and the type of nitrocellulose membrane used for making the biosensors. The amount of AUNP-Aptamer-HRP conjugates on the conjugate pad affected the intensities of both the test line and the control line. We compared the dispensing times of the conjugates on the conjugate pad and four times dispensing was found to show the best results. (Figure 27). The peak intensity did not increase for dispensing the conjugates more than four times. Saturation of the AUNP-aptamer-HRP conjugates on the test line occurred and the excess conjugates moved onto the control zone. The amount of streptavidin-biotin aptamer on the test zone was also optimized increasing the sensitivity of the biosensors. We tested different concentrations of the biotin-aptamer conjugated with streptavidin. Increasing the biotin-aptamer concentration to 4 OD was ideal for the biosensor, showing the best sensitivity (Figure 28).

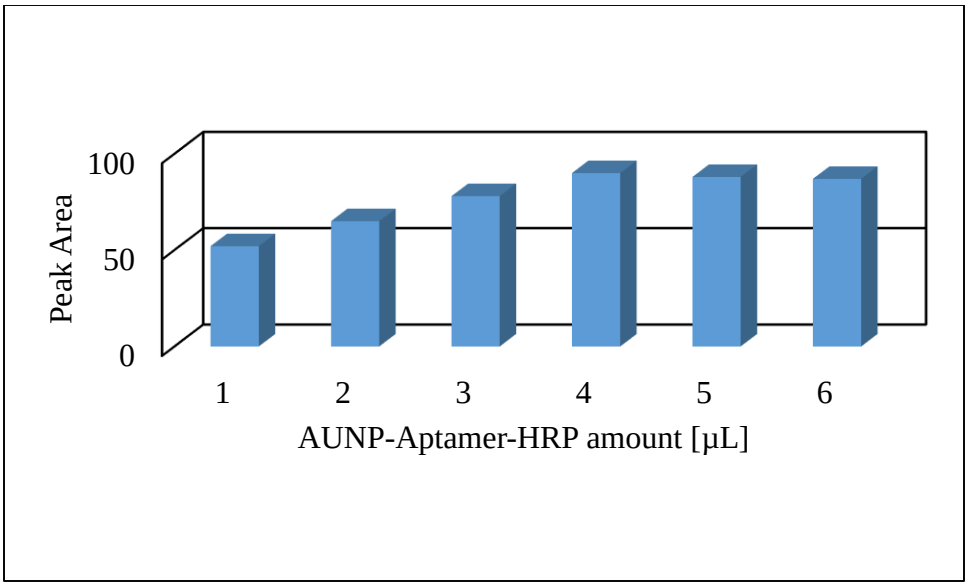

Figure 27. Graph showing the optimization for the AUNP-Aptamer-HRP.

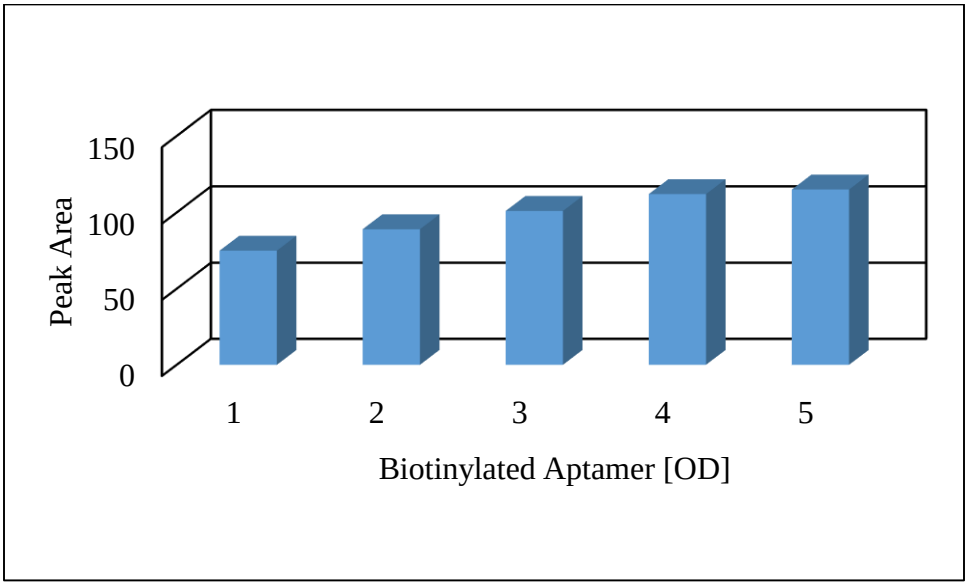

Figure 28. Graph showing the optimization for Biotinylated-Aptamer concentration.

The performance of the biosensor was also affected by the components of the running buffer. Different buffers including PBS, PBS (1%BSA), 1/15 SSC, PBST and PBST (1% BSA) were tested. All the buffers showed a response for the PDGF-BB detection, but the best performance (signal) was observed with the PBST (1% BSA) buffer (Figure 29). Therefore we selected PBST (1% BSA) as the running buffer for the lateral flow biosensors. The biosensors

were also tested for interference with other protein targets like IgG, IgM, Casein and HAS. No control signals were seen for each of the non-specific protein targets tested on the biosensor. Samples containing PDGF-BB mixed with each of the non-specific targets were tested on the biosensor. The lateral flow biosensor could detect PDGF-BB even in the presence of other non-specific targets, proving that the biosensor is selective and sensitive only for PDGF-BB. Since quantitative analysis relies on the stability of the analyte signal and reproducibility of the assay, six different biosensors were tested with 0/75 nM concentrations of PDGF-BB to determine the reproducibility of the biosensor. The relative standard deviation (RSD) for the lateral flow biosensor detecting PDGF-BB was about 5.5 % (figure 30). The calibration plot Figure 31 shows that the peak area vs the concentration of PDGF-BB is linear over the 0.05nM – 10nM range, with a detection limit of 0.05nM. The intensity of the peak area increased as the concentration of the PDGF-BB increased in the sample solution.

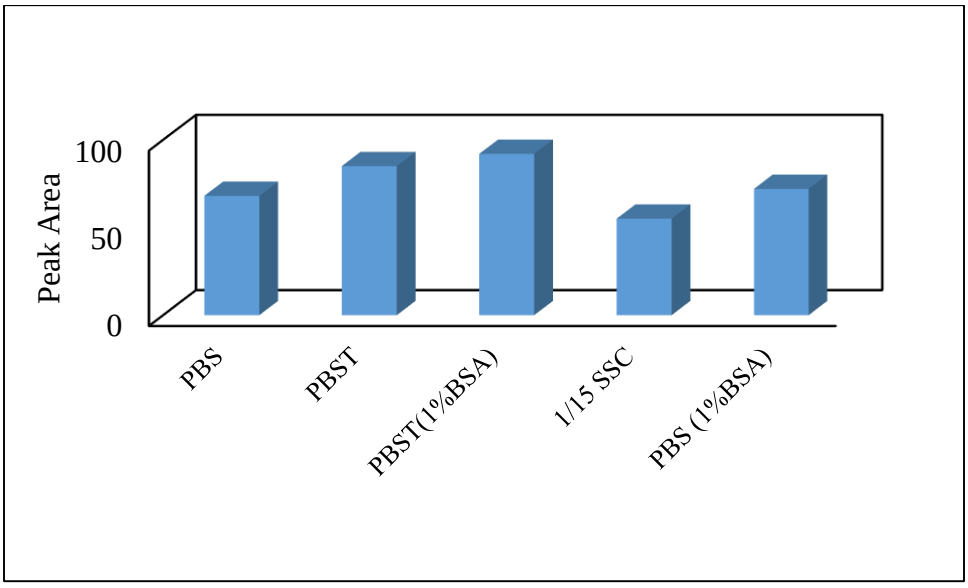

Figure 29. Graph showing the optimization of different buffer systems.

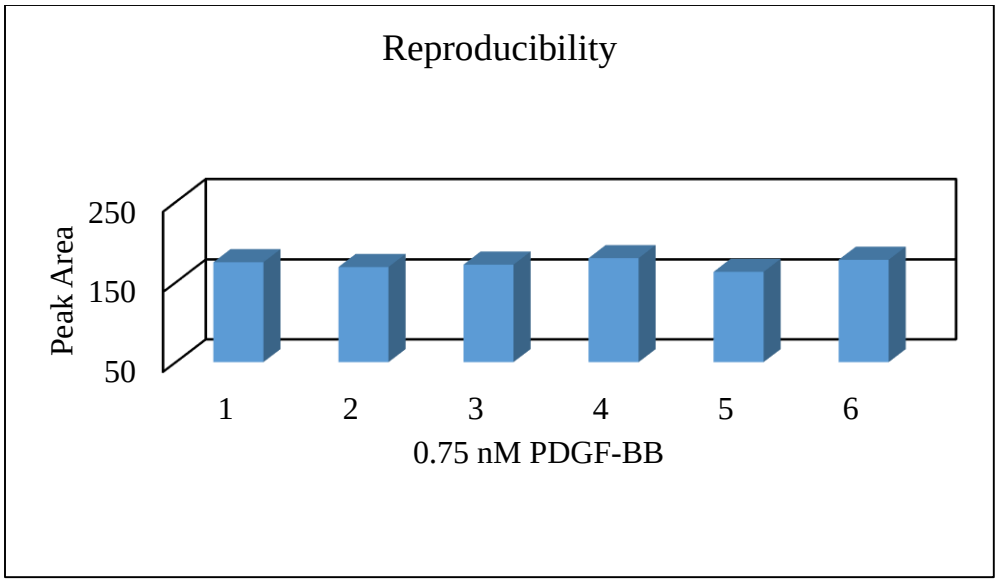

Figure 30. Graph showing the reproducibility of the lateral flow biosensor.

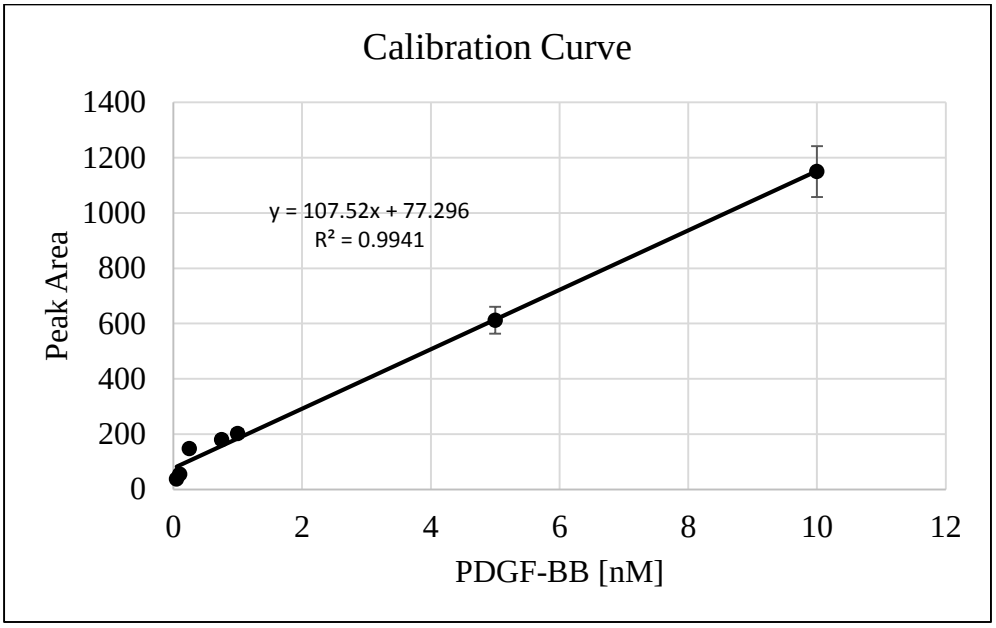

Figure 31. Graph showing the calibration curve for the detection of PDGF-BB.

4.4. Conclusion

In summary, we have successfully developed a method for the amplification of the captured AUNP on the test line using HRP and AEC substrate. The dual labeled AUNP-aptamer-HRP based biosensor can detect PDGF-BB with a detection limit of 0.05 nM and a linear range of 0.05 nM –

10 nM. The biosensor takes advantage of the unique optical and binding properties of AUNPs and also uses aptamers which are known for their selectivity to detect PDGF-BB. HRP when reacted with AEC substrate gives a red product therefore lowering our detection limit by amplifying the signal. The biosensor is fast, sensitive and selective for the detection of PDGF-BB, showing good reproducibility.

CHAPTER 5. MAGNETIC BEAD BASED COLORIMETRIC DETECTION OF CEA

This chapter focuses on the development of a colorimetric system for the detection of CEA. The colorimetric system works on the principle of sandwich hybridization between an aptamer, an antibody and CEA. Magnetic beads coated with streptavidin and horseradish peroxidase are also incorporated into this colorimetric system, taking advantage of their unique individual properties. Firstly, an introduction on the importance of detecting CEA, and why we need a low cost, fast, simple and accurate colorimetric method. It is followed by a discussion on the step wise detailed procedure for the colorimetric system, along with the various optimizations performed to make the colorimetric system sensitive and selective for CEA. A combined result and discussion section about the analytical performance of the system is presented next, followed by a summary of this study at the end.

5.1. Introduction

Cancer, one of the most dangerous and fatal disease is known to have a very low survival rate. Early detection of cancer greatly improves the survival rate for patients and reduces fatalities. For the early detection, biomarkers have gained considerable interest in the past few decades.[114] CEA is one of the well-known biomarker found overexpressed in breast cancer, colon cancer, ovarian cancer and many more.[115] CEA levels found in healthy individuals are about 3.4 ng/mL and 2.5ng/mL for males and females respectively. The CEA concentration doubles for smokers.[116] CEA not only helps in the diagnosis, but it also helps to monitor the progress of treatment for a patient. In many cases, CEA have been monitored over a certain period of time to monitor the reappearance of cancer after treatment.[116, 117]

As discussed in the earlier section, there are antibodies and aptamers for the detection of CEA. Currently, methods like radioimmunoassay, fluorescence immunoassay,

chemiluminescence immunoassay and many other methods are used for the clinical diagnosis of CEA.[118-120] Even though sensitive; these methods suffer from drawbacks related to the use of antibodies. Aptamers have shown equal or better selectivity and sensitivity for CEA detection. The advantages that aptamers have over antibodies are resulting in the replacement of antibodies for such antigen target detection. Therefore, there is a need for a detection system that is fast, low cost, sensitive and selective for CEA.

5.2. Material and Methods

Biotin Aptamer for CEA: 5'- /5BiosG/AG GGG GTG AAG GGA TAC CC -3'

Streptavidin-Magnetic beads (SMB) were purchased from Thermo Fischer Scientific. Anti-Carcino Embryonic Antigen CEA antibody (Mouse monoclonal) was bought from Abcam. Sodium chloride-sodium citrate (SSC) buffer (pH 7.0), Phosphate buffer saline with tween (PBST), phosphate buffer saline (PBS, PH 7.4,), bovine serum albumin (BSA), and CEA protein were purchased from Sigma-Aldrich. 3, 3', 5, 5'-Tetramethylbenzidine (TMB), stopping solution and horseradish peroxidase (HRP) were purchased from Sigma Aldrich. Micropipettes (1 µL , 20 µL, 200 µL and 1000 µL), micro-centrifuge tubes and step shaker were from VWR. Cary 100 UV-Vis spectrophotometer from Agilent technologies was used for all the absorbance readings.

5.3. Method for Detection

A detection scheme illustrating the principle is shown in Figure 32. Briefly, 5uL Streptavidin coated magnetic beads were taken in a vial, washed three times using magnetic separation with PBST (0.05% tween) and finally resuspended in 50µL PBSB (1% BSA). Biotin-aptamer (0.5nM) was then added to the SMB solution and incubated for 20 min at RT on the shaker. The strong Biotin-Streptavidin interaction immobilized the aptamer on the SMB; after the immobilization was complete the washing cycle was repeated with PBST (1% tween) to remove

all the unbound biotin-aptamers. CEA of a known concentration was then added to the solution, incubated for 30 min at RT on the shaker. Aptamer being specific for CEA recognizes and binds it tightly. All unbound CEAs were washed off using PBST (1%BSA). The antibody-HRP which is also specific for CEA is then incubated in the solution for 30 min at RT. A sandwich is formed between the aptamer, CEA and the antibody immobilizing the CEA on the SMBs. Excess antibody-HRPs were washed off using PBST(1% tween). HRP being an enzyme has been used widely for signal amplification purposes. In our experiment TMB was used as a substrate, which reacts with HRP to produce a Blue colored solution having an absorbance peak at 630-650nm. A stopping solution is added after 5 min to stop the reaction between the HRP and TMB, changing the color to yellow. The absorbance peak stabilizes and sensitivity increases 2-3 folds by adding the stopping solution. Figure 33 Shows the detection of 10 ng/mL CEA using the colorimetric system. The yellow color indicated the presence of CEA in the sample, while the absorbance readings quantify the amount of CEA based on the calibration curve. A Color change from blue to yellow is observed in the sample tube after adding the stopping solution. The control tube which has no CEA present shows neither the blue color nor the yellow color. TMB when added to the sample containing CEA, reacts with the trapped HRP on the SMBs giving a blue color. The appearance of the blue color indicated the presence of the CEA in the sample solution and is used fot the qualitative detection. For the quantitative detection, the stopping solution is added and absorbance is measured at 450 nm using the Cary 100 UV-Vis spectrophotometer.

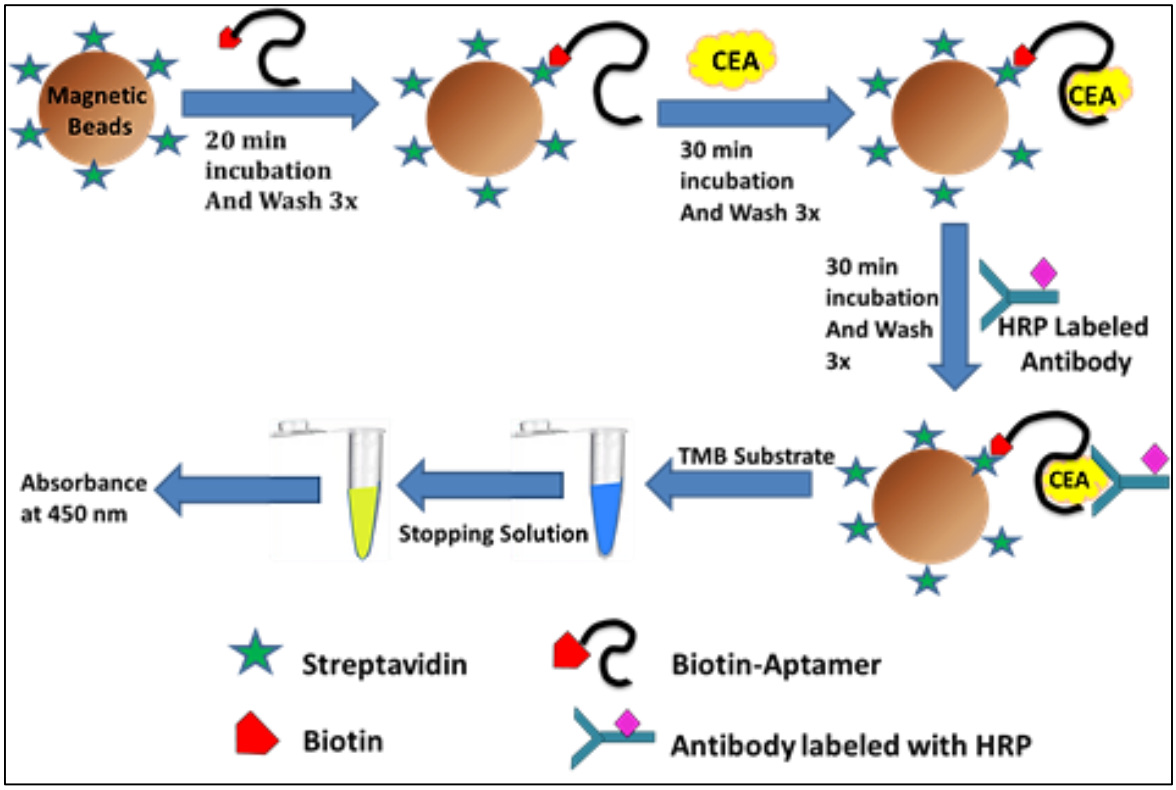

Figure 32. Shows the stepwise representation for the detection of CEA.

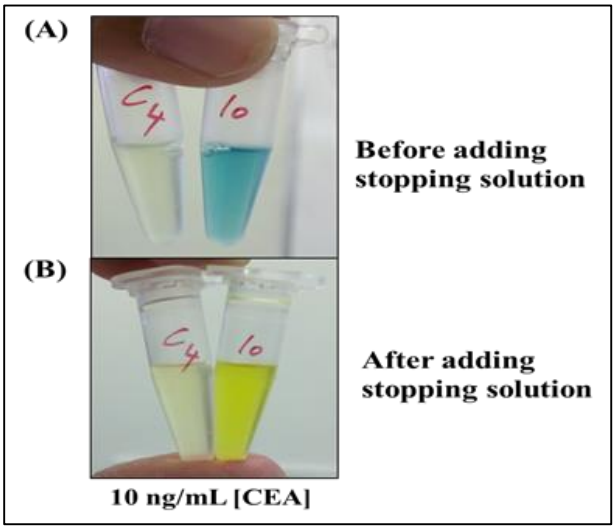

Figure 33: Colorimetric response for 10 ng/mL CEA concentration.

5.4. Results and Discussion

Various optimizations were performed to make the colorimetric detection of CEA sensitive. Optimizations were done using 15 ng/mL CEA concentration and a reaction time of 5 min unless otherwise stated. Figure 34 shows the absorbance signals for different amounts of SMB indicating that 5 µL SMB showed the best results. Using 25 µL SMB did not increase the signal significantly, so 5 µL was chosen for further optimizations. The absorbance response for CEA is also sensitive towards the amount of Aptamer added to bind the SMB. Different concentrations of aptamer ranging from 0.01 nM – 1.5 nM were tested; Figure 35 shows the increase in absorbance from 0.01 nM to 0.5 nM after which the signal saturated. More Aptamers on the MB surface results in a higher absorbance signal as more CEA could get captured for the sandwich hybridization in the next step. The Aptamer concentration 0.5 nM saturated the SMB surface and no more aptamers could get immobilized, resulting in the same response for higher concentrations of the aptamer added to the SMB. Antibody-HRP concentration also affected the absorbance for CEA detection. Figure 36 shows absorbance response for different dilutions of Antibody-HRP, 10 times diluted (50 µg) being the best. Absorbance for 15 ng/mL CEA decreased as the Antibody-HRP was diluted further. Diluting the Antibody-HRP solution further reduced the number of HRP molecules present in the solution, therefore reducing the absorbance signal for CEA detection.

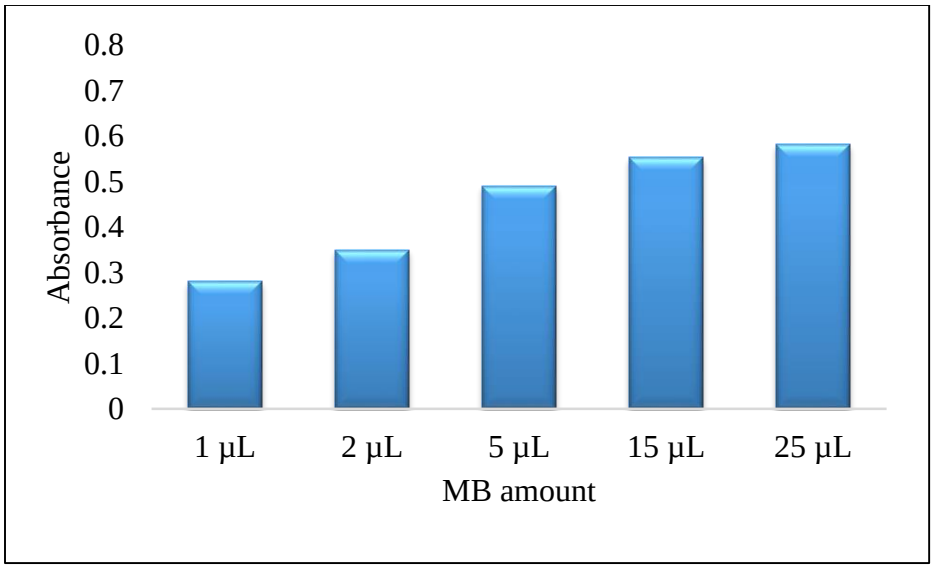

Figure 34. Graph showing optimization for different amounts of SMB.

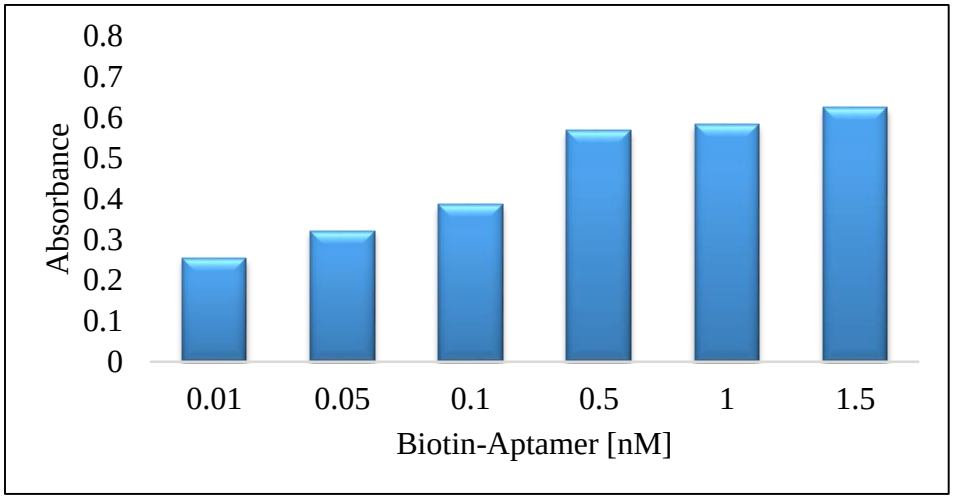

Figure 35. Optimization for the concentration of biotin-aptamer.

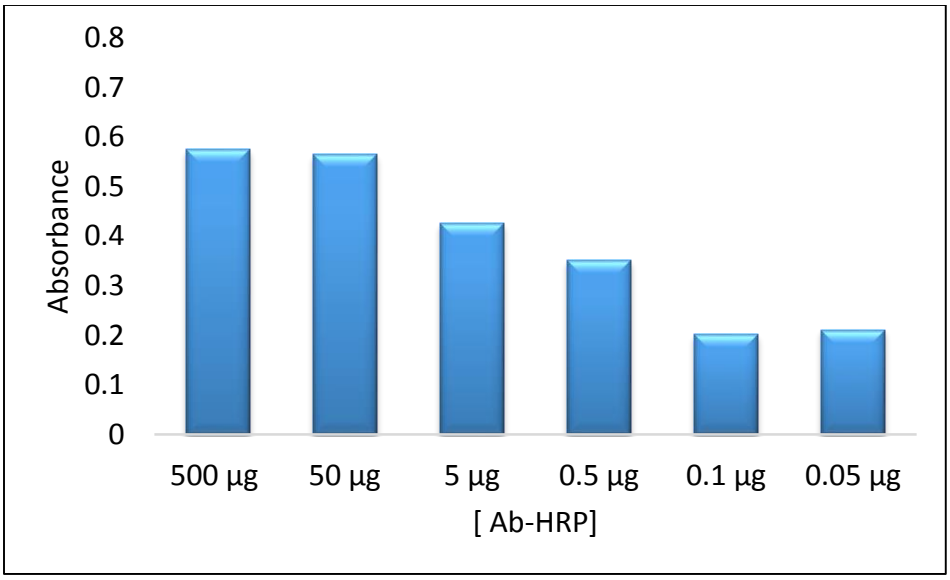

Figure 36. Optimization for different concentrations of Antibody-HRP.

Since quantitative analysis relies on the stability of the analyte signal and reproducibility of the system, five colorimetric assays were performed simultaneously for 5ng/mL, 15ng/mL and 60ng/mL; all of them showed good reproducibility with RSD ranging from 5-8%. Figure 37 shows the reproducibility of 15ng/mL CEA concentration with RSD 5.42% indicating that the colorimetric detection system is reproducible and accurate. The Colorimetric detection system was also tested for interference using other Protein like PDGF, Thrombin and Human IgG. Briefly, 500nM of each analyte was tested using our colorimetric detection system. Absorbance signals for these proteins were same as the control (buffer). Different concentrations of CEA were also tested with the mixture of all three proteins. Absorbance signals shown in Figure 38 indicate that the colorimetric detection system is selective and sensitive for CEA. Other proteins do not cause any interference with the absorbance signals of CEA. The system was also tested in complex biological matrix by spiking the solution with Plasma samples. CEA was detected successfully with up to 20 µL plasma spiked in the solution. Using the colorimetric system a detection limit of 1.5 ng/mL of

CEA was achieved. The system has a linear dynamic range of 1.5 ng/mL to 180 ng/mL for CEA shown in Figure 39.

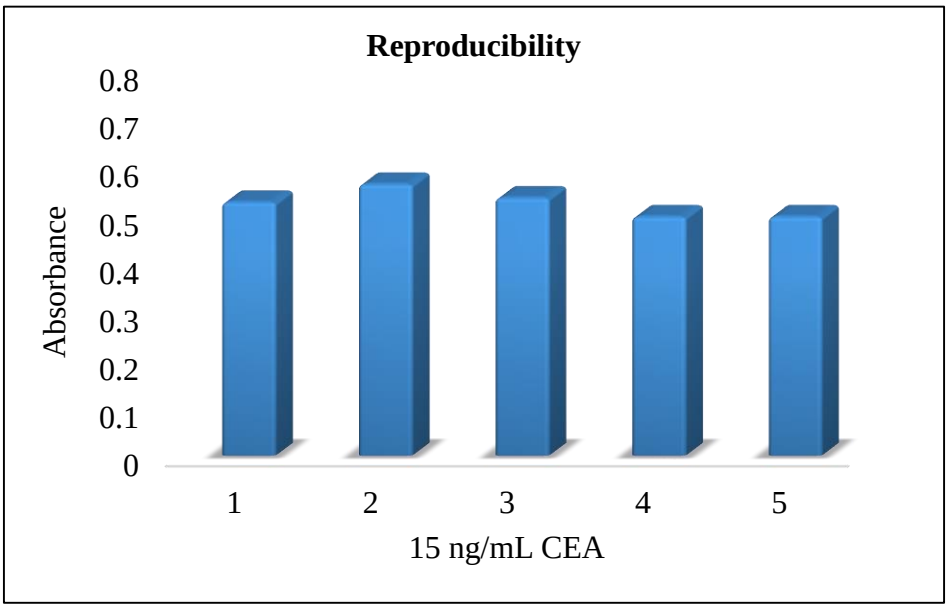

Figure 37. Graph showing the reproducibility.

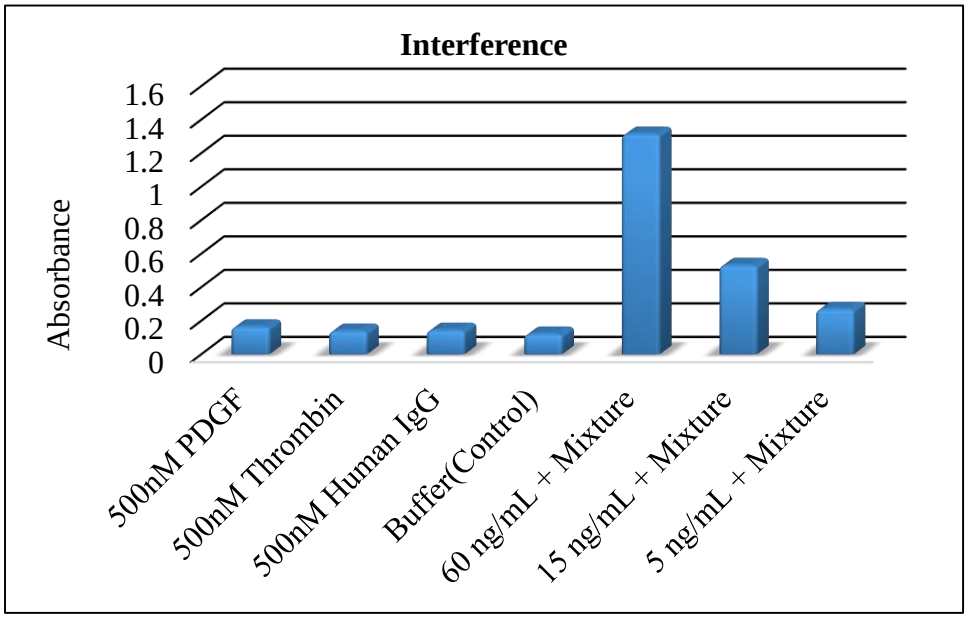

Figure 38. Graph showing the interference with non-specific proteins.

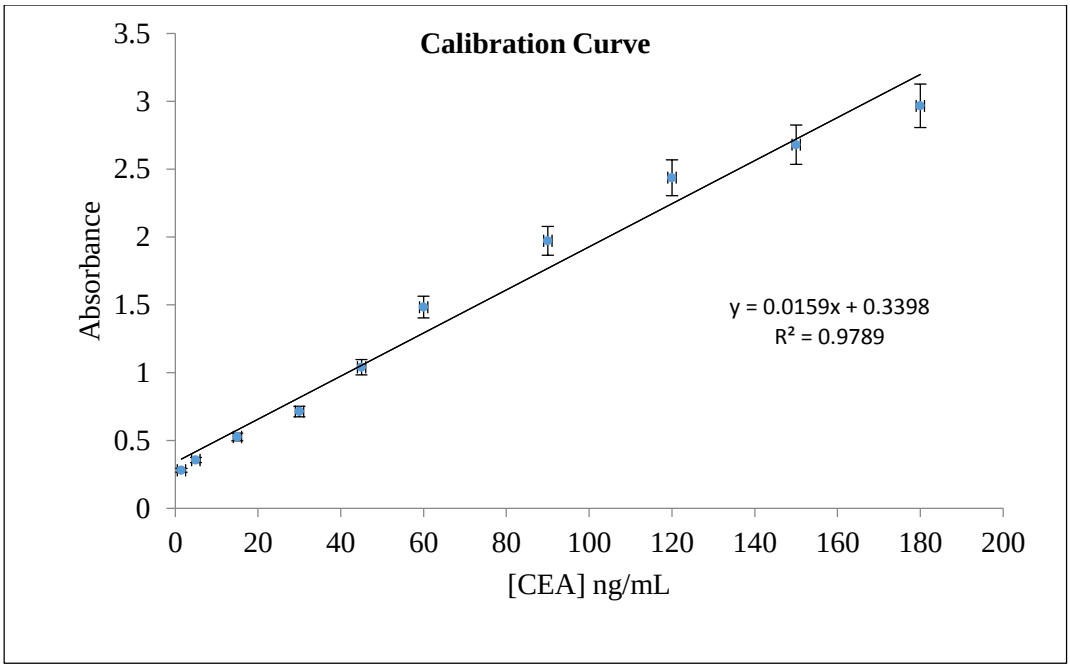

Figure 39. Graph showing the calibration curve for the colorimetric detection.

5.5. Conclusion

In conclusion, we have developed a simple and sensitive colorimetric method for the detection of Carcinoembryonic antigen (CEA) by using streptavidin magnetic beads, Biotin-Aptamer and Antibody-HRP. The colorimetric system uses the molecular recognition properties of Aptamer and Antibody to successfully detect CEA with a detection limit of 1.5 ng/mL and a 1.5ng/mL – 180ng/mL linear range. The CDS was also used successfully to detect CEA in complex biological matrix (plasma). The colorimetic detection method developed here was improved in the next study. The antibody used for the sandwich hybridization capture of the CEA target was replace by an aptamer syste. The detection was focused on MCF-7 cells which have several MUC1 expressed on their surface. Aptamers specific for the MUC1 was incorporated into the colorimetric detection system and the CDS was made more feasable, reducing the cost, assay time and sensitivity.

CHAPTER 6. MAGNETIC BEAD BASED COLORIMETRIC DETECTION SYSTEM FOR MCF-7 BREAST CANCER CELLS

6.1. Introduction

Mucin 1 (MUC1) are transmembrane glycoproteins overexpressed on MCF-7 cells in primary and metastatic breast cancers. In this study, biotin-aptamers (BApt) highly specific for MUC1 are combined with streptavidin-magnetic beads (SMB) for the development of a magnetic bead-aptamer based colorimetric (MBAC) system that enables the qualitative and quantitate detection of MCF-7 breast cancer cells. Firstly, an introduction on the importance of detecting MCF-7 breast cancer cells followed by a detailed discussion on the procedure for the CDS. A combined results and discussion section will focus on the various optimizations performed to make the CDS sensitive and selective for the MCF-7 cells. The analytical performance of the CDS is presented next, followed by a summary of this study at the end.

6.2. Material and Methods

MUC 1 aptamer: 5′-/ 5Biosg/ GCA GTT GAT CCT TTG GAT ACC CTG G-3′

Streptavidin-Magnetic beads (SMB) were purchased from Thermo Fischer Scientific. MCF-7 cell line was bought from ATCC. Sodium chloride-sodium citrate (SSC) buffer (pH 7.0), Phosphate buffer saline with tween (PBST) and phosphate buffer saline (PBS, PH 7.4,) were purchased from Sigma-Aldrich. 3, 3’, 5, 5’-Tetramethylbenzidine (TMB), stopping solution and horseradish peroxidase (HRP) were purchased from Sigma Aldrich. Micropipettes (1 µL, 20 µL, 200 µL and 1000 µL), micro-centrifuge tubes and step shaker were from VWR. Cary 100 UV-Vis spectrophotometer from Agilent technologies was used for all the absorbance readings. EMEM culture buffer, FBS, cell culture plates and Trypsin were purchased from Sigma Aldrich.

6.3. Assay Procedure

Figure 40 illustrates the principle of the SMB-BApt based MBAC system for the detection of MCF-7 cells. Streptavidin coated MBs were labelled with biotin-Apt to form complex 1. Briefly, SMB were taken in a vial, washed three times using magnetic separation with PBST (0.05% tween) and finally suspended in PBSB (1% BSA). BApt were then added to the SMB and incubated at room temperature (RT) for 20 min on a shaker. The strong streptavidin-biotin interaction helped label many BApt on the SMB surface. After the successful immobilization the SMB-BApt complex were washed three times using magnetic separation and PBST (1% tween) to remove all the unbound BApt. Complex 1 was finally re-suspended in PBSB and stored at 4˚C. MCF-7 cells have many surface proteins (MUC1) for aptamer binding, therefore the same BApt was conjugated with streptavidin-horse radish peroxidase (SHRP) to form complex 2. The BApt was mixed with SHRP in a vial for 20 min at RT, on a shaker. After adding 500 µL PBS to the mixture, the solution was centrifuged for 20 minutes at 6000 rpm at 4˚C using the Amicon Ultra Centrifugal Filter from Millipore. The washing step was repeated 3 times, as a result the unbound BApts and SHRPs were filtered off while the BApt-SHRP complex solution in the filter was diluted with PBS and stored at 4˚C.

In presence of MCF-7 cells, aptamers specific for MUC1 on the MCF-7 cell surface capture the cells forming a sandwich type hybridization shown in figure 40 (A). The SMB-BApt complex 1 capture the MCF-7 cells onto the MB surface. Since there are many MUC1 proteins on the MCF-7 cell surface, aptamers from the BApt-SHRP complex 2 also bind forming the SMB-BApt-MCF-7-BApt-SHRP complex. A strong magnet then introduced for magnetic separation helps separate all the unbound MCF-7cells and the components of complex two from the SMB-BApt-MCF-7-BApt-SHRP complex. The above washing step was repeated 3 times with PBST (1% tween).

Substrate TMB or 3, 3', 5, 5'-Tetramethylbenzidine is then added to the complex. TMB which reacts with HRP, an enzyme used widely for signal amplification, gives a blue colored solution for the qualitative detection. A stopping reagent (Sigma Aldrich) is then added after 5 min to stop the reaction between the HRP and TMB, changing the color to yellow for the qualitative detection. The absorbance of the solution was then measured at 450nm giving us a signal readout corresponding to the number of MCF-7 cells in the sample. In the absence of MCF-7 cells, components of complex 2 get washed off during the magnetic separation and washing steps. As a result, addition of the TMB substrate will give no color as HRP is not immobilized onto the SMBs of complex 1. Figure 41 shows the typical qualitative response for the MBAC system in the presence of 0 MCF-7 cells (control) and increasing amounts of MCF-7 cells. In the absence of MCF-7 cells no blue color is observed, while the intensity of the blue color in the presence of MCF-7 cells increases as the number of cells in the sample increase.

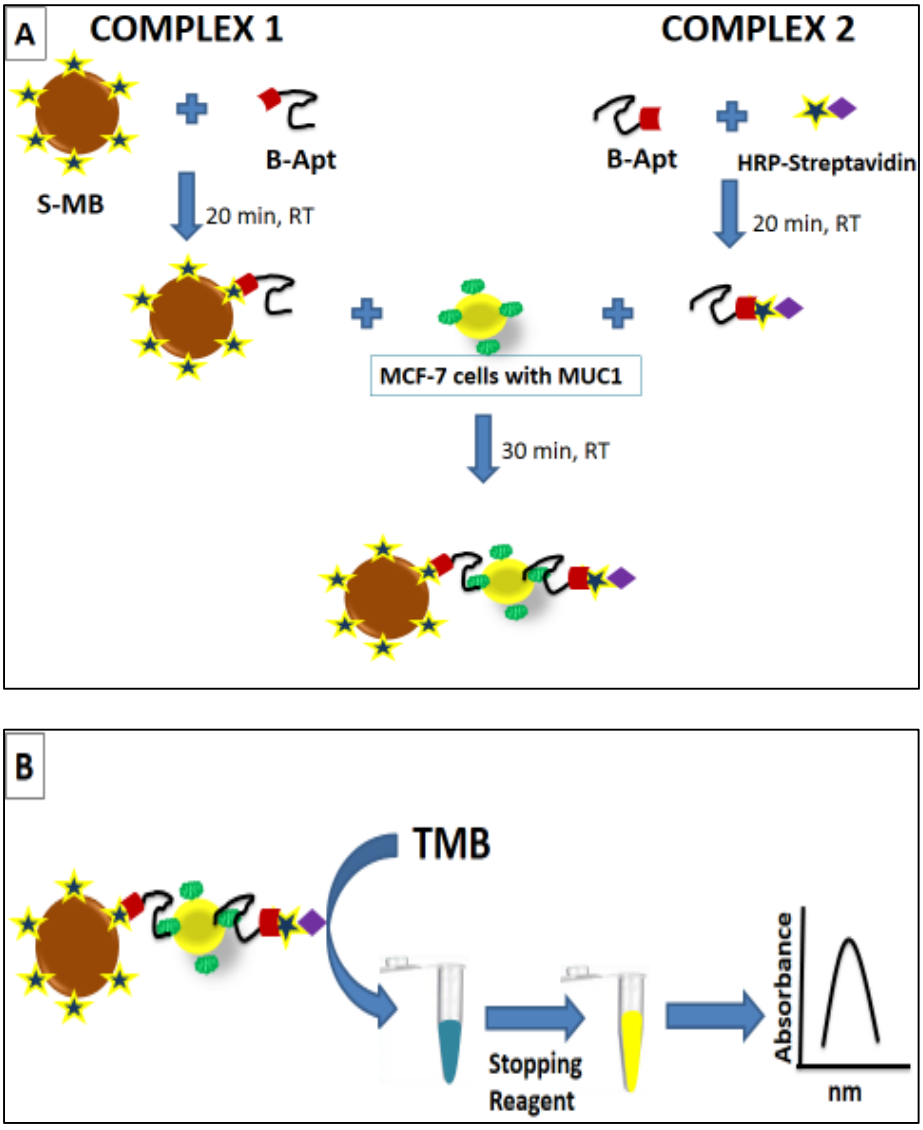

Figure 40. Schematic representation of the magnetic bead based colorimetric assay.

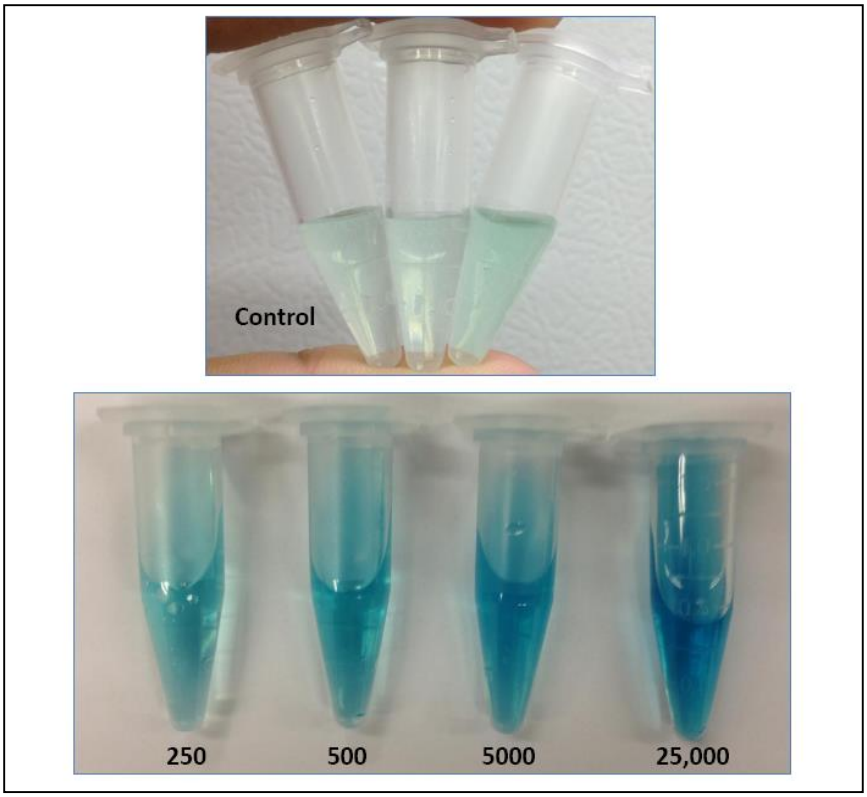

Figure 41. Typical photo images for the magnetic bead based colorimetric assay.

6.3.1. MCF-7 Cell Culture

For culturing the MCF-7 cells, we used EMEM culture buffer supplemented with 10% FBS and 1% penicillin/streptomycin. The cells were kept in a culture flask at 37 ˚C with a concentrated 5% CO_2 atmosphere. After the MCF-7 cells reached approximately 90 to 95 % confluence on the plates, we removed the media and washed the cells with PBS buffer twice. After washing, 2-3 mL of warm (37 ˚C) 0.25% Trypsin was added to dislodge the cells from the flask surface. The dispersal of the cells took about 5-10 minutes. Once the MCF-7 cell layer was dispersed (5min at 37 ˚C), we added about 8 mL of the growth media and aspirated the cells by gently pipetting the solution, which was then transferred to a sterile 10 mL centrifuge tube. This was done to deactivate the trypsin and separate the clumps of cells formed during trypsinization. A cell count using the cell counter was done to know the exact number of cells in 10 mL solution. The cells were then

separated from the growth media by centrifuging the mixture at 15000 rpm for 5 minutes in a centrifuge. The supernatant (trypsin/media) was separated by pipetting out the solution and the pellet was re-dispersed in 10 mL PBS. TO collect the cells for testing on the colorimetric detection system we centrifuged the cells again at 15000 rpm for 5min. After the centrifugation, the cells were collected in 1 mL tubes containing PBS. To continue the culture of the MCF-7 cells for future experiments, 1 mL of the cells were transferred to fresh growth medium (24 mL) in a new sterile flasks. The flask with the MCF-7 cells were incubate at 37°C in humidified 5% CO2 atmosphere until further use. Growth media which was EMEM with FBS and penicillin was changed every two days to ensure good cell growth.

6.3.2. Optimizations of Complex 1

Analytical parameters including the amount of SMB, BApt concentration, SHRP concentration and incubation time for complex 1 and complex 2 would also effect the response of the MBAC system. In the current study, all the optimizations have been done using 10,000 MCF-7 cells unless otherwise stated. SMB amount in complex 1 played a major role in the sensitive detection of MCF-7 cells using the MBAC system. Figure 42 presents the absorbance readings for MCF-7 cells with different concentrations of SMBs on the MBAC system. It can be seen that the absorbance reading for MCF-7 cells increases greatly with the increase of SMB concentration up to 1 mg, after which the absorbance readings saturate for 2 mg and 2.5 mg. Therefore, a concentration of 1 mg for SMBs were used for the preparation of complex 1. The amount of BApt labelled on SMBs were also optimized. Different concentrations of BApt ranging from 0.01 nmol – 1.5 nmol were tested on the MBAC system. Figure 43 shows the absorbance readout for different BApt concentrations indicating an increase in the absorbance reading from 0.01 nmol to 0.05 nmol, proving that higher number of BApt on the SMB surface

results in a higher absorbance signal as more MCF-7 cells can be captured. The BApt concentration of 0.05 nmol saturated the SMB surface resulting in a constant absorbance readout for higher BApt concentrations. Biotin-Streptavidin interactions have been used widely to label several DNAs, aptamers and antibodies onto different nanoparticle surfaces. Figure 44 presents the response for different incubation times on the MBAC system. Incubating the SMB and BApt for 20 min gave the ideal response for the detection of MCF-7 cells. Therefore, 20 min was chosen as the incubation time for the formation of complex 1. Incubating the SMB and BApt for less than 20 minutes resulted in a decrease in the absorbance signal, while incubating the two components for more than 20 minutes showed no great enhancement in the absorbance readings.

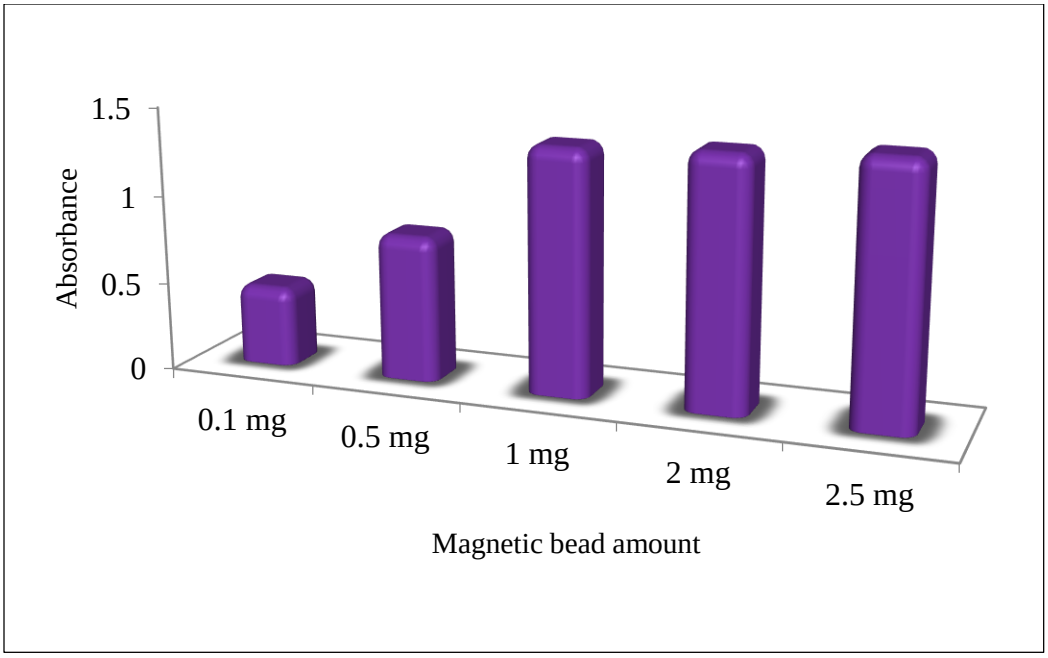

Figure 42. Graph showing the effect of Magnetic Bead amount on the MBAC system.

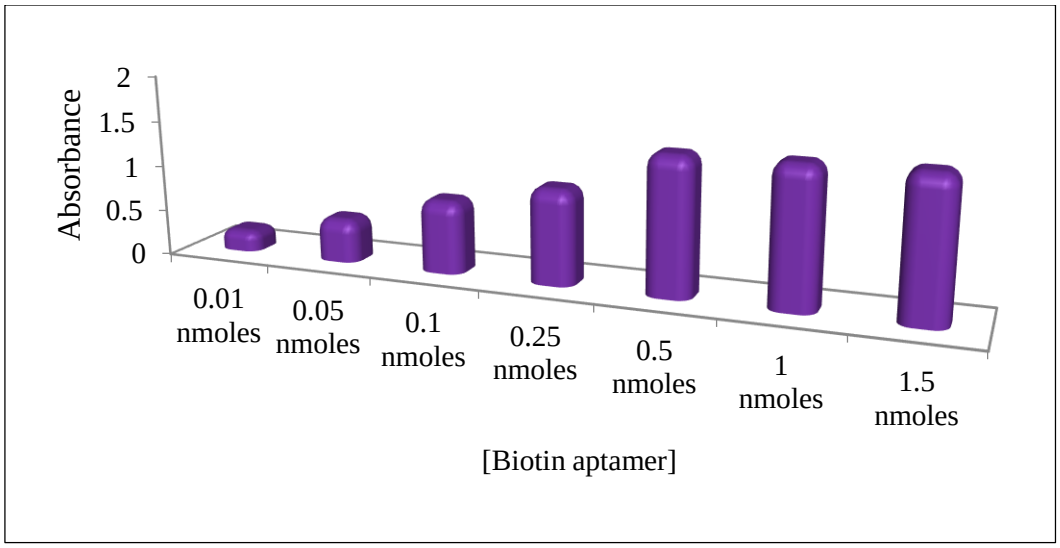

Figure 43. Optimization for the Biotin-Aptamer concentration used in complex 1.

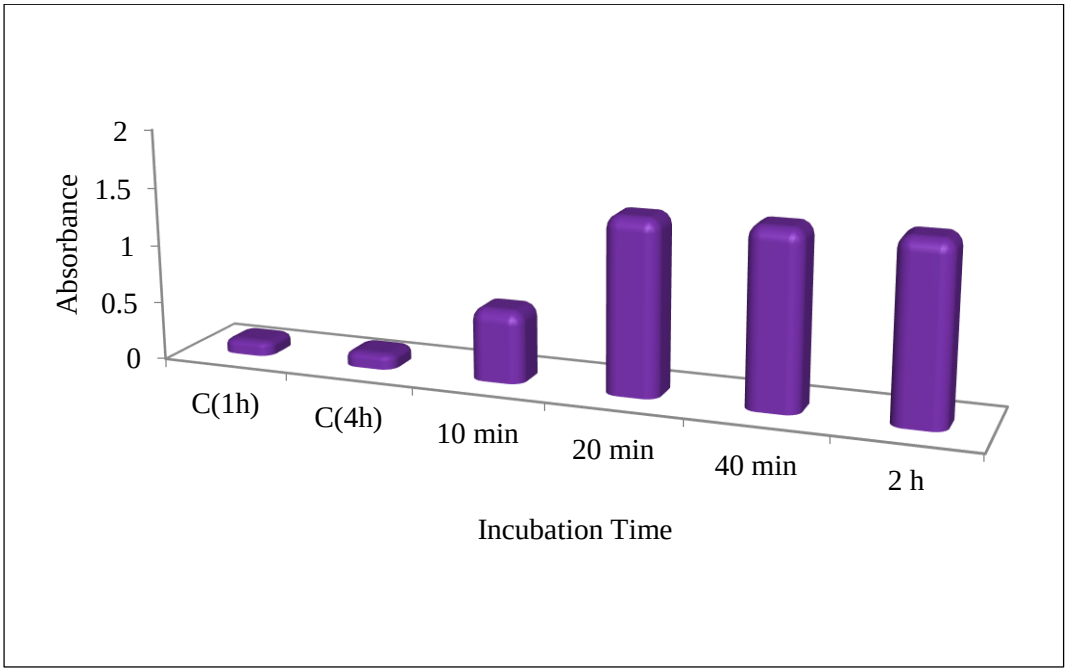

Figure 44. Graph showing the optimization for different incubation times for complex 1.

6.3.3. Optimizations of Complex 2

Optimizations for components of complex 2 were also performed using 10,000 MCF-7 cells. First, we studied the effect of BApt concentration on the absorbance response of the MBAC system. To obtain the best absorbance readout for 10,000 MCF-7 cells, different

concentrations of the BApt were conjugated with a constant amount of SHRP in complex 2. Figure 45 shows absorbance readings for different BApt concentrations on the MBAC system. It can be seen that the absorbance increased up to 1 nmol; a further increase in the BApt concentration does not increase the absorbance greatly, indicating a saturation of the amount of BApt needed to bind the MCF-7 cells. Therefore, 1 nmol of biotinylated aptamer was used as the optimal concentration throughout the entire study. The response of the MBAC system was also affected by the amount of SHRP used in complex 2. Different concentrations of SHRP were conjugated to BApts for optimizing the ideal amount of SHRP in complex 2. Figure 46 presents the response for different SHRP concentrations on the MBAC system, indicating that 10µL of 1mg/ml SHRP concentration was optimal to achieve the best absorbance readout. The incubation time for the formation of SMB-BApt-MCF-7-BApt-SHRP complex was optimized to ensure sensitive detection of MCF-7 cells using the MBAC system. Figure 47 presents the absorbance response for different incubation times of complex 1, MCF-7 cells and complex 2. Corresponding absorbance readouts shown for different incubation times indicate that 30 min was sufficient for capturing the MCF-7 cells and forming the SMB-BApt-MCF-7-BApt-SHRP complex.

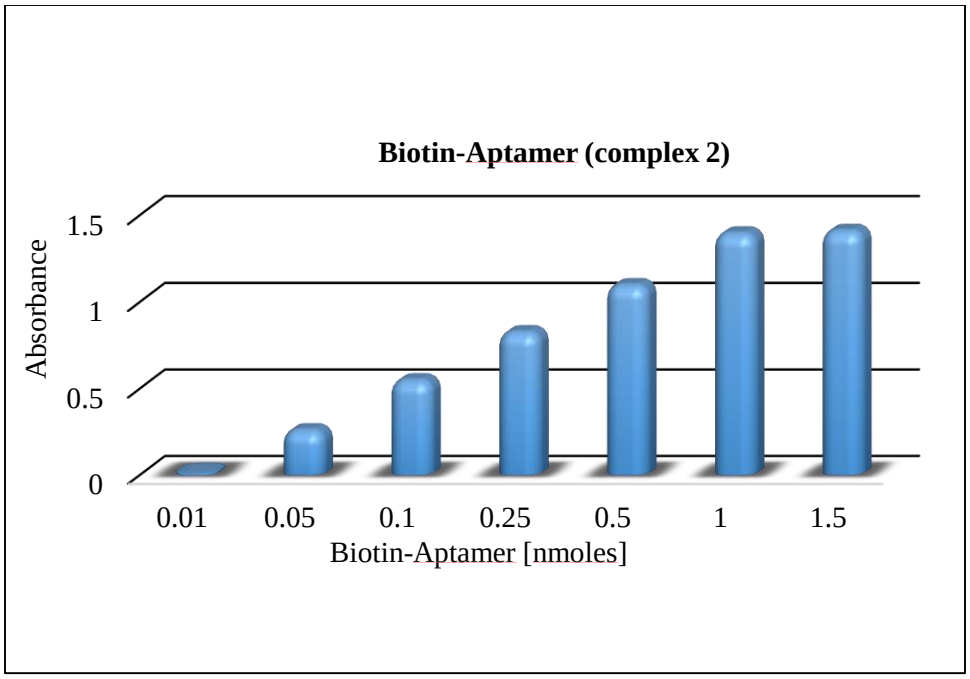

Figure 45. Optimization for the concentration of Biotin-Aptamer in complex 2.

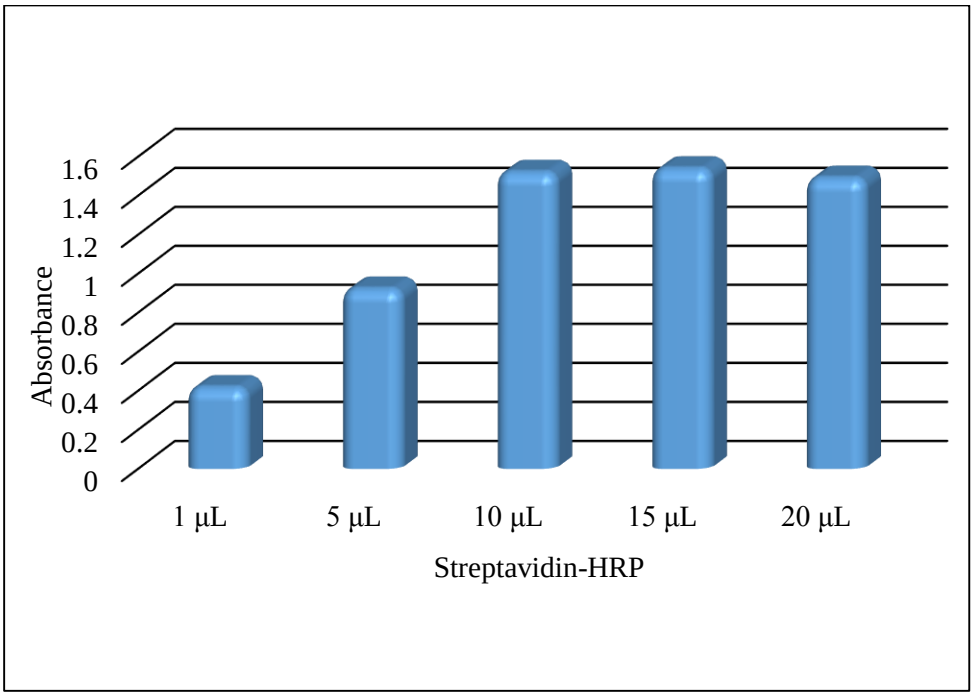

Figure 46. Effect of different concentrations of Streptavidin-HRP on the MBAC system.

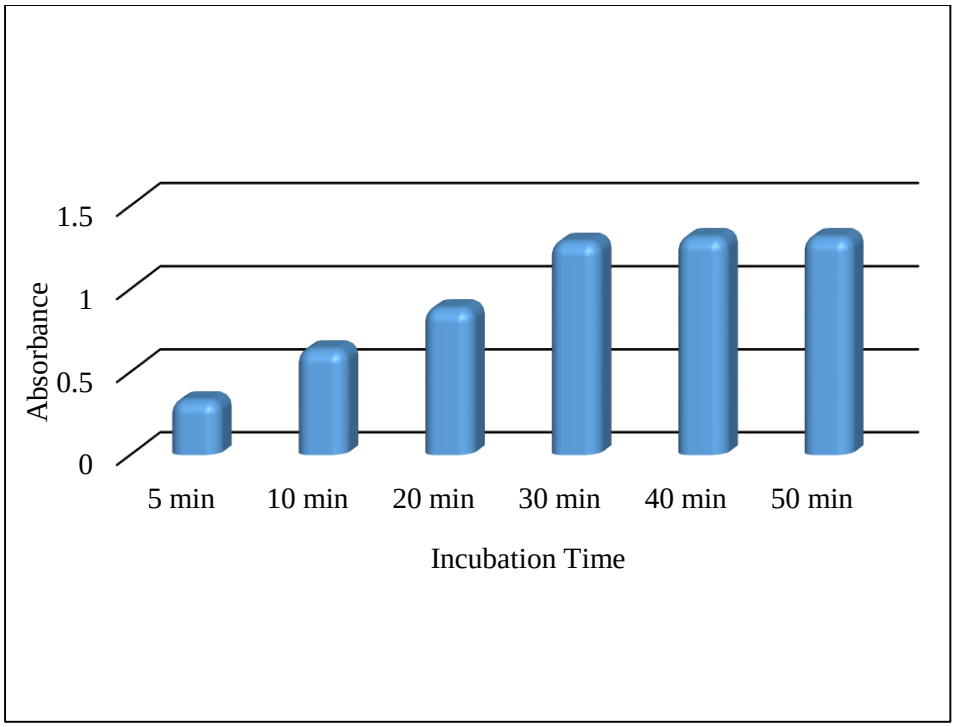

Figure 47. Optimization for the incubation time of complex 1, MCF-7 cells and complex 2.

6.3.4. Analytical Performance

Since quantitative analysis relies on the stability of the analyte signal and reproducibility of the system, six colorimetric assays with 5000 MCF-7 cells were performed simultaneously using the MBAC system. Figure 48 shows the absorbance readouts for reproducibility of the MBAC system with an RSD of 4.72% indicating that the MCF-7 detection system is reproducible and reliable. To assess the selectivity of the MBAC system, other cancer cell lines (CCL-2, CCL-119 and CCL-185) mixed with MCF-7 cells have been tested on the MBAC system. The MBAC system was tested with 0.5 million CCL-2, CCL-119 and CCL-185 cells. Figure 49 shows the blue bars that represent individual absorbance readouts for each cell line, and the mixture of MCF-7 cells with each individual cell lines on the MBAC system. Excellent selectivity for MCF-7 cell detection was achieved over other

cancer cell lines. The specificity of the MBAC system is certainly attributed to the high molecular recognition property of aptamers.

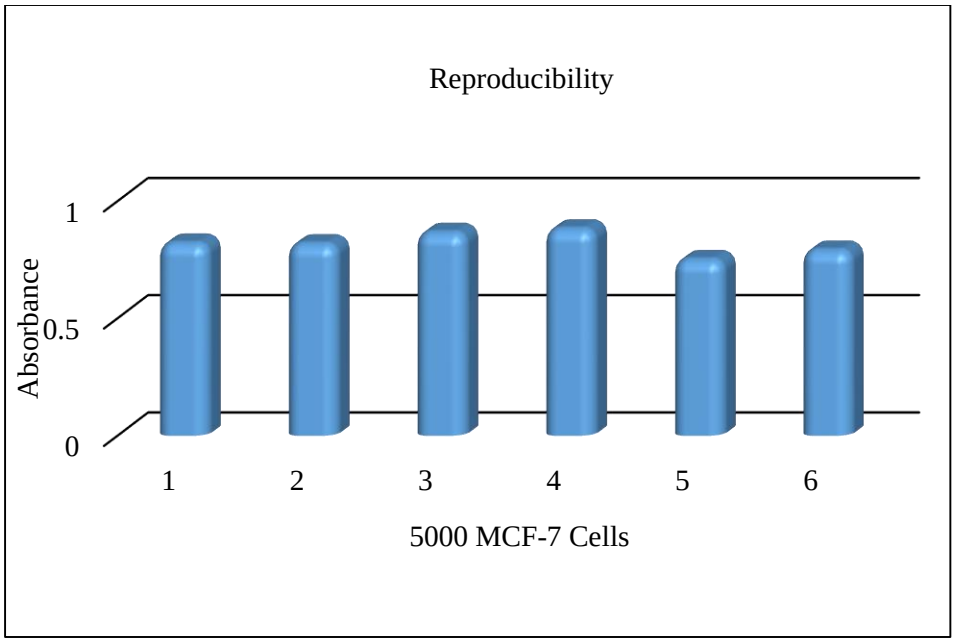

Figure 48. Graph showing the reproducibility of the MBAC system with 5000 MCF-7 cells.

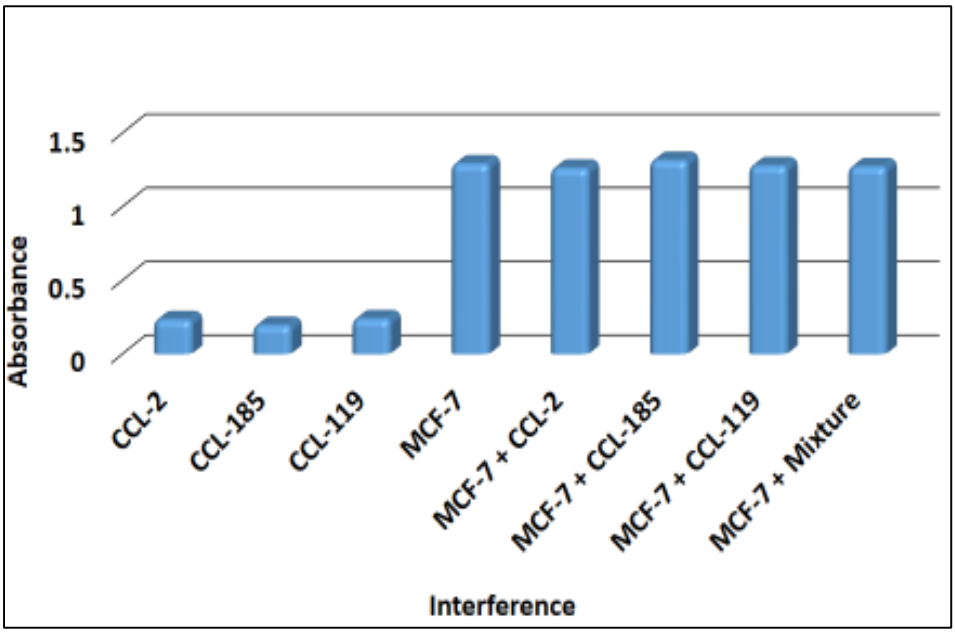

Figure 49. Graph showing the specificity of the MBAC system.

.

Under optimal experimental conditions, the performance of the MBAC system was examined with different number of MCF-7 cells. Quantitative detections were performed by measuring the absorbance readouts with a UV-Vis spectrometer. Well defined peaks were observed at 450nm, increasing in intensity with the increase in the number of MCF-7 cells. Figure 50 shows the absorbance peaks at 450nm vs number of MCF-7 cells, the inset shows the linear calibration curve for the absorbance response from the MBAC system ranging from 250 cells to 50,000 cells. A detection limit of 250 cells was obtained with the MBAC system using the absorbance readouts. Also, visual judgement of the blue color could be used to differentiate 250 MCF-7 cells from the control experiment.

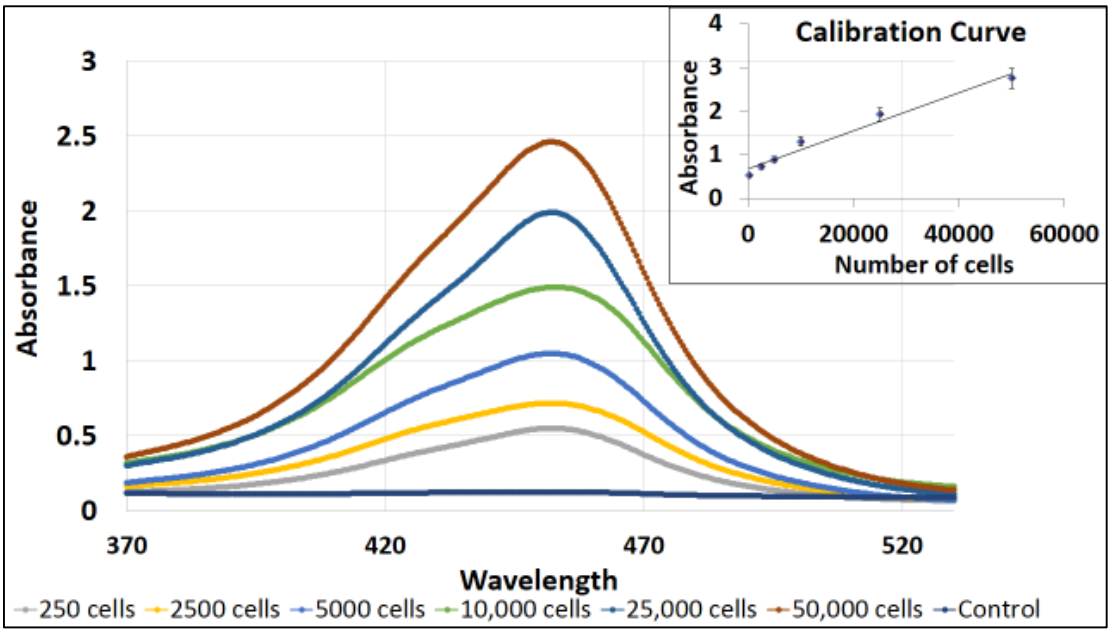

Figure 50. Absorbance response shown for different number of MCF-7 cells.

To demonstrate the feasibility of the MBAC system for detection of MCF-7 cancer cells in biological fluids, the system was applied to detect human blood samples spiked with the MCF-7 cells. The MBAC system was first tested with different volumes of blood to determine the effect on the system. It was found that there was no interference caused by blood when the

volume is less than 5 µL per tube, but significant decrease of the signal was observed after adding 10 µL blood per tube. Figure 51 shows the calibration curve for the MBAC response in 5 µL blood spiked with different amounts of MCF-7 cells. The MBAC system could successfully detect 1000 MCF-7 cells in blood, showing a good linear absorbance response for the increasing number of MCF-7 cells in the sample.

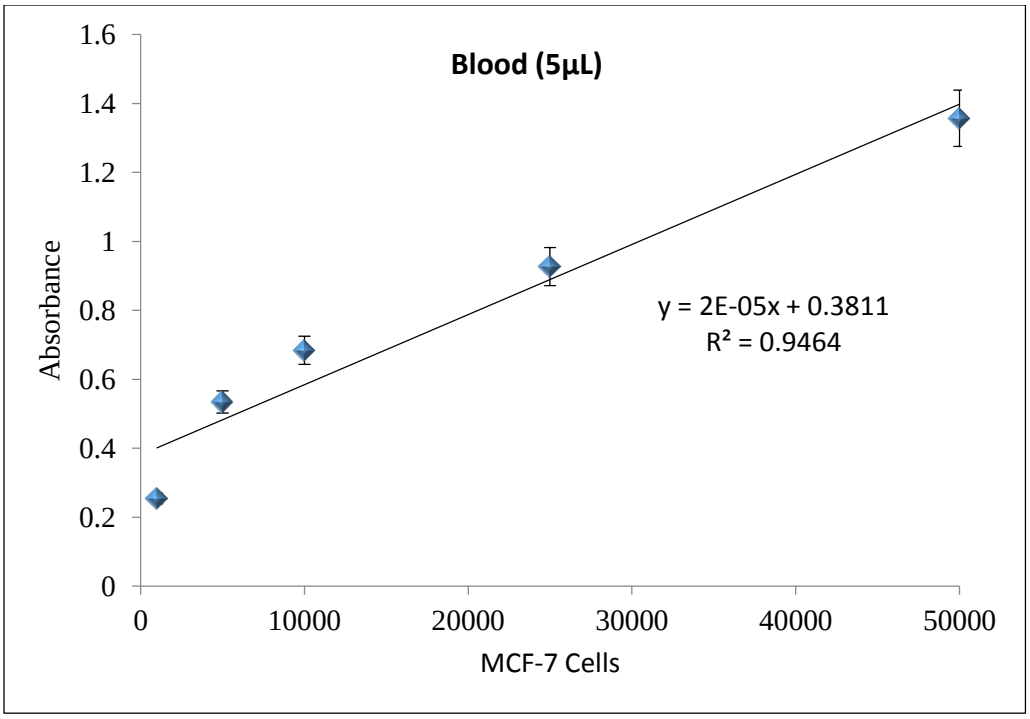

Figure 51. Calibration curve for the MBAC system.

6.5. Conclusion

In summary, we developed a colorimetric detection system based on streptavidin coated magnetic beads, biotinylated aptamers and horseradish peroxidase for the detection of MUC1 on the surface of MCF-7 breast cancer cells. Compared to the colorimetric detection method for CEA, this MBAC system utilizes a pair of aptamers for the detection. Also, complex 1 and 2 are prepared separately, which saves time during the testing of MCF-7 cells reducing the total assay time for detecting MCF-7 cells to about 30 minutes. Analytical parameters tested on the MBAC system

prove that it is reliable with an RSD of 4.72% and specific for the detection of MCF-7 cells, showing no interference with other cancer cell lines. The MBAC system also shows a good detection limit of 250 cells and a dynamic linear range from 250 to 50,000 MCF-7 cells. The colorimetric system was also successful in detecting MCF-7 cells in complex biological matrixes like blood. The MBAC system offers a rapid, simple and cost effective system for the detection of MCF-7 cells. Due to the reliability and accuracy of the detection system, it can also be used for monitoring the progression of the breast cancer patient.

CHAPTER 7. CROSS-FLOW AMPLIFICATION ON LATERAL FLOW BIOSENSORS FOR THE ULTRASENSITIVE DETECTOIN OF MCF-7 CELLS

7.1. Introduction

Amplification techniques have made detection methods more sensitive for their targets helping in the early detection, diagnosis and treatment of several diseases. Signal amplification increases the intensity of the detectable signal for ultra-low concentrations, making the detection method more sensitive. In chapter 4, we incorporated the use of HRP for the detection of PDGF-BB making the lateral flow strips more sensitive for the target analyte. HRP when combined with its substrate (AEC) amplified the red color on the test zone increasing the signal intensity. In this study, we developed a cross flow amplification method which was used to improve the sensitivity of the lateral flow biosensors for the detection of MCF-7 breast cancer cells. A pair of aptamers, specific for the MUC1 proteins overexpressed on the MCF-7 cell surface are used to capture the AUNPs on the test zone via the sandwich type hybridization assay. The AUNPs used in this study are dual labeled with aptamers (specific for MUC1) and ssDNA oligonucleotides (For cross flow). The ssDNA oligonucleotide labeled onto the AUNP-Aptamer conjugates (Conjugates 1) are complimentary to ssDNA labeled onto a different set of AUNPs (conjugates 2). After the assay is complete the conjugate 2 are introduced onto the lateral flow strips, complementary binding between the ssDNA oligonucleotides immobilize additional AUNPs onto the test zone, therefore enhancing the intensity of the test zone. The cross flow technique developed in this study is a good signal amplification method showing no significant background noise or interference. The cross flow amplification method reduced the detection limit of the MCF-7 cells by 5-fold compared to the colorimetric method. The system showed good reproducibility and a linear dynamic range to quantify the number of MCF-7 cells in the sample solution.

7.2. Materials and Methods

The following equipment and reagents were used in this study: The Airjet AJQ 3000 dispenser, Biojet BJQ 3000 dispenser, clamshell laminator and the guillotine cutting module CM 4000 were bought from Biodot LTD (Irvine, CA). The Portable strip reader, DT1030, was purchased from Shanghai Aubio Tech. Co., LTD (Shanghai, China). Streptavidin from Streptomyces avidinii, $Na_3PO_4 \cdot 12H_2O$, $HAuCl_4$, trisodium citrate, sucrose, Tween 20, Triton X-100, sodium chloride-sodium citrate (SSC) buffer (pH 7.0), phosphate buffer saline (PBS, PH 7.4, 0.01 M), bovine serum albumin (BSA), and PDGF-BB were purchased from Sigma-Aldrich. Glass fibers (GFCP000800), cellulose fiber sample pads (CFSP001700), laminated cards (HF000MC100) and nitrocellulose membranes (HFB24004) were provided by Millipore (Bedford, MA). The serum, aptamers and oligonucleotide probe used in this study were obtained from Integrated DNA Technologies, Inc. (Coralville, IA) and have the following sequences:

Primary Aptamer for MUC1:

5′-/5ThioMC6-D/ GCA GTT GAT CCT TTG GAT ACC CTG G -3′

Secondary Aptamer for MUC1:

5′-/ 5Biosg/ GCA GTT GAT CCT TTG GAT ACC CTG G-3′

DNA oligonucleotide (control probe):

5′-/ 5Biosg/ CCA GGG TAT CCA AAG GAT GAA CTG C- 3′

All buffer solutions were prepared using ultrapure (>18MΩ cm) water from a Millipore Milli-Q water purification system (Billerica, MA).

7.2.1. Preparation of Aptamer-AUNP-ssDNA Dual Conjugates

The conjugates were prepared by the reported method[28] with slight modifications. Briefly, 1mL 5-fold solution of AUNPs were prepared using the centrifuge. To the 5-fold AUNP solution,

7.05µM dATP was added and incubated for 15minutes. SDS (1%) with a final concentration of 0.01% was then added to the solution and incubated for about 10 min. SDS stabilizes the AUNP solution and prevents unwanted aggregation in the next step, which is the addition of NaCl (2M) with a final concentration of 0.01M in the 1mL AUNP solution. After addition of salts, thiolated aptamer 0.3 OD and thiolated ssDNA 0.3 OD was added, the solution was kept on a shaker at RT for 3 h. Unbound thiolated aptamers and ssDNA were removed from the AUNP-aptamer conjugate solution by centrifugation (12,000 rpm; 20 min) and washing using PBS, this was done three times. After the final wash the pellet was re-suspended in 1mL eluent buffer (20 mM Na3PO4 · 12H2O, 5% BSA, 0.25% Tween 20, and 10% sucrose). Equal ratios of the aptamer and ssDNA were added to the AUNP solution to ensure equal binding of both the probes. The conjugates were successful in detecting MCF-7 cells and performing the cross flow amplification on the lateral flow strips.

The AUNP-ssDNA (conjugates 2) for the cross flow pad were prepared using the same method mentioned above. The conjugates 2 had only the ssDNA complementary to the ssDNA on the conjugate 1.

7.2.2. Preparation of Aptamer-Based Lateral Strip Biosensor with the Cross Flow Modification

The lateral strip biosensor has five main components: sample pad, conjugate pad, nitrocellulose membrane, absorption pad and the plastic backing layer. For this study, the strips were modified with another set of sample pad and conjugate pad assembly overlapping the lateral flow strips for cross flow purposes. We dispensed one test zones and one control zone on the nitrocellulose membrane, one for capturing MCF-7 cells and the other for capturing the excess conjugates. The control zone was dispensed to check the working of the biosensor and the quality of the conjugates. Sample pads were pretreated with a buffer (pH 8.0) containing 0.25% Triton X-

100, 0.05 M Tris-HCl, and 0.15 mM NaCl. This was done to ensure the proper movement of the analytes onto the conjugate pad. Aptamer-AUNP-ssDNA conjugates (conjugate 1) and AUNP-ssDNA (conjugate 2) were dispensed onto two separate glass fiber conjugate pads using the AirJet dispenser. The dispensed conjugate pads were then dried for 1h at 37 °C and stored at 4 °C until further use. For the nitrocellulose membrane, we first prepared the secondary biotinylated aptamer conjugated with streptavidin for immobilization onto the membrane. Briefly, 50 nmoles of the secondary biotinylated aptamer for MCF-7 cells were mixed with 250 µL of 2 mg/mL streptavidin. After incubating it for 1h at RT, 400 µL of PBS was added for the washing step. Excess unbound biotinylated aptamer was removed by centrifugation for 20 minutes with a Millipore filter (cutoff 30,000 D) at 6000 rpm. The conjugates were washed twice again and finally diluted to a volume of 500 µL with PBS. Using the BioJet dispenser the streptavidin-biotinylated aptamer conjugates and the control zone were dispensed onto the nitrocellulose membrane. The distance between each zones was around 0.2 cm and there were a total of two zones on the biosensor (Test zone 1: MCF-7 cells, Zone 2: control zone). The control zone was a biotinylated DNA probe complementary to the primary PDGF aptamer, prepared using the same technique as above. After dispensing the nitrocellulose membrane was dried at RT for 1h and stored at 4 ˚C. A plastic backing layer was used to assemble all the components together, using a clamshell laminator. All the membranes overlapped each other by 2mm, which made the migration of solution from one pad to the other fluent and smooth during the assay. Biosensors with a width of 3 mm were cut using the guillotine cutting module CM 4000. The cross flow strips which comprised of only two components, the sample pad and the conjugate pad, overlapped the nitrocellulose membrane by 2 mm before the test zone and the control zone (illustrated in figure 52).

7.2.3. Assay Procedure

A total volume of 80 μL, with the desired number of MCF-7 cells in running buffer (PBST containing 1%BSA) was added onto the sample application pad. The solution through capillary action then migrated onto the conjugate pad, where the AUNP-aptamer conjugates captured the specific target. The AUNP-aptamer-target complex then migrated onto the nitrocellulose membrane where they were captured by the Biotinylated aptamers on the test zones. The biosensor was washed with 15 μL buffer (PBST containing 1%BSA), two times at intervals of 5 minutes each. The test zones and the control zone were evaluated visually within 10 min. For the quantitative measurements, the optical intensity of the red band was observed using the portable "strip reader" combined with the "AuBio strip reader" software.

For the cross flow amplification, buffer solution PBST (1%BSA) with a total volume of 30 μL was added onto the sample application pad of the cross flow strips. The solution which then migrated onto the conjugate pad of the cross flow strips helped move the conjugates 2 onto the nitrocellulose membrane of the lateral flow strips. When the conjugate 2 come in contact with the conjugate 1, the intensity of the test zone is amplified. The complementary ssDNA on conjugate 1 and conjugate 2 interact forming dsDNA, immobilizing additional AUNPs on the test zone, and therefore intensifying the signal. Results were obtained by recording the optical responses with the strip reader after 10 min of assay time.

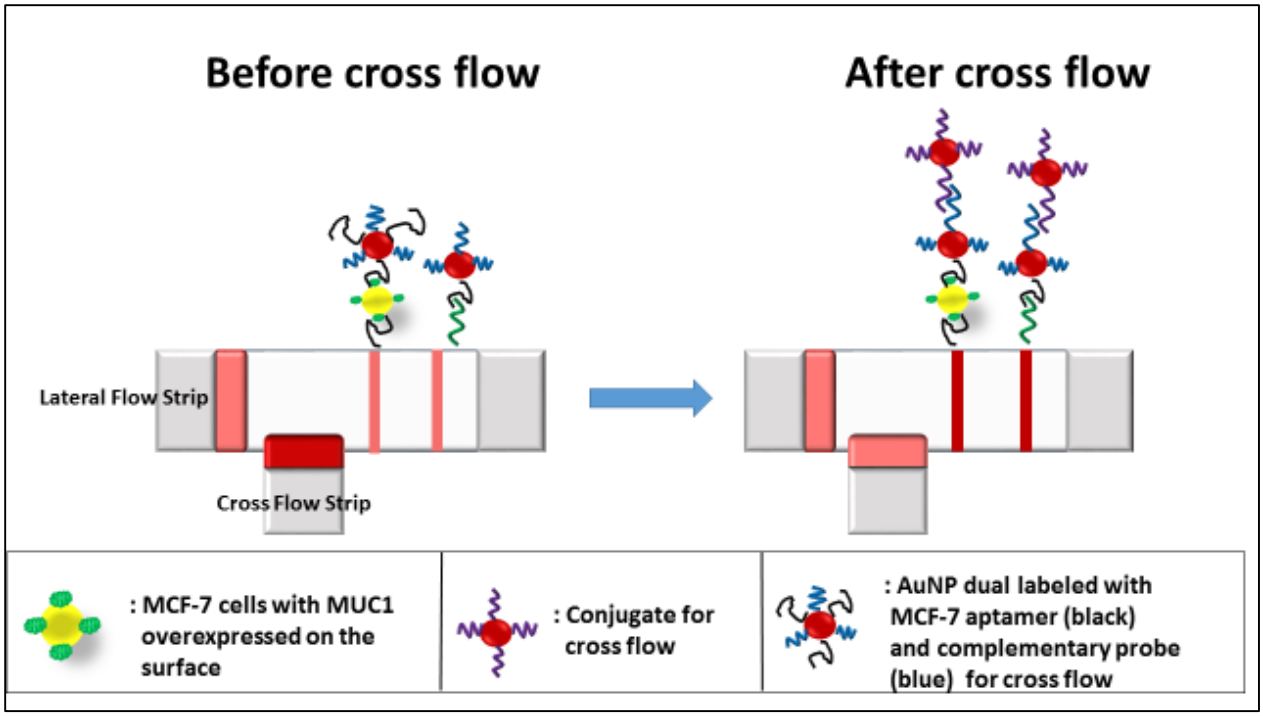

Figure 52. Schematic representation of the Cross flow principle.

7.3. Results and Discussion

The cross flow amplification principle shown in figure 52 indicate the lateral flow strips which are normal biosensor strips for the detection of MCF-7 cells and the cross flow strips which are composed of sample pad and conjugate pad. The cross flow strip overlaps the lateral flow strip by 2 mm just before the test and control zones. The conjugate 1 (Aptamer-AUNP-ssDNA) are dispensed on the conjugate pad of the lateral flow strips while the conjugate 2 (AUNP-ssDNA) are dispensed on the conjugate pad of the cross flow strips. After the assay is complete, Aptamer-AUNP-ssDNA conjugates are captured on the test zone in presence of the target MCF-7 cells. The conjugate 2 from the cross flow strips are then activated by adding buffer to the sample pad. The AUNP-ssDNA (conjugate 2) get immobilized onto the test zone via the complementary binding between the ssDNA on both the conjugates. The increased number of AUNPs on the test zone increases the intensity of the test zone, therefore increasing the sensitivity of the lateral flow

biosensors. One major optimization important for the cross flow amplification on the lateral flow biosensors was the type of nitrocellulose membrane used in the preparation of the strips. Two types of nitrocellulose membrane were compared, 3 minute and the 4 minute. The 4 minute nitrocellulose membrane had smaller pores compared to the 3 minute membrane. As shown in figure 53, 3 minute membranes showed a slightly better response compared to the 4 minute membrane. This may be because of the slightly larger pore size of the 3 minute membrane, making it easy for the large complex of AUNPs and captured cells to move freely onto the test zone. The small pores of the 4 minute membrane might have trapped some of the AUNP-MCF-7 cell complexes, resulting in a lower intensity on the test zone.

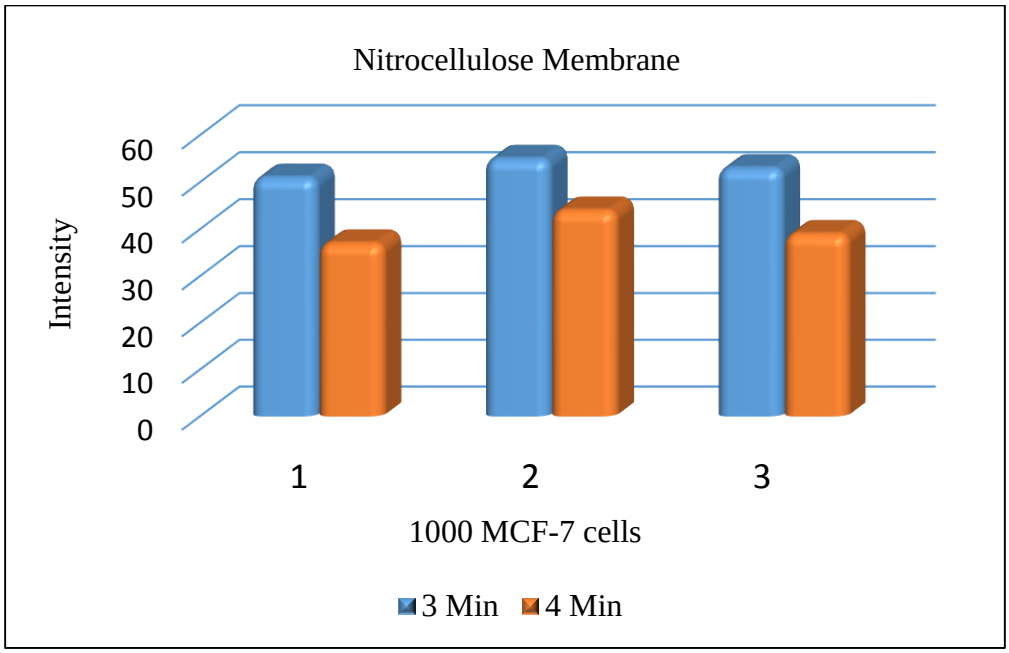

Figure 53. Graph showing the optimization for the nitrocellulose membrane.

Other optimizations included the test line concentration, conjugate amount and the buffer system. Different concentrations of the biotinylated aptamer were dispensed on the test zone (figure 54). The intensity of the test zone for 1000 MCF-7 cells increased till a concentration of 200 nmoles, after which the signal saturated. So, 4x dispensed test line at a concentration of 200

nmoles was chosen for the lateral flow biosensors. For the conjugate amount optimization, different amounts of Aptamer-AUNP-ssDNA were dispensed onto the conjugate pad and tested against a concentration of 1000 MCF-7 cells. Using the AirJet dispenser, dispensing the conjugates 3 times onto the conjugate pad showed the best response for 1000 MCF-7 cells. Dispensing more times resulted in the saturation of the test line intensity. Figure 55 shows a graph representing the response for different dispensing times of the conjugates on the conjugate pad for 1000 MCF-7 cells. Different buffer systems were also tested on the lateral flow biosensors to find the optimal running buffer showing the maximum intensity for the MCF-7 cell detection. Figure 56 shows that PBST (1% BSA) gave the best response compared to other buffers like PBST, PBSB and 1/4 SSC (1% BSA) that were also tested on the biosensor. PBST (1% BSA) was chosen as the running buffer for all the samples tested on the lateral flow strips.

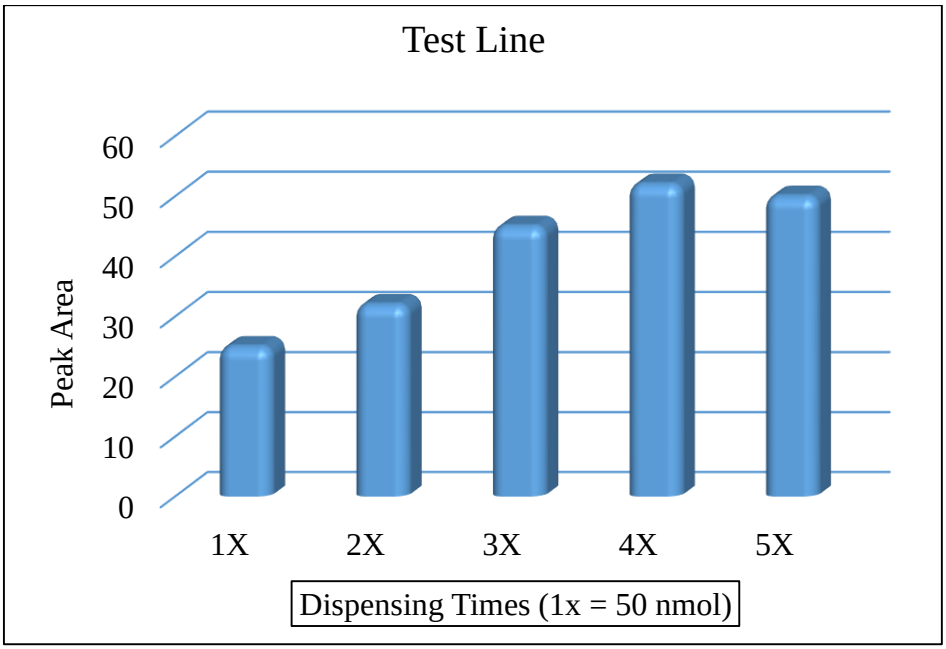

Figure 54. Graph showing the optimization for the test line dispensing times.

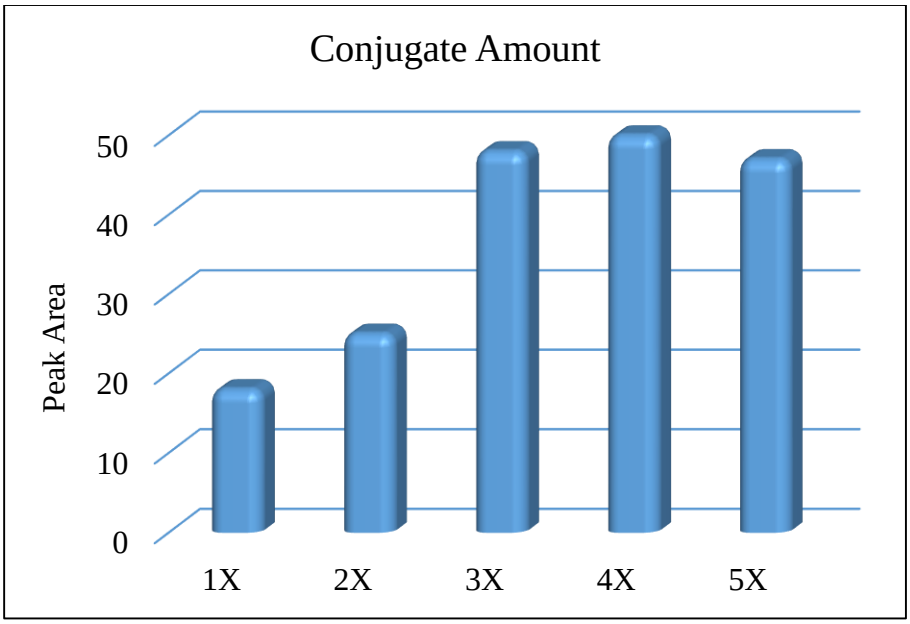

Figure 55. Graph showing optimization for conjugate amount.

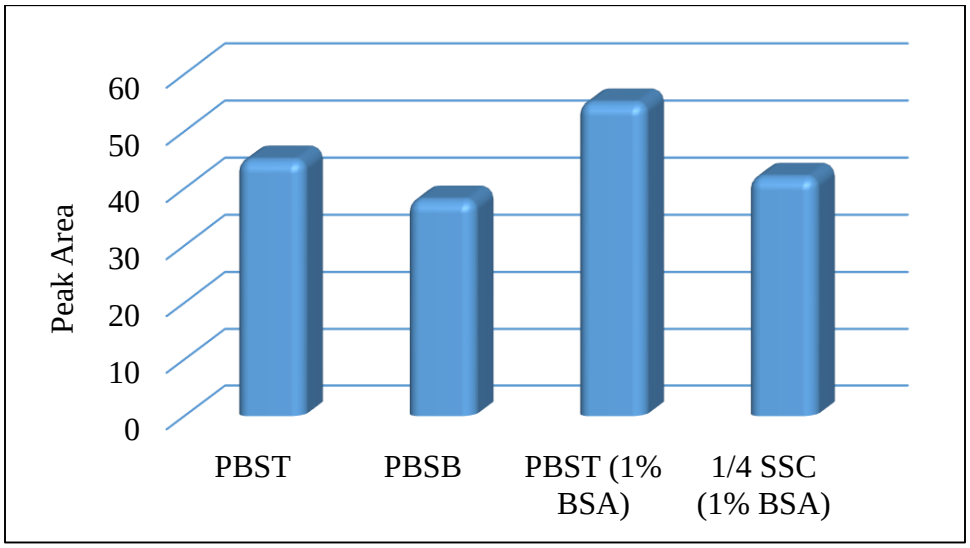

Figure 56. Image showing the optimization for different running buffers.

After the parameters for the lateral flow biosensors were optimized, the strips were tested with different concentrations of MCF-7 cells. Figure 57 shows the response recorded using the Aubio strip reader for different amounts of MCF-7 cells tested on the lateral flow strips. These assays were run without the cross flow amplification, achieving a detection limit of 500 cells and

a linear dynamic range of 500 to 100,000 cells. Once the detection limit and optimal parameters of the lateral flow strips were determined, we incorporated the cross flow amplification to see the amplification effect. The cross flow strips which overlapped the lateral flow strip by 2 mm, were activated by adding just the running buffer PBST (1% BSA) on the sample pad. The conjugates 2 which are AUNP-ssDNA were then rehydrated by the buffer and pushed onto the nitrocellulose membrane of the lateral flow strips, where they came in contact with the test zone, leading to the amplification of the test line intensity. Figure 58 shows the increase in intensity of the test zone before and after the use of the cross flow amplification method for the detection of 500 MCF-7 cells. The intensity of the test line is barely visible before the cross flow amplification, while after the amplification method the red line on the test zone is clearly visible, indicating successful amplification.

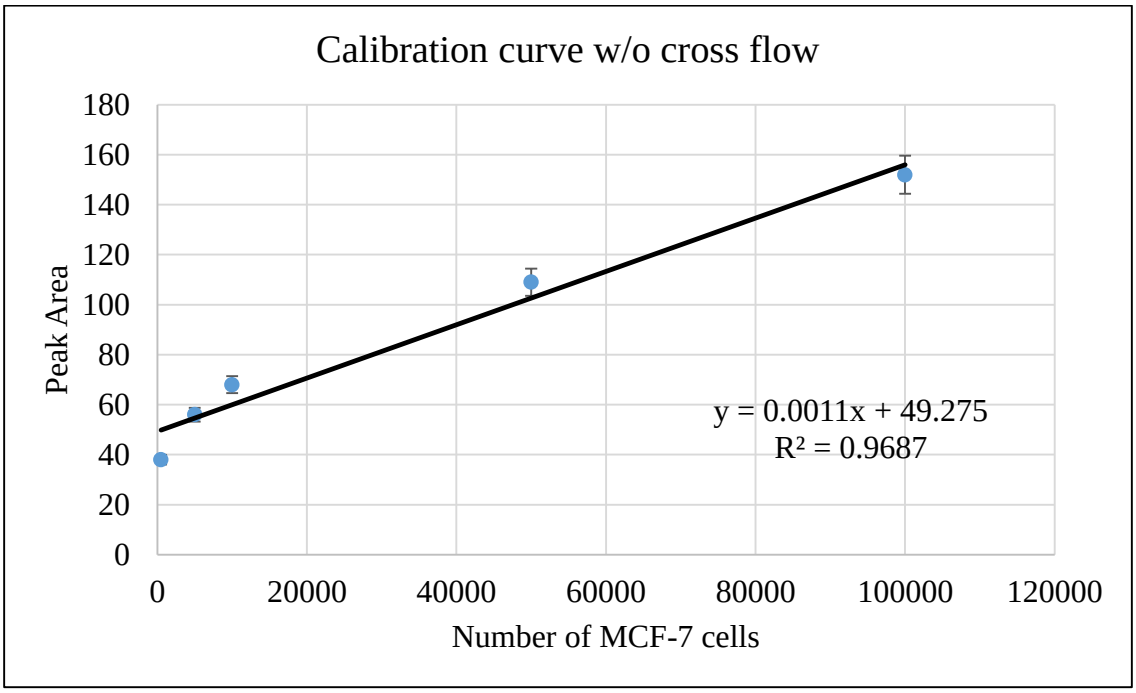

Figure 57. Calibration curve for different MCF-7 concentrations without cross flow amplification.

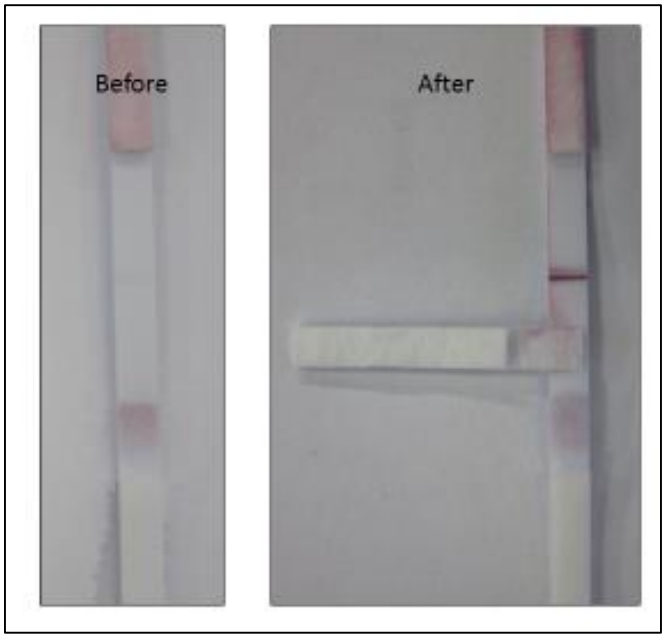

Figure 58. Image showing the amplification effect using the cross flow method.

The analytical performance of the lateral flow strips with the cross flow amplification was also tested. To check the reproducibility of the Cross flow amplification method, we took six strips and tested equal concentration of the MCF-7 cells on each. Once the assay was complete, the cross flow amplification was performed to check the intensity of the test zone after the amplification process. Figure 59 shows the response for six different lateral flow strips after the cross flow amplification detecting 50 MCF-7 cells. The quantitative response were recorded using the GoldBio strip reader and the RSD was calculated to be 6.5 %. Interference using other cell line like CCL-2, CCL-185 and CCL-119 were also tested on the lateral flow strips with cross flow amplification. None of the non-specific cell lines showed any response on the test zone, they also did not cause any interference for the detection of the MCF-7 cells on the strips. Figure 60 shows the image for the cross flow amplification on the lateral flow biosensors detecting different number of MCF-7 cells in running buffer. The detection limit using the cross flow amplification reduced

to about 50 MCF-7 cells, which is a 10-fold increase in sensitivity. The linear range with the amplification method ranged from 50 to 10,000 MCF-7 cells shown in figure 61.

Figure 59. Image showing the reproducibility for the cross flow amplification method.

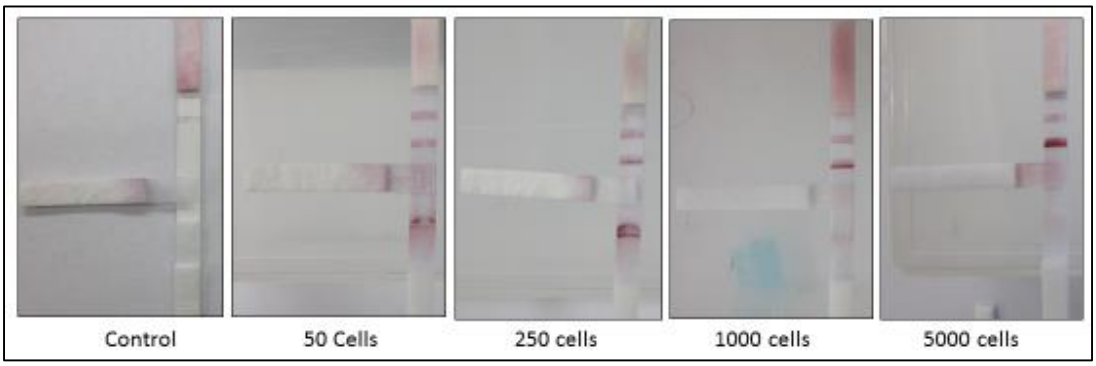

Figure 60. Image showing the response for different MCF-7 cells after the cross flow amplification.

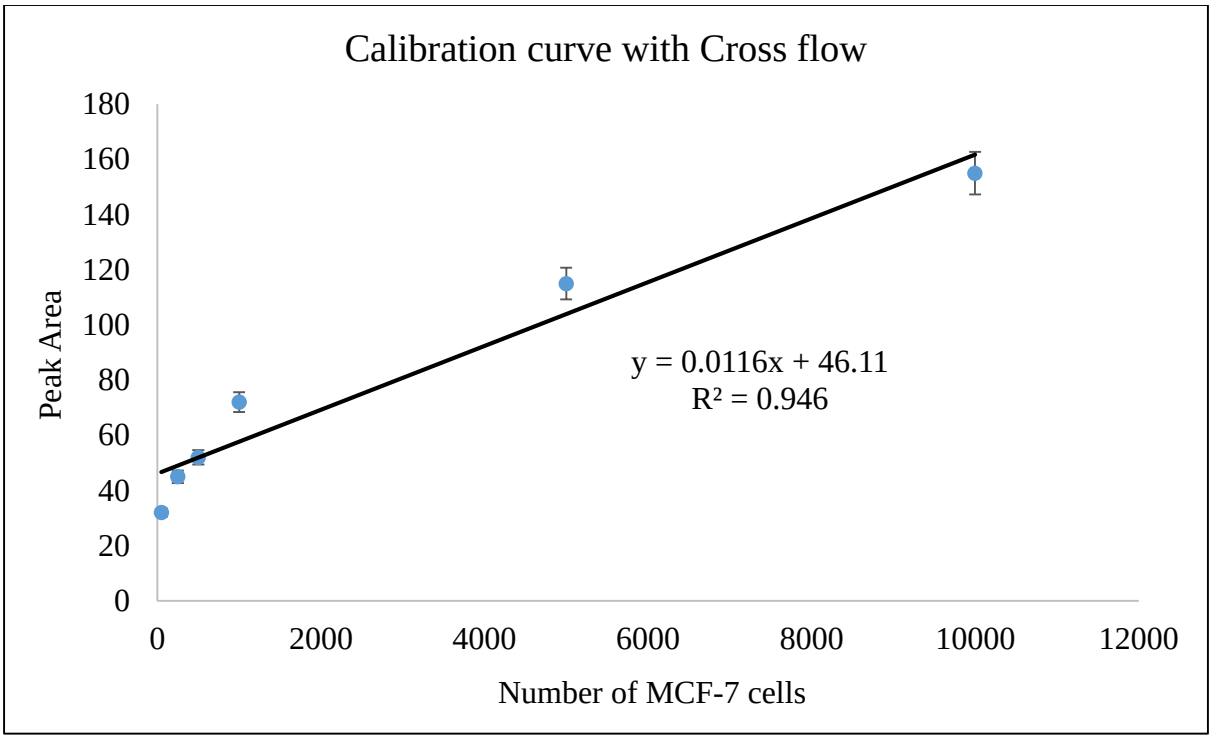

Figure 61. Calibration curve for different MCF-7 concentrations after the cross flow amplification.

7.4. Conclusion

In this study, we successfully developed a cross flow amplification method which could amplify the intensity of the test zone, greatly improving the sensitivity of the lateral flow biosensors for the detection of MCF-7 cells. The incorporated cross flow strip made of only the conjugate pad and sample pad could amplify the intensity of the test zone within minutes resulting in a 10-fold increase in sensitivity. The detection limit of the lateral flow biosensors was lowered to 50 MCF-7 cells compared to the 500 MCF-7 cell detection limit, without cross flow amplification. The method developed in this study is a good example for the cross flow amplification technique, which could also be incorporated for the detection of other targets. The use of two complementary ssDNA on separate AUNP conjugates is simple, fast, low-cost and reliable. Interference was not observed using the cross flow technique as the ssDNA only bound to its complementary counterpart on the test zone. In the absence of the complementary ssDNA

the cross flow conjugates could not get immobilized on the test zone, therefore giving no false positives. The amplification method also showed good reproducibility with an RSD of 6.5 %. For improving the amplification procedure we could incorporate the use of HRP labels onto conjugate 2, which would lead to a dual amplification procedure. The HRP once trapped onto the test zone will be introduced to a substrate which would further amplify the intensity of the test zone.

CHAPTER 8. SUMMARY

In this dissertation, we studied the development of new methods for the simple, fast and cost effective detection of protein biomarkers. The development of a lateral flow biosensor for thrombin by Liu et al. inspired the work described in this dissertation. The thrombin biosensors incorporated the use of aptamers and AUNPs, showing the proof of concept for protein detection on lateral flow biosensors. Proteins are great biomarkers for the early detection and diagnosis of several major diseases. As early detection greatly improves the survival rate in patients, we focused our research on improving the lateral flow strips, making it more sensitive for the detection of protein biomarkers.

The biosensors were first tested for the multiple detection of protein biomarkers. PDGF-BB and thrombin were selected as the model targets for detection. Separate aptamers specific for their respective targets were conjugated with AUNPs and dispensed on the conjugate pad. Test zones for each target were prepared by dispensing the secondary aptamers for both the PDGF-BB and thrombin onto the nitrocellulose membrane. In presence of the targets, sandwich type hybridization captured the AUNPs onto the test zones giving red colored bands. The lateral flow biosensors were successfully developed for the multiple detection of the two protein biomarker targets. The two targets did not show any interference for each other and both the targets could be detected simultaneously. A detection limit of 1 nM for PDGF-BB and 1.5 nM for thrombin was achieved with a good linear detection range. Although the biosensor showed good sensitivity with a detection limit above the cut-off values for both the targets, we wanted to make the biosensors more sensitive lowering the detection limit even further.

Amplification techniques, well known for lowering the detection limit by amplifying the detectable signal have gained a lot of interest in the past few decades. To improve the sensitivity

of the lateral flow biosensor we incorporated the use of horseradish peroxidase (HRP). AUNPs were dual labeled with aptamers and HRP molecules for the detection of PDGF-BB. HRP when combined with its substrate (AEC) produced a red insoluble product, which increased the red color of the test zone, amplifying the signal intensity. Using the HRP amplification technique we lowered the detection limit to 0.05 nM PDGF-BB, which was a 20-fold increase in sensitivity compared to the lateral flow biosensors without HRP amplification. We also modified the conjugate preparation method by incorporating the use of dATP, which formed a monolayer of adenosine around the AUNP protecting it from aggregation during the aging process. Out of the four different mononucleotides, dATP covered AUNPs were found to have a higher salt tolerance than AUNPs protected by other mononucleotides. The controlled salt concentration and dATP monolayer on the AUNPs facilitate the ligand exchange reaction between the incoming thiol-aptamer and the outgoing dATP. The new method for conjugate preparation reduced the preparation time to about 5 h compared to the traditional method which took 50 h. Also the amount of thiolated-aptamer used for conjugation was reduced to 0.3 OD from 1 OD, reducing the reagent cost for each batch of conjugate prepared. The new method of conjugate preparation was faster, cheaper and showed equal sensitivity compared to the traditional method.

To improve the platform for protein biomarker detection, moving towards real patient samples, we developed a colorimetric detection system. Streptavidin-magnetic beads, biotinylated-antibodies, biotinylated-aptamers and streptavidin-HRP were combined in a systematic manner for the detection of Carcinoembryonic antigen, used as a model target. The colorimetric system relied on the reaction between HRP and its substrate (TMB). In presence of the target, HRP reacted with its substrate giving a yellow color, showing absorbance at 450 nm. This method was successfully developed for the qualitative and quantitative detection of CEA, with a detection limit

of 1.5 ng/mL. A fast, simple and sensitive method was developed for the detection of the synthesized CEA protein biomarker.

To move closer to our goal, which is real patient sample testing, we further improved the colorimetric detection system. MCF-7 breast cancer cells which overexpress MUC1 proteins on their surface, were cultured and used as model targets. Aptamer specific for the MUC1 protein were used to capture the MCF-7 cells in a sandwich type hybridization. HRP labeled onto the aptamer then reacted with its substrate (TMB) giving a yellow color, showing absorbance at 450 nm. Compared to the previous colorimetric system, this new improved MBAC system was cheaper, faster and simpler. The same aptamer was used to complete the sandwich type hybridization as several MUC1 surface proteins are expressed on one MCF-7 cell surface. Antibodies, replaced by aptamers reduced the cost for running the MBAC test. Also, complex 1 and 2 are prepared separately, which saves time during the testing of MCF-7 cells reducing the total assay time for detecting MCF-7 cells to about 30 minutes. The MBAC system showed good reproducibility with no interference from other cancer cell lines. A detection limit of 250 MCF-7 cells was easily achievable using the MBAC system.

The detection of MCF-7 cells was further tested on the lateral flow biosensors with the cross flow amplification method to improve the sensitivity. AUNPs were dual labelled with aptamers (specific for MUC1) and ssDNA (cross flow probe) for the detection of MCF-7 cells. After the MCF-7 cells were captured on the test zone, the cross flow conjugates were activated from the cross flow strips. The AUNP-ssDNA cross flow conjugates as a result of complementary binding got trapped on the test zone, binding to the dual labelled Aptamer-AUNP-ssDNA conjugates. The accumulation of additional AUNPs on the test zone increased the intensity of the test zone, improving the sensitivity for MCF-7 cell detection. Without the cross flow amplification,

lateral flow strips could detect 500 MCF-7 cells showing good reproducibility with an excellent linear detection range. Incorporation of the cross flow amplification method reduced the detection limit to 50 MCF-7 cells, improving the sensitivity 10-folds compared to the normal lateral flow strips.

In this dissertation, we have successfully development Lateral flow biosensors and colorimetric methods for a number of protein biomarker targets. Amplification of the two methods using HRP and cross flow amplification greatly improved the sensitivity of the detection systems. The lateral flow biosensors and the colorimetric methods are great point-of-care detection systems which can be further improved by using dual amplification. AUNPs could be labeled with aptamers (specific for target), HRP and ssDNA (cross flow) for a dual amplification system. The cross flow amplification combined with the HRP amplification would surely be a powerful system for detection of protein biomarkers in patient samples.

REFERENCES

(1) Tuerk, C.; Au, L. *Science (Washington, D. C.)* **1990**, *249*, 505–510.

(2) Ellington, A. D.; Szostak, J. W. *Nature (London)* **1990**, *346*, 818–822.

(3) Stadtherr, K.; Wolf, H.; Lindner, P. *Anal. Chem.* **2005**, *77*, 3437-3443.

(4) Potyrailo, R. A.; Conrad, R. C.; Ellington, A. D.; Hieftje, G. M. *Anal. Chem.* **1998**, *70*, 3419 3425.

(5) Stojanovic, M. N.; Landry, D. W. *J. Am. Chem. Soc.* **2002**, *124*, 9678-9679.

(6) Herr, J. K.; Smith, J. E.; Medley, C. D.; Shangguan, D.; Tan, W. *Anal. Chem.* **2006**, *78*, 2918.

(7) Nimjee, S. M.; Rusconi, C. P.; Sullenger, B. A. *Annu. Rev. Med.* **2005**, *56*, 555-583.

(8) Liss, M.; Petersen, B.; Wolf, H.; Prohaska, E. *Anal. Chem.* **2002**, *74*, 4488- 4495.

(9) Shuman, M. A.; Majerus, P. W. *J. Clin. Invest.* **1976**, *58*, 1249–1258.

(10) Zhu, H.; Klemic, J. F.; Chang, S.; Bertone, P.; Casamayor, A.; Klemic, K. G.; Smith, D.; Gerstein, M.; Reed, M. A.; Snyder, M. *Nat. Genet.* **2000**, *26*, 283–289.

(11) Bichler, J.; Siebeck, M.; Maschler, R.; Pelzer, H.; Fritz, H. *Blood Coag. Fibrinol.* **1991**, *2*, 129–133.

(12) Potyrailo, R. A.; Conrad, R. C.; Ellington, A. D.; Hieftje, G. M. *Anal. Chem.* **1998**, *70*, 3419–3425.

(13) Furtado, L. M.; Su, H.; Thomson, M. *Anal. Chem.* **1999**, *71*, 1167–1175.

(14) Bizzarri, A. R.; Cannistraro, S. *Nanomedicine* **2007**, *3*, 306–310.

(15) Sano, T.; Smith, C. L.; Cantor, C. R. *Science* **1992**, *258*, 120-122.

(16) Zhang, H.; Wang, Z.; Li, X.-F.; Le, X. C. *Angew. Chem., Int. Ed.* **2006**, *45*, 1576-1580.

(17) German, I.; Buchanan, D. D.; Kennedy, R. T. *Anal. Chem.* **1998**, *70*, 4540-4545.

(18) Ostergaard, J.; Heegaard, N. H. H. *Electrophoresis* **2006**, *27*, 2590-2608.

(19) Turkevich, L.; Berezovski, M.; Nutiu, R.; Li, Y.; Krylov, S. N. *Anal. Chem*. **2003**, *75*, 1382-1386.

(20) Craig, D. B.; Arriaga, E. A.; Wong, J. C. Y.; Lu, H.; Dovichi, N. J. *J. Am. Chem. Soc*. **1996**, *118*, 5245-5253.

(21) Wu, D.; Regnier, F. E. *Anal. Chem*. **1993**, *65*, 2029-2035.

(22) Yang, W.-C.; Schmerr, M. J.; Jackman, R.; Bodemer, W.; Yeung, E. S. *Anal. Chem*. **2005**, *77*, 4489-4494. (g) Pavski, V.; Le, X. C. *Curr. Opin. Biotechnol*. **2003**, *14*, 65-73.

(23) Fredriksson, S.; Gullberg, M.; Jarvius, J.; Olsson, C.; Pietras, K.; Gustafsdottir, S. M.; Ostman, A.; Landergren, U. *Nat. Biotechnol*. **2002**, *20*, 473-477.

(24) Plotz, C. M.; Singer, J. M. *Am. J. Med.* **1956**, *21*, 888–892.

(25) Kohn, J. *Immunology* **1968**, *15*, 863–865.

(26) Millipore, C. *A Short Guide: Developing Immunochromatographic Test Strips*; 1996.

(27) Hui Xu, Xun Mao,Qingxiang Zeng, Shengfu Wang, Abdel-Nasser Kawde, and Guodong Liu *Anal. Chem.* **2009,** *81*, 669–675

(28) Xun Mao, Meenu Baloda, Anant S. Gurung, Yuehe Lin, Guodong Liu,* Electrochemistry Communications 10 (2008) 1636–1640

(29) Hongquan Zhang, Xing-Fang Li, and X. Chris Le* *Department of Laboratory Medicine and Pathology, Uni*V*ersity of Alberta, Edmonton, Alberta, Canada T6G 2G3*

(30) Han, M.; Gao, X.; Su, J.; Nie, S. *Nat. Biotechnol.* **2001**, *19*, 631–635.

(31) Kim, Y. M.; Oh, S. W.; Jeong, S. Y.; Pyo, D. J.; Choi, E. Y. *Envrion. Sci. Technol.* **2003**, *37*, 1899–1904.

(32) Gale, N. W.; Yancopoulos, G. D. *Genes Dev*. **1999**, *13*, 1055-1066.

(33) Battegay, E. J.; Rupp, J.; Iruela-Arispe, L.; Sage, E. H.; Pech, M. *J. Cell Biol.* **1994**, *125*, 917-928.

(34) Thommen, R.; Humar, R.; Misevic, G.; Pepper, M. S.; Hahn, A. W. A.; John, M.; Battegay, E. J. *J. Cell Biochem.* **1997**, *64*, 403-413.

(35) Folkman, J. Angiogenesis in Cancer, Vascular, Rheumatoid and Other Diseases. *Nature Med.* **1995**, *1*, 27-31.

(36) Heldin, C.-H. *EMBO J.* **1992**, *11*, 4251-4259.

(37) Seymour, L.; Dajee, D.; Bezwoda, W. R. *Breast Cancer Res. Treat.* **1993**, *26*, 247-252.

(38) Lindmark, G.; Sundberg, C.; Glimelius, B. L.; Rubin, K.; Gerdin, B. *Lab. Invest.* **1993**, *69*, 682-689.

(39) Yosida, K.; Kuniyasu, H.; Yasui, W.; Kitadai, Y.; Toge, T.; Tahara, E. *J. Cancer Res. Clin. Oncol.* **1993**, *119*, 401-407.

(40) Antoniades, H. N.; Galanopoulos, T.; Neville-Golden, J.; O'Hara, C. J. *Proc. Natl. Acad. Sci., U.S.A.* **1993**, *89*, 3942-3946.

(41) Plate, K. H.; Breier, G.; Farrell, C. L.; Risau, W. *Lab. Invest.* **1992**, *67*, 529-534.

(42) Raines, E. W.; Bowen-Pope, D. D.; Ross, R. *Handbook in Experimental Pharmacology*; Sporn, M. B., Roberts, A. B., Eds.; Springer: Heidelberg, 1990, pp 173-262.

(43) Blaskovich. M. A.; Lin, Q.; Delarue, F. L.; et al. *Nat. Biotechnol.* **2000**, *18* (10), 1065-1070.

(44) Tuerk, C.; Au, L. *Science (Washington, D. C.)* **1990**, *249*, 505–510.

(45) Ellington, A. D.; Szostak, J. W. *Nature (London)* **1990**, *346*, 818–822.

(46) Stadtherr, K.; Wolf, H.; Lindner, P. *Anal. Chem.* **2005**, *77*, 3437-3443.

(47) Potyrailo, R. A.; Conrad, R. C.; Ellington, A. D.; Hieftje, G. M. *Anal. Chem.* **1998**, *70*, 3419-3425.

(48) Stojanovic, M. N.; Landry, D. W. *J. Am. Chem. Soc.* **2002**, *124*, 9678-9679.

(49) Herr, J. K.; Smith, J. E.; Medley, C. D.; Shangguan, D.; Tan, W. *Anal. Chem.* **2006**, *78*, 2918-2924.

(50) Nimjee, S. M.; Rusconi, C. P.; Sullenger, B. A. *Annu. Rev. Med.* **2005**, *56*, 555-583.

(51) Liss, M.; Petersen, B.; Wolf, H.; Prohaska, E. *Anal. Chem.* **2002**, *74*, 4488- 4495.

(52) Shuman, M. A.; Majerus, P. W. *J. Clin. Invest.* **1976**, *58*, 1249–1258.

(53) Leitzel, K.; Bryce, W.; Tomita, J.; Manderino, G.; Tribby, I.; Thomason, A.; Billingsley, M.; Podczaski, E.; Harvey, H.; Bartholomew, M.; et al. *Cancer Res.* **1991**, *51* (16), 4149- 4154.

(54) Zhu, H.; Klemic, J. F.; Chang, S.; Bertone, P.; Casamayor, A.; Klemic, K. G.; Smith, D.; Gerstein, M.; Reed, M. A.; Snyder, M. *Nat. Genet.* **2000**, *26*, 283–289.

(55) Bichler, J.; Siebeck, M.; Maschler, R.; Pelzer, H.; Fritz, H. *Blood Coag. Fibrinol.* **1991**, *2*, 129–133.

(56) Potyrailo, R. A.; Conrad, R. C.; Ellington, A. D.; Hieftje, G. M. *Anal. Chem.* **1998**, *70*, 3419–3425.

(57) Furtado, L. M.; Su, H.; Thomson, M. *Anal. Chem.* **1999**, *71*, 1167–1175.

(58) Bizzarri, A. R.; Cannistraro, S. *Nanomedicine* **2007**, *3*, 306–310.

(59) Plotz, C. M.; Singer, J. M. *Am. J. Med.* **1956**, *21*, 888–892.

(60) Kohn, J. *Immunology* **1968**, *15*, 863–865.

(61) Millipore, C. *A Short Guide: Developing Immunochromatographic Test Strips*;1996.

(62) Hui Xu, Xun Mao,Qingxiang Zeng, Shengfu Wang, Abdel-Nasser Kawde, and Guodong Liu *Anal. Chem.* **2009,** *81*, 669–675

(63) Ivo M. B. Francischetti.; Jesus G. Valenzuela.; and Jose´ M. C. Ribeiro, *Biochemistry* **1999,** *38*, 16678-16685.

(64) Qiang Zhao.; Xiufen Lu.; Chun-Gang Yuan.; Xing-Fang Li.; and X.; Chris Le, *Anal. Chem.* **2009,** *81*, 7484–7489.

(65) V. Fuster.; L. Badimon.; J. J. Badimon.; J. H. Chesebro, *N. Engl. J. Med*. **1992**, 326, 242 ± 250.

(66) R. Ross, *Nature* **1993**, 362, 801 ± 809.

(66) P. Libby, *Circulation* **1995**, 91, 2844 ± 2850.

(67) Md. Aminur Rahman.; Jung Ik Son.; Mi-Sook Won.; and Yoon-Bo Shim, *Anal. Chem.* **2009,** *81*, 6604–6611. [1] V.

(68) Fabien Le Floch.; Hoang A. Ho.; and Mario Leclerc**.** *Anal. Chem*. **2006,** 78, 4727-4731.

(69) Baldrich, E.; Acero, J. L.; Reekmans, G.; Laureyn, W.; O'Sullivan, C. K. *Anal. Chem.* **2005**, *77*, 4774–4784.(9) Bichler, J.; Siebeck, M.; Maschler, R.; Pelzer, H.; Fritz, H. *Blood Coag.Fibrinol.* **1991**, *2*, 129–133.

(70) Potyrailo, R. A.; Conrad, R. C.; Ellington, A. D.; Hieftje, G. M. *Anal. Chem.***1998**, *70*, 3419–3425.

(71) Bizzarri, A. R.; Cannistraro, S. *Nanomedicine* **2007**, *3*, 306–310.

(72) Hui Xu.; Xun Mao.; Qingxiang Zeng.; Shengfu Wang.; Abdel-Nasser Kawde.; and Guodong Liu.; *Anal. Chem.* **2009,** *81*, 669–675

(73) Tuerk, C.; Gold, L. *Science (Washington, D. C.)* **1990**, *249*, 505–510.

(74) Ellington, A. D.; Szostak, J. W. *Nature (London)* **1990**, *346*, 818–822.

(75) Ho, H. A.; Leclerc, M. *J. Am. Chem. Soc.* **2004**, *126*, 1384–1387.

(76) Bang, G. S.; Cho, S.; Kim, B. G. *Biosens. Bioelectron.* **2005**, *21*, 863–870.

(77) Xun Mao.; Yunqing Ma.; Aiguo Zhang.; Lurong Zhang.; Lingwen Zeng.; and Guodong Liu.; *Anal. Chem.* **2009**, *81*, 1660–1668

(78) Smironov, I.; Shafer, R. H. *Biochemistry* **2000**, *39*, 1462–1468.

(79) Guodong Liu.; Xun Mao.; Joseph A. Phillips.; Hui Xu.; Weihong Tan.; and Lingwen Zeng. *Anal. Chem.* **2009**, *81*, 10013–10018

(80) Qiang Zhao.; Xiufen Lu.; Chun-Gang Yuan.; Xing-Fang Li and X. Chris Le. *Anal. Chem.* **2009,** *81*, 7484–7489

(81) Suttiporn Pinijsuwan.; Patsamon Rijiravanich.; Mithran Somasundrum.; and Werasak Surareungchai. *Anal. Chem.* **2008**, *80*, 6779–6784.

(82) Savka I. Stoeva.; Jae-Seung Lee.; Jennifer E. Smith.; Steven T. Rosen.; and Chad A. Mirkin. *J. AM. CHEM. SOC*. **2006**, 128, 8378-8379

(83) Mulvaney, P. *Langmuir* **1996**, *12*, 788-800.

(84) Kelly. K. L.; Coronado. E.; Zhao. L. L.; Schatz. G. C. *J. Phys. Chem. B* **2003**, *107*, 668-677.

(85) He. X.; Zhong. Z.; Guo. Y.; Lv. J.; Xu. J.; Zhu. M.; Li. Y.; Liu. H.;Wang. S.; Zhu. Y.; Zhu. D. *Langmuir* **2007**, *23*, 8815-8819.

(86) Cheng-Ju Yu; and Wei-Lung Tseng; *Langmuir* **2008,** *24*, 12717-12722

(87) Yi-Ming Chen; Cheng-Ju Yu; Tian-Lu Cheng; and Wei-Lung Tseng. *Langmuir* **2008,** *24,* 3654-3660.

(88) Wenting Zhao.; Li Lin.; and I-Ming Hsing. *Bioconjugate Chem.* **2009,** *20,* 1218–1222

(89) L. W. Wang, B. Liu, H. Yin, J. Wei, X. Qian, L. Yu, *JNMU ELSEVIER*, 2007-21(5):277-281.

(90) Berinstein NL, *J Clin Oncol* 2002; 20: 2197-207.

(91) G. R. Hashemi Tabar and C. L. Smith, *WASJ,* 2010, 16-21

(92) A. C. Perkins and S. Missailidis, *Q J Nucl Mol Imaging*, 2007, 51(4): 292-6.

(93) R. Genc¸ , D. Murphy, A. Fragoso, M. Ortiz, and C. K. O'Sullivan, *Anal chem*, 2011, *83* (2),

563–570.

(94) A. S. sundblad, E. M. Pellicer, L. Ricci, *Human Pathol,* 1996, 27, 297-301.

(95) D. E. Haagensen, S. J. Kister, J. P. Vandevoorde, J. B. Gates, e. K. Smart, H. J. Hansen, S. A.Wells, *Cancer*, 1978, 42, 1512-1519.

(96) B. Jezersek, J. Cervek, Z. Rudolf, S. Novakovic, *Cancer Lett*, 110, 137-144

(97) S. Shousha, t. Lyssiotis, V.M. Godfrey, P. J. Scheuer, *Br. Med.J.,* 1979, 1, 777-779.

(98) L. Gold, D. Brown, Y. He, T. Shtatland, B. S. Singer and Y. Wu, *The proceedings of the Natoinal Academy of Sci.*, 1997, 94:59-64

(99) C. Tuerk, L. Au, *Science* 1990, *249*, 505–510.

(100) A. D. Ellington, J. W. Szostak, *Nature,* 1990, *346*, 818–822.

(101). K. Stadtherr, H. Wolf, P. Lindener, *Anal. Chem.* 2005, *77*, 3437-3443.

(102) R. A. Potyrailo, R. C. Conrad, A. D. Ellington, g. M. Hieftje, *Anal Chem*, 1988, 70, 3419-4325.

(103). M. N. Stojanovic, D. W. Landry, *J. Am. Chem. Soc.* 2002, *124*, 9678-9679

(104) J. K. Herr, J. E. Smith, C. D. Medley, D. Shangguan, Tan, W. Tan, *Anal. Chem.* 2006, *78*, 2918-2924.

(105) J. E. Smith, D. M. Colin, Z. Tang, D. shangguan, C. Lofton and W. Tan, *Anal Chem,* 2007, 79: 3075-3082.

(106) E. Baldrich, JL. Acero, G. Reekmans, W. Laureyn, CK. O'ullivan, *Anal Chem*, 2005, 77: 4774-84.

(107) JF. Lee, GM, stovall, AD. Ellington, *Curr opin chem biol*, 2006, 10:282-9.

(108) JW. Guthrie, CL. Hamula, H. zhang, XC. Le, *Methods*, 2006, 38:324-30.

(109) H. Xu, X. Mao, Q. Zeng, S. Wang, A. N. Kawde and G. Liu, *Anal chem*, 2009, 81, 669-675

(110) S.L Clark and V. T. Remcho, *Electrophoresis,* 2002, 23(9): 1335-40.

(111) D. M. P. Thompson, J. Krupey, S. freefman, P. gold, *Proc. Nat. A cad. Sci,* 1969, 64, 161-167.

(112) M. Szturmowicz, W. Tomkowski, A. Fijalkowska, A. Sakowicz, S. Filipecki, *Eur. J. cancer*, 1995, 31, S264.

(113) V. Villena, A. Lopez-Encuentra, J. Echave-Sustaeta, P. Martin-Escribano, B. Oruno-de-solo, J. Estenzo-Alfaro, *cancer,* 1996, 78, 736.

(114) H. Yang, Q. Ahu, D. Li, P. Lin, M. Din, J. Xu, *Fresenius J. Anal. Chem*, 2001, 370, 88-91.

(115) J. Yuan, G. Wang, K. Majima, K. Matsumoto, *Anal Chem,* 2001,73, 1869-1876.

(116) G.F. Blackburn, H.P. Shah, J.H. Kenten, J. Laland, R.A. Kamin, J. Link, J. Peterman, M. J. powell, A. Shah, D. B. Talley, *Clin. Chem.* 1991, 37, 1471-1664.

(117) Shuman, M. A.; Majerus, P. W. *J. Clin. Invest.* **1976**, *58*, 1249–1258.

(118) Zhu, H.; Klemic, J. F.; Chang, S.; Bertone, P.; Casamayor, A.; Klemic, K. G.; Smith, D.; Gerstein, M.; Reed, M. A.; Snyder, M. *Nat. Genet.* **2000**, *26*, 283–289.

(119) Bichler, J.; Siebeck, M.; Maschler, R.; Pelzer, H.; Fritz, H. *Blood Coag. Fibrinol.* **1991**, *2*, 129–133.

(120) Potyrailo, R. A.; Conrad, R. C.; Ellington, A. D.; Hieftje, G. M. *Anal. Chem.* **1998**, *70*, 19-3425.

(121) Furtado, L. M.; Su, H.; Thomson, M. *Anal. Chem.* **1999**, *71*, 1167–1175.

(122) Bizzarri, A. R.; Cannistraro, S. *Nanomedicine* **2007**, *3*, 306–310.

(123) Plotz, C. M.; Singer, J. M. *Am. J. Med.* **1956**, *21*, 888–892.

(124) Kohn, J. *Immunology* **1968**, *15*, 863–865.

(125) Millipore, C. *A Short Guide: Developing Immunochromatographic Test Strips*; 1996.

(126) Cho, Y. J.; Lee, D. H.; Kim, D. O.; Min, W. K.; Bong, K. T.; Lee, G. G.; Seo, J. H. *J. Agric. Food Chem.* **2005**, *53*, 8447–8451.

(127) Shim, W.; Yang, Z.; Kim, J.; Choi, J.; Je, J.; Kang, S.; Kolosova, A.; Eremin,S.; Chung, D. *J. Agric. Food Chem.* **2006**, *54*, 9728–9734.

(128) Sithigorngul, P.; Rukpratanporn, S.; Pecharaburanin, N.; Suksawat, P.; Longyant, S.; Chaivisuthangkura, W. *J. Microbiol. Methods* **2007**, *71*, 256–264.

(129) Tuerk, C.; Gold, L. *Science (Washington, D. C.)* **1990**, *249*, 505–510.

(130) Ellington, A. D.; Szostak, J. W. *Nature (London)* **1990**, *346*, 818–822.